Université de Montréal

Évaluation tridimensionnelle de la reconstruction du ligament croisé antérieur

par

Julien Montreuil

Programme de Sciences Biomédicales

Faculté de Médecine

Mémoire présenté à la Faculté des études supérieures

en vue de l'obtention du grade de maîtrise en

Sciences Biomédicales

Option musculosquelettique

22 novembre 2019

Université de Montréal

Faculté de Médecine

Ce mémoire intitulé

Évaluation tridimensionnelle de la reconstruction du ligament croisé antérieur

Présenté par
Julien Montreuil

A été évalué(e) par un jury composé des personnes suivantes
Dr. Stefan Parent
Président-rapporteur

Dr. Frédéric Lavoie
Directeur de recherche

Dr. Jacques A. De Guise
Codirecteur

Dr. Moreno Morelli
Membre du jury

Résumé

Le ligament croisé antérieur (LCA) demeure un des ligaments du genou le plus souvent blessé. Un mauvais positionnement des tunnels osseux est souvent mis en cause dans les échecs de reconstructions du LCA. Une meilleure compréhension biomécanique du phénomène devient essentielle. Par l'utilisation de l'imagerie biplanaire stéréoradiographique à faible irradiation EOS^{tm}, notre groupe a développé une méthode de reconstruction 3D permettant une description morphologique osseuse remarquable. Par l'entremise de ce système, un référentiel permet d'évaluer, de manière automatisée, précise et reproductible, le positionnement tridimensionnel des tunnels osseux. Notre groupe souhaite partager ce référentiel afin d'assister les chirurgiens orthopédistes à restaurer une biomécanique optimale dans les reconstructions du LCA.

Mots-clés :

Genou

Ligament croisé antérieur

Reconstruction LCA

Imagerie tridimensionnelle

EOS^{tm} imaging

Imagerie biplanaire stéréoradiographique

Abstract

The anterior cruciate ligament (ACL) remains one of the most injured ligament of the knee. Mispositioning the tunnels remains a common cause of ACL reconstruction failure. A better biomechanical description of this phenomenon is therefore essential. Using the low irradiation biplanar stereoradiographic EOS^{tm} imaging system, our group developed a 3D reconstruction method allowing a precise morphologic description of the knee. With this system, the tridimensional positioning of the femoral tunnel can be evaluated in a novel, computerized, precise and reproducible coordinate system. With this referential, our group wish to assist orthopedic surgeons in the restoration of optimal biomechanics in ACL reconstructions.

Keywords:

Knee

Anterior cruciate ligament

ACL Reconstruction

Tridimensional imaging

EOS^{tm} imaging

Biplanar stereoradiographic x-ray

Table des matières

Liste des tableaux

Chapitre 1

Chapitre 2

Liste des figures

Chapitre 1

Chapitre 2

Liste des sigles et abréviations

ACL: Anterior cruciate ligament

ACLR: Anterior cruciate ligament reconstruction

AP: Antero-posterior

CAS: Computer-assisted surgery

CT: Computed Tomography

DRB: Dynamic reference bases ICC:

Intra-class correlation

LCA: Ligament croisé antérieur

LIR: Lateral intercondylar ridge

MRI: magnetic resonance imaging

XR: X-rays

Remerciements

Je tiens à remercier chaleureusement le docteur Frédéric Lavoie, qui m'a initié à la chirurgie orthopédique au tout début de mes études en médecine. Son support et dynamisme auront potentialisé mon intérêt en biomécanique et imagerie orthopédique. Je suis grandement reconnaissant pour sa confiance dans le projet ambitieux de compléter ce mémoire sans interruption d'activités cliniques.

L'équipe du LIO, sous la supervision de Jacques de Guise, aura été déterminante dans ce projet. Je remercie sincèrement Thierry Cresson et Lulu Zhou par leur contribution immense dans la concrétisation de ce projet. Je remercie également tous les étudiants et collègues impliqués dans la réalisation de ce travail. Sans votre support, ce travail n'aurait pas été possible.

Merci.

Introduction

La reconstruction du ligament croisé antérieur

Histoire

Il est fascinant que des papyrus datant de l'Égypte ancienne (-2000 BC) aient décrit des structures stabilisatrices du genou. Bien que des textes de la Grèce antique d'Hippocrate (-400 BC) ont témoigné d'instabilité post-traumatique du genou, l'anatomiste grec de l'Empire Romain Galien de Pergamon (129-199 AD), fut le premier à décrire ces stabilisateurs intra-articulaires du genou en les nommant « ligament genu cruciata ». (1) Ce n'est ensuite qu'au 19e siècle, en Allemagne, que l'importance du ligament croisé antérieur (LCA) dans la cinématique du genou fut soulignée. En effet, les frères Weber, en 1836, ont noté une translation antéropostérieure du tibia lorsque le LCA était réséqué. Plus encore, ceux-ci ont décrit les deux faisceaux du ligament et la distribution des tensions durant l'amplitude du mouvement du genou. (2)

Anatomie, fonction & biomécanique

Le ligament croisé antérieur est donc une structure du genou intra-capsulaire, mais extra-synoviale. Il origine de la face postéro-médiale du condyle fémoral latéral, s'étend distalement avec une orientation oblique vers la région antéro-médiale du plateau tibial. L'insertion tibiale est environ à 15 mm du rebord tibial antérieur, médialement à l'attache de la corne antérieure du ménisque externe. (3) Par cette orientation, le ligament croisé antérieur procure 85% de la stabilité quant à la translation antérieure du tibia par rapport au fémur. Le LCA est un stabilisateur secondaire en termes de rotation tibiale et angulation varus/valgus. (4, 5) La longueur moyenne de ce ligament est de 32 mm et sa largeur varie de 7 à 12 mm. Comme plusieurs ligaments, il est composé d'une matrice organisée de fibres, principalement de collagène de type I. Par sa viscoélasticité, le LCA peut subir des déformations sans dommages structurels. (6) Tel que souligné précédemment, le LCA est en fait composé de deux faisceaux, nommés selon leur insertion au niveau du tibia ; le faisceau antéro-médial et le faisceau

postéro-latéral. Ces faisceaux sont isolés dès la vie fœtale. Le faisceau antéro-médial est surtout responsable de limiter la translation antérieure du tibia. Il est sous tension durant l'entièreté de l'amplitude de mouvement du genou, mais surtout en flexion. Le faisceau postéro-latéral, lui, est soumis à une plus grande variété de tensions. Il est sous tension lorsque le genou est en extension, tandis qu'il est relâché en milieu de flexion. Le faisceau postérolatéral contribue principalement à une stabilité rotatoire du tibia. Ainsi, les différentes portions du ligament se partagent les tensions à travers l'amplitude de mouvement du genou et lui confèrent une importante stabilité. (7)

Pathoanatomie de la rupture du LCA

Robert Adams, en 1837, fût le premier à décrire un cas clinique de rupture du ligament croisé antérieur. (2) Bien que prenant place dans un contexte traumatique, notons que 70% des ruptures du LCA surviennent sans contact. (8) Le mécanisme typique implique souvent un athlète effectuant une décélération soudaine avec un changement de direction. Ce pivot cause une hyper-extension, une rotation et une flexion latérale, avec un stress en valgus au genou qui, par le fait même, met sous tension le LCA qui cède. Ces mécanismes sont souvent observés au soccer, football, basketball et en ski alpin. Les études biomécaniques ont souligné que les femmes auraient une prédisposition à avoir une faiblesse du genou en valgus, ce qui pourrait en partie expliquer une incidence de rupture du LCA près de 3 fois plus grande que les hommes. (8) (9) Des données épidémiologiques indiqueraient qu'environ 400 000 reconstructions du LCA sont performées chaque année à travers le monde. (8) (7) De plus, avoir une échancrure intercondylienne étroite, un ligament de petite taille ainsi qu'une pente tibiale postérieure élevée ont tous été identifiés comme facteurs de risque anatomiques pour une rupture du LCA, mais également pour l'échec d'une reconstruction subséquente. (10) Lors d'une rupture, la membrane synoviale couvrant les ligaments croisés couvre les extrémités libres et rétractées du LCA, expliquant ainsi le potentiel de guérison négligeable. Sans cette structure stabilisatrice importante, la blessure peut causer une instabilité et une cinématique anormale du genou. Par une histoire comportant un mécanisme de blessure attendu et un examen physique précis, les cliniciens peuvent diagnostiquer précisément une rupture du ligament croisé antérieur. La

disponibilité actuelle des examens d'imagerie en résonance magnétique permet d'objectiver la rupture ainsi que les atteintes concomitantes aux autres structures du genou.

Traitement conservateur

Un traitement conservateur par la combinaison d'une réadaptation avec une stabilisation mécanique externe lors des activités est une option raisonnable avec ces blessures. En 1983, Noyes a partagé les résultats d'une série de patients avec rupture du LCA traités de façon non-opératoire ; le tiers de patients ont été capables de continuer leurs activités habituelles, un autre tiers de patients étaient fonctionnels, mais ont dû modifier significativement leurs activités, tandis que le dernier tiers démontrait une instabilité significative persistante qui nécessiterait une chirurgie. (10) La décision commune entre le patient et le chirurgien d'opter pour un traitement conservateur est surtout influencée par le niveau d'activité, voire la demande fonctionnelle sur le genou, l'âge et l'occupation. La présence de blessures concomitantes aux autres ligaments ou aux ménisques peut aussi influencer la décision. Néanmoins, un patient sans ligament croisé antérieur est à risque d'épisodes de subluxation. Cette biomécanique altérée met le genou, en particulier les ménisques et le cartilage, en souffrance. Une incidence d'arthrose post-traumatique de 50% d'ici 15 ans est décrite dans la littérature. (11) Un énorme champ de recherche en orthopédie tente de mieux comprendre le développement d'arthrose suite à une rupture du ligament croisé antérieur. (12) Bien qu'il n'y ait pas de seuil pour un traitement chirurgical, les patients de plus de 60 ans procèdent rarement à une reconstruction. Certains experts soutiennent qu'un test « pivot shift » toujours positif trois mois suivant la blessure est le meilleur prédicteur pour une instabilité, voire la nécessité d'une chirurgie. (13)

Traitement chirurgical

Le chirurgien anglais Sir Arthur William Mayo-Robson est décrit comme étant le premier à avoir effectué une réparation du LCA en 1895. (2) Par contre, la reconstruction du LCA avec greffon autologue tel qu'on la connait aujourd'hui a initialement été décrite par Ernest William Hey Groves en 1917. (14) Les résultats défavorables des réparations primaires du ligament natif

ont écarté ces procédures depuis les années 1970. Toutefois, les avancées récentes en génie biomédical permettent le développement de techniques prometteuses de réparation primaire avec sutures combinées à un échafaudage bioactif permettant de couvrir l'espace entre les extrémités du ligament rompu. (12, 15)

Néanmoins, depuis les années 1990s, la reconstruction du LCA avec autogreffe ou allogreffe demeure le traitement chirurgical de choix pour la majorité des chirurgiens orthopédistes. Bien que les techniques de reconstruction intra-articulaire soient unanimement utilisées, des techniques de reconstruction extra-articulaire ont historiquement été décrites et sont toujours pratiquées afin de mieux contrer les forces de translation et rotationnelles. (16) Jusqu'à tout récemment, l'approche chirurgicale de la reconstruction du LCA était effectuée à l'aide d'une grande arthrotomie afin de bien visualiser l'échancrure intercondylienne. Parallèlement, l'évolution des techniques d'arthroscopie a permis de significativement modifier la chirurgie et sa réadaptation. (17, 18) Initialement, deux incisions étaient faites pour la procédure. La première pour prélever le greffon et préparer le tunnel tibial. La deuxième, pour percer le tunnel fémoral à l'aide de guide. (19) La reconstruction du LCA par arthroscopie se fait dorénavant par une ou deux incisions. (20) La technique « transtibiale » utilise la même incision puisque le tunnel tibial guide le tunnel fémoral. Avec cette technique, les dispositifs d'aide au perçage du tunnel fémoral tendent à placer celui-ci dans une position isométrique, plus haute sur le mur du condyle latéral fémoral. D'un autre côté, une deuxième incision antéro-médiale pour un positionnement indépendant du tunnel fémoral, bien que reproduisant anatomiquement la biomécanique du LCA, crée un greffon plus oblique à risque de se buter sur le ligament croisé postérieur durant la flexion du genou. (20) Somme toute, les techniques « transtibiales » sont progressivement abandonnées pour des techniques de positionnement anatomique du tunnel fémoral, offrant une stabilité rotatoire similaire au LCA sain.

Pour poursuive, le choix de greffon pour la reconstruction du LCA est habituellement entre un tissu autologue ou allogénique. Les allogreffes peuvent provenir autant du tendon achilléen, rotulien, du quadriceps, des ischio-jambiers ou même des muscles jambiers. Les

risques accrus de transmission de virus, le coût et un taux d'échec supérieur ont rendu cette option moins populaire. (21, 22) Les greffes autologues, davantage utilisées, peuvent être prélevées des ischio-jambiers, du tendon rotulien ou du tendon du quadriceps. Le chirurgien italien Riccardo Galeazzi en 1934, serait le premier à avoir utilisé les ischio-jambiers comme greffon pour sa reconstruction anatomique du LCA. (23) Le tendon patellaire (ou rotulien), avec la technique « bone-tendon-bone » a longtemps été idéalisé comme greffon par son potentiel rapide de guérison par l'interface osseux dans les tunnels. De plus, par une haute résistance à la traction et une rigidité accrue, ce greffon a des propriétés biomécaniques intéressantes. (24) Toutefois, des revues systématiques ont soulignées des douleurs significatives à la face antérieure du genou par rapport aux autres types de greffe. (25) Ainsi, l'autogreffe des tendons des muscles gracilis et semi-tendineux demeure la plus fréquente lors des reconstructions du LCA, par une douleur chronique diminuée et des propriétés biomécaniques comparables. (26)

Positionnement du tunnel fémoral

Les concepts de positionnement du tunnel fémoral en isométrie face au positionnement anatomique dans la reconstruction du LCA font objet d'un continuel débat. L'objectif d'un placement du tunnel favorisant l'isométrie est d'éviter les variations de tension durant la flexion et l'extension du genou afin de minimiser les ruptures. (7) Tel que mentionné précédemment, un tunnel fémoral favorisant l'isométrie se verra dans une position haute sur le mur médial du condyle fémoral latéral alors que l'empreinte anatomique est connue pour être plus basse. Plus encore, c'est cette position plus basse qui confère une contrainte rotatoire au ligament natif. (27, 28) Effectivement, des études ont démontrés qu'un positionnement à l'intérieur de l'empreinte anatomique réplique mieux la cinématique du genou sain : un placement antérieur du tunnel fémoral causerait une restriction du greffon en flexion tandis qu'un placement postérieur causerait, lui, une tension excessive en extension (29, 30) L'importance clinique d'un placement adéquat du tunnel fémoral a été démontrée dans la littérature : un placement non-anatomique serait à l'origine d'un haut taux de révision. (31, 32)

Plusieurs descriptions cadavériques de l'attache fémorale du ligament croisé antérieur ont permis d'identifier des repères anatomiques valides. Le « lateral intercondylar ridge » (LIR) est défini comme étant la démarcation antérieure de l'empreinte du LCA. Perpendiculairement au LIR, le « bifurcate ridge » a été identifié comme la séparation entre l'attache des faisceaux antéro-médial et postéro-latéral. (7, 33-35) En plus d'une description anatomique, certaines méthodes ont été proposées pour assurer une description quantitative et reproductible du positionnement anatomique du tunnel fémoral. Une des techniques répandues demeure l'Horloge. (29, 36) Comme la vue coronale de l'échancrure intercondylienne est semi-circulaire, il était naturel de décrire la position anatomique du tunnel ainsi ; 2 heures (genou gauche) et 10 heures (genou droit). Toutefois, des experts ont rapidement critiqué la description d'une structure tridimensionnelle à l'aide d'un référentiel bidimensionnel. Effectivement, la technique de l'horloge ne tenant pas compte de la profondeur de l'échancrure, sa précision et reproductibilité ont été mises en doute. (36) Pour poursuivre, la technique de quadrant de Bernard & Hertel demeure une référence pour décrire le positionnement anatomique du tunnel fémoral. Ce groupe a initialement soulevé que la position de l'insertion fémorale du LCA était à 24.8% en profondeur à partir du rebord postérieur du condyle latéral et à 28.5% de la hauteur du condyle par rapport à la ligne de Blumensaat. (37) Traitant de coordonnées dans un plan sagittal, son applicabilité peropératoire avec une vue en arthroscopie est limitée. Néanmoins, la standardisation de ce référentiel a mené à plusieurs études et méta-analyses précisant la position anatomique du tunnel fémoral. (35, 38-40) Ces coordonnées sont à la base des récentes avancées en chirurgie assistée par ordinateur par la navigation peropératoire (41), mais également dans le cadre d'études de chirurgie robotique active. (42, 43) La description de nouveaux repères anatomiques reproductibles, tel que le « apex of deep cartilage », pour guider le placement anatomique du tunnel fémoral est également encourageante. (44, 45) En outre, peu de descriptions tridimensionnelles reproductibles de la position anatomique du tunnel fémoral ont été proposées depuis la technique radiographique du quadrant en 1997.

L'imagerie EOS^{mc}

Histoire

Le système d'imagerie EOS^{mc} est un système d'imagerie corporelle biplanaire stéréo radiographique. Cette technologie est issue des travaux du physicien Georges Charpak dans la détection des rayons X. Celui-ci s'en est mérité le Prix Nobel de Physique en 1992. Ce type d'imagerie est donc fondé sur des capteurs radiologiques basse-dose. Avec cette faible irradiation, l'utilisation, particulièrement en pédiatrie, en devient très intéressante. Dans la dernière décennie, ses applications en imagerie tridimensionnelle musculosquelettique ont été multiples.

Principes & Utilisation

Effectivement, depuis 2007, EOS^{mc} est devenu une référence en imagerie tridimensionnelle musculosquelettique. Un avantage de ce système est que le patient demeure dans une position fonctionnelle de mise en charge. Étant également à l'échelle, les paramètres cliniques de longueur ou de volume extraits de ces images sont fiables. EOS^{mc} transforme les photons en électrons, minimisant la distorsion et l'irradiation subséquente : près de 8-10 fois moins qu'une radiographie conventionnelle et environ 1000 fois moins qu'une tomodensitométrie. (46, 47). Ce système procède à une capture simultanée et calibrée d'images orthogonales. L'utilisation de cette technologie permet des reconstructions tridimensionnelles précises du système squelettique, apportant une nouvelle approche aux pathologies orthopédiques, particulièrement en chirurgie de la colonne et dans les déformations des membres inférieurs. (47, 48)

Méthodologie, Perspectives et Hypothèses

Devant des proportions de mauvais positionnement de tunnels dans la reconstruction du LCA atteignant entre 25 et 65% (49), face à l'impact clinique qu'a un positionnement adéquat et par l'émergence de technologies d'imagerie tridimensionnelle, notre groupe a tenté de se pencher sur des questions qui seront explorées dans ce mémoire :

- Est-ce que l'imagerie EOS^{mc} est un outil fiable pour la modélisation tridimensionnelle du genou, particulièrement dans le contexte de la reconstruction du ligament croisé antérieur ?
- Y a-t-il un protocole de réalisation à suggérer pour améliorer la modélisation 3D du genou avec l'imagerie biplanaire stéréoradiographique et assurer sa généralisabilité ?
- Quelles sont les coordonnées tridimensionnelles du centre anatomique du LCA dans l'échancrure intercondylienne ?
- Est-il possible de développer un nouveau référentiel tridimensionnel pouvant guider le positionnement adéquat du tunnel fémoral à l'aide de l'imagerie stéréoradiographique biplanaire d'EOS^{mc} ?
- Établir la précision, la reproductibilité et l'applicabilité d'un tel référentiel.

Ce mémoire est rédigé en intégrant une continuité entre deux articles. Le premier chapitre, *Biplanar stereo-radiographic imaging as a new reference in tridimensional evaluation of tunnels positioning in ACL reconstruction,* vise surtout à valider les reconstructions tridimensionnelles du genou provenant de l'imagerie EOS^{mc}. Le deuxième chapitre, *Femoral tunnel placement analysis in ACL reconstruction using a novel tridimensional referential with biplanar stereo-radiographic (EOS^{tm}) imaging,* de son côté, explore une nouvelle méthode pour décrire les coordonnées tridimensionnelles du tunnel fémoral à l'aide de l'imagerie EOS^{mc}.

Nous croyons d'abord que l'imagerie EOS^{mc} permettra une description tridimensionnelle précise de la morphologie osseuse du genou. Nous souhaitons proposer ces reconstructions radiographiques biplanaires comme outil dans l'évaluation des reconstructions du ligament croisé antérieur. Dans un optique de généralisabilité, nous partagerons un protocole de réalisation de reconstruction tridimensionnelle du membre inférieur avec l'imagerie EOS^{mc}. Nous croyons que les modèles 3D seront obtenus rapidement et avec une bonne reproductibilité inter-observateur. Nous prévoyons que l'utilisation des incidences obliques rendra les reconstructions plus précises qu'avec les projections AP-LAT par une identification facilitée des repères anatomiques, incluant les tunnels fémoraux. En fait, nous croyons que l'analyse surfacique des modèles 3D venant d'EOS^{mc} démontrera un écart de moins de 2 mm avec les modèles venant de tomodensitométrie. Cette validation des reconstructions permettra de développer un nouveau référentiel dans l'échancrure intercondylienne décrivant le positionnement tridimensionnel du tunnel fémoral.

Dans un deuxième temps, nous croyons qu'un référentiel cylindrique, combinant la technique de l'Horloge ainsi que la grille de Bernard & Hertel est un moyen efficace de décrire objectivement l'emplacement de l'ouverture intra-articulaire du tunnel fémoral. Notre groupe souhaite valider un tel référentiel, évaluer sa reproductibilité et son applicabilité. Avec ce référentiel, nous évaluerons la position réelle du tunnel fémoral de patients ayant procédés à une reconstruction du ligament croisé antérieur. Somme toute, nous croyons que cette méthode ouvrira la porte à une multitude d'applications préopératoires, d'outils peropératoires ainsi que de méthodes d'évaluation post-opératoires.

Références introduction

1. Marshall JL, Wang JB, Furman W, Girgis FG, Warren R. The anterior drawer sign: what is it? The Journal of sports medicine. 1975;3(4):152-8.

2. Schindler OS. Surgery for anterior cruciate ligament deficiency: a historical perspective. Knee Surg Sports Traumatol Arthrosc. 2012;20(1):5-47.

3. Fu FH, Schulte KR. Anterior cruciate ligament surgery 1996. State of the art? Clinical orthopaedics and related research. 1996(325):19-24.

4. Markolf KL, Mensch JS, Amstutz HC. Stiffness and laxity of the knee--the contributions of the supporting structures. A quantitative in vitro study. J Bone Joint Surg Am. 1976;58(5):583-94.

5. Arnoczky SP. Anatomy of the anterior cruciate ligament. Clinical orthopaedics and related research. 1983(172):19-25.

6. Larson RL, Tailon M. Anterior Cruciate Ligament Insufficiency: Principles of Treatment. The Journal of the American Academy of Orthopaedic Surgeons. 1994;2(1):26-35.

7. Rayan F, Nanjayan SK, Quah C, Ramoutar D, Konan S, Haddad FS. Review of evolution of tunnel position in anterior cruciate ligament reconstruction. World J Orthop. 2015;6(2):252-62.

8. Boden BP, Dean GS, Feagin JA, Jr., Garrett WE, Jr. Mechanisms of anterior cruciate ligament injury. Orthopedics. 2000;23(6):573-8.

9. Prodromos CC, Han Y, Rogowski J, Joyce B, Shi K. A meta-analysis of the incidence of anterior cruciate ligament tears as a function of gender, sport, and a knee injury-reduction regimen. Arthroscopy. 2007;23(12):1320-5.e6.

10. Schillhammer CK, Reid JB, 3rd, Rister J, Jani SS, Marvil SC, Chen AW, et al. Arthroscopy Up to Date: Anterior Cruciate Ligament Anatomy. Arthroscopy. 2016;32(1):209-12.

11. Ajuied A, Wong F, Smith C, Norris M, Earnshaw P, Back D, et al. Anterior cruciate ligament injury and radiologic progression of knee osteoarthritis: a systematic review and meta-analysis. Am J Sports Med. 2014;42(9):2242-52.

12. Nau T, Teuschl A. Regeneration of the anterior cruciate ligament: Current strategies in tissue engineering. World J Orthop. 2015;6(1):127-36.

13. Kostogiannis I, Ageberg E, Neuman P, Dahlberg LE, Friden T, Roos H. Clinically assessed knee joint laxity as a predictor for reconstruction after an anterior cruciate

ligament injury: a prospective study of 100 patients treated with activity modification and rehabilitation. Am J Sports Med. 2008;36(8):1528-33.

14. Ratliff AH. Ernest William Hey Groves and his contributions to orthopaedic surgery. Bristol medico-chirurgical journal (1963). 1983;98(367):98-103.

15. Murray MM, Flutie BM, Kalish LA, Ecklund K, Fleming BC, Proffen BL, et al. The BridgeEnhanced Anterior Cruciate Ligament Repair (BEAR) Procedure: An Early Feasibility Cohort Study. Orthopaedic journal of sports medicine. 2016;4(11):2325967116672176.

16. Marcacci M, Zaffagnini S, Iacono F, Neri MP, Loreti I, Petitto A. Arthroscopic intra- and extra-articular anterior cruciate ligament reconstruction with gracilis and semitendinosus tendons. Knee Surg Sports Traumatol Arthrosc. 1998;6(2):68-75.

17. Kieser CW, Jackson RW. Eugen Bircher (1882-1956) the first knee surgeon to use diagnostic arthroscopy. Arthroscopy. 2003;19(7):771-6.

18. Paessler HH, Deneke J, Dahners LE. Augmented repair and early mobilization of acute anterior cruciate ligament injuries. Am J Sports Med. 1992;20(6):667-74.

19. Harner CD, Marks PH, Fu FH, Irrgang JJ, Silby MB, Mengato R. Anterior cruciate ligament reconstruction: endoscopic versus two-incision technique. Arthroscopy. 1994;10(5):502-12.

20. Garofalo R, Moretti B, Kombot C, Moretti L, Mouhsine E. Femoral tunnel placement in anterior cruciate ligament reconstruction: rationale of the two incision technique. Journal of orthopaedic surgery and research. 2007;2:10.

21. Brown MJ, Carter T. ACL Allograft: Advantages and When to Use. Sports medicine and arthroscopy review. 2018;26(2):75-8.

22. Grassi A, Nitri M, Moulton SG, Marcheggiani Muccioli GM, Bondi A, Romagnoli M, et al. Does the type of graft affect the outcome of revision anterior cruciate ligament reconstruction? a meta-analysis of 32 studies. The bone & joint journal. 2017;99-b(6):714-23.

23. Ferretti AMD. A Historical Note on Anterior Cruciate Ligament Reconstruction. Journal of Bone & Joint Surgery - American Volume. 2003;85(5):970-1.

24. Foster TE, Wolfe BL, Ryan S, Silvestri L, Kaye EK. Does the graft source really matter in the outcome of patients undergoing anterior cruciate ligament reconstruction? An evaluation of autograft versus allograft reconstruction results: a systematic review. Am J Sports Med. 2010;38(1):189-99.

25. Mohtadi N, Chan D, Barber R, Oddone Paolucci E. A Randomized Clinical Trial Comparing Patellar Tendon, Hamstring Tendon, and Double-Bundle ACL Reconstructions: Patient-Reported and Clinical Outcomes at a Minimal 2-Year Follow-up. Clinical journal of sport medicine : official journal of the Canadian Academy of Sport Medicine. 2015;25(4):32131.

26. Samuelsen BT, Webster KE, Johnson NR, Hewett TE, Krych AJ. Hamstring Autograft versus Patellar Tendon Autograft for ACL Reconstruction: Is There a Difference in Graft Failure Rate? A Meta-analysis of 47,613 Patients. Clinical orthopaedics and related research. 2017;475(10):2459-68.

27. Fu FH, Bennett CH, Lattermann C, Ma CB. Current trends in anterior cruciate ligament reconstruction. Part 1: Biology and biomechanics of reconstruction. Am J Sports Med. 1999;27(6):821-30.

28. Jepsen CF, Lundberg-Jensen AK, Faunoe P. Does the position of the femoral tunnel affect the laxity or clinical outcome of the anterior cruciate ligament-reconstructed knee? A clinical, prospective, randomized, double-blind study. Arthroscopy. 2007;23(12):1326-33.

29. Musahl V, Plakseychuk A, VanScyoc A, Sasaki T, Debski RE, McMahon PJ, et al. Varying femoral tunnels between the anatomical footprint and isometric positions: effect on kinematics of the anterior cruciate ligament-reconstructed knee. Am J Sports Med. 2005;33(5):712-8.

30. Dabirrahmani D, Christopher Hogg M, Walker P, Biggs D, Mark Gillies R. Comparison of isometric and anatomical graft placement in synthetic ACL reconstructions: A pilot study. Computers in Biology and Medicine. 2013;43(12):2287-96.

31. Marchant BG, Noyes FR, Barber-Westin SD, Fleckenstein C. Prevalence of nonanatomical graft placement in a series of failed anterior cruciate ligament reconstructions. Am J Sports Med. 2010;38(10):1987-96.

32. Sadoghi P, Kropfl A, Jansson V, Muller PE, Pietschmann MF, Fischmeister MF. Impact of tibial and femoral tunnel position on clinical results after anterior cruciate ligament reconstruction. Arthroscopy. 2011;27(3):355-64.

33. Colombet P, Robinson J, Christel P, Franceschi JP, Djian P, Bellier G, et al. Morphology of anterior cruciate ligament attachments for anatomic reconstruction: a cadaveric dissection and radiographic study. Arthroscopy. 2006;22(9):984-92.

34. Pearle AD, McAllister D, Howell SM. Rationale for Strategic Graft Placement in Anterior Cruciate Ligament Reconstruction: I.D.E.A.L. Femoral Tunnel Position. American journal of orthopedics (Belle Mead, NJ). 2015;44(6):253-8.

35. Hwang MD, Piefer JW, Lubowitz JH. Anterior cruciate ligament tibial footprint anatomy: systematic review of the 21st century literature. Arthroscopy. 2012;28(5):728-34.

36. Han Y, Hart A, Martineau PA. Is the clock face an accurate, precise, and reliable measuring tool for anterior cruciate ligament reconstruction? Arthroscopy. 2014;30(7):84955.

37. Bernard M, Hertel P, Hornung H, Cierpinski T. Femoral insertion of the ACL. Radiographic quadrant method. The American journal of knee surgery. 1997;10(1):14-21; discussion -2.

38. Parkar AP, Adriaensen M, Vindfeld S, Solheim E. The Anatomic Centers of the Femoral and Tibial Insertions of the Anterior Cruciate Ligament: A Systematic Review of Imaging and Cadaveric Studies Reporting Normal Center Locations. American Journal of Sports Medicine. 2017;45(9):2180-8.

39. Forsythe B, Kopf S, Wong AK, Martins CA, Anderst W, Tashman S, et al. The location of femoral and tibial tunnels in anatomic double-bundle anterior cruciate ligament reconstruction analyzed by three-dimensional computed tomography models. J Bone Joint Surg Am. 2010;92(6):1418-26.

40. Lee JK, Lee S, Seong SC, Lee MC. Anatomy of the anterior cruciate ligament insertion sites: comparison of plain radiography and three-dimensional computed tomographic imaging to anatomic dissection. Knee Surgery Sports Traumatology Arthroscopy. 2015;23(8):2297-305.

41. Luites JW, Wymenga AB, Blankevoort L, Eygendaal D, Verdonschot N. Accuracy of a computer-assisted planning and placement system for anatomical femoral tunnel positioning in anterior cruciate ligament reconstruction. The international journal of medical robotics + computer assisted surgery : MRCAS. 2014;10(4):438-46.

42. Petermann J, Kober R, Heinze R, Frölich JJ, Heeckt PF, Gotzen L. Computer-assisted planning and robot-assisted surgery in anterior cruciate ligament reconstruction. Operative Techniques in Orthopaedics. 2000;10(1):50-5.

43. Burkart A, Debski RE, McMahon PJ, Rudy T, Fu FH, Musahl V, et al. Precision of ACL tunnel placement using traditional and robotic techniques. Comput Aided Surg. 2001;6(5):270-8.

44. Hart A, Sivakumaran T, Burman M, Powell T, Martineau PA. A Prospective Evaluation of Femoral Tunnel Placement for Anatomic Anterior Cruciate Ligament Reconstruction Using 3-Dimensional Magnetic Resonance Imaging. Am J Sports Med. 2018;46(1):192-9.

45. Hart A, Han Y, Martineau PA. The Apex of the Deep Cartilage: A Landmark and New Technique to Help Identify Femoral Tunnel Placement in Anterior Cruciate Ligament Reconstruction. Arthroscopy. 2015;31(9):1777-83.

46. Deschenes S, Charron G, Beaudoin G, Labelle H, Dubois J, Miron MC, et al. Diagnostic imaging of spinal deformities: reducing patients radiation dose with a new slot-scanning Xray imager. Spine. 2010;35(9):989-94.

47. Ilharreborde B, Dubousset J, Le Huec JC. Use of EOS imaging for the assessment of scoliosis deformities: application to postoperative 3D quantitative analysis of the trunk. European spine journal : official publication of the European Spine Society, the European Spinal Deformity Society, and the European Section of the Cervical Spine Research Society. 2014;23 Suppl 4:S397-405.

48. Illes T, Somoskeoy S. The EOS imaging system and its uses in daily orthopaedic practice. Int Orthop. 2012;36(7):1325-31.

49. Behrend H, Stutz G, Kessler MA, Rukavina A, Giesinger K, Kuster MS. Tunnel placement in anterior cruciate ligament (ACL) reconstruction: quality control in a teaching hospital. Knee Surg Sports Traumatol Arthrosc. 2006;14(11):1159-65.

Chapitre 1: Biplanar stereo-radiographic imaging as a new reference in tridimensional evaluation of tunnels positioning in ACL reconstruction

Soumis et en révision ;

Journal of Orthopaedic Research

Journal of Orthopaedic Research

Biplanar stereo-radiographic imaging as a new reference in tridimensional evaluation of tunnels positioning in ACL reconstruction

Journal:	*Journal of Orthopaedic Research*
Manuscript ID	Draft
Wiley - Manuscript type:	Research Article (Member)
Date Submitted by the Author:	n/a
Complete List of Authors:	Montreuil, Julien; CRCHUM, LIO Thibeault, Félix; University of Montreal Lavoie, Frédéric; CHUM, Orthopaedics Cresson, Thierry; CRCHUM, LIO deGuise, Jacques; CRCHUM, LIO
Keywords:	ACL, Modeling, Knee, Biomechanics
Areas of Expertise:	Tridimensional modeling, Stereoradiographic imaging

Article

Biplanar stereo-radiographic imaging as a new reference in tridimensional evaluation of tunnels positioning in ACL reconstruction

MONTREUIL, Julien[1,2] ; LAVOIE, Frédéric[3] ; THIBEAULT, Felix[4] ; CRESSON, Thierry[1] ; DE GUISE, Jacques A.[1]

Affiliations

1. Laboratoire de recherche en Imagerie et Orthopédie de l'ETS (LIO)
2. McGill Division of Orthopaedic Surgery, Montreal General Hospital (MGH)
3. Service de chirurgie orthopédique, Centre Hospitalier de l'Université de Montréal (CHUM)
4. Faculté de Médecine, Université de Montréal

Abstract word count: 245

Text Word count: 3496

Contributions statement

JM designed and conceptualized the study, performed segmentations, reconstructions, analysis, interpretation of results and drafted the manuscript. *FL* designed and conceptualized the study, performed analysis, interpretation of results and revised the manuscript. Also obtained research ethics committee approval for data collection. *FT* performed segmentations, reconstructions and assisted in drafting the manuscript. *TC* & *JdG* supervised all computerization tasks, including providing personalized software for modeling and analysis.

All authors have read and approved the final submitted manuscript.

Manuscript presented at the ORS 2019 annual meeting in Austin, Texas

Address for Correspondence:

Julien Montreuil MD

Laboratoire de recherche en Imagerie et Orthopédie de l'ETS (LIO) du Centre de Recherche du Centre Hospitalier de l'Université de Montréal (CRCHUM)

900 St Denis St, Montreal, QC, H2X 0A9

Abstract

The objective is to evaluate precisely and reproducibly tridimensional positioning of bone tunnels in anterior cruciate ligament (ACL) reconstructions. To propose biplanar stereoradiographic imaging as a new reference in tridimensional evaluation of ACL reconstruction (ACLR). Two evaluators reconstructed pre- and post-operative knees, using two different stereoradiographic projections, for a total of 144 knee 3D models from EOS^{tm}. A surface analysis by distance mapping allowed us to evaluate the differences or errors between the homologous points of the EOS^{tm} and CT-Scan reconstructions. At the femur, we obtained a mean (95% confidence level) error of 1.5 mm (1.3-1.6) for the surface analysis between the EOS^{tm} models compared to the CT reconstructions when using AP-Lat projections, compared to 1.0 mm (1.0 – 1.1) with oblique projections. At the proximal tibia, they differed by 1.2 mm (1.0-1.4) in AP-Lat, and 1.1 mm (1.1-1.3) in oblique. For the femoral tunnel placement analysis, the total radius difference between the two imaging modalities was 0.8 mm (0.4-1.2) in AP-Lat and 0.6 mm (0.0-1.2) in oblique views. The femoral apertures positioning on EOS^{tm} models were within 4.3 mm (3.0-5.7) of those on CT-Scan reconstructions; which were 4.6 mm (3.5-5.6) with the oblique views. Furthermore, a difference of 9.3^{o} (7.2-11.4) in tunnel orientation was obtained with AP-Lat projections; compared to the 8.3^{o} (6.6-10.0) with oblique views. According to the intra and inter-reproducibility analysis of our knee 3D models, EOS^{tm} biplanar X-Ray images proved to be fast, efficient and precise in the design of ACLR 3D models with respect to CT-Scan.

Key words:

- Knee, ACL, Tridimensional modeling, Stereoradiographic imaging, Biomechanics of ligament, Imaging and radiology

Introduction

The anterior cruciate ligament (ACL) is an important stabilizer and surely one of the most injured ligament of the knee (1). Worldwide, around 400 000 ACL reconstructions (ACLR) are performed in a year (2). Nonanatomical tunnel positioning is often implicated in failed ACLR (3). Common errors can lead to a vertical graft, causing instability and impingement in the intercondylar notch. Furthermore, anterior placement of femoral tunnel could lead to restriction and tightness of the graft in knee flexion (2, 4). An anatomical placement of the femoral tunnel better resists the rotational force and may reduce the risk of subsequent osteoarthritis (5, 6). Location of the ACL anatomic footprint correlating to the Bernard and Hertel grid has been widely studied by radiologic and cadaveric studies (7). Several methods have been proposed to reach an accurate femoral tunnel placement. Surgical femoral guides do not appear to be precise and are associated with high variability of tunnel positioning (8). Because the femoral notch is essentially semi-circular, the clock-face technique was proposed to describe femoral tunnel positioning (9). However, using a two-dimensional representation of a tridimensional structure has raised concerns. Even without taking the depth and anteroposterior position of the clock-face into account, the inter-rater reliability of the clock-face grading system was found to be poor (10). Despite the historical two-dimensional characterization of ACL tunnels, it remains difficult to define ACL tunnel placement using 2D methods (11). Recent methods to improve femoral tunnel 3D positioning involve Computed-Assisted Surgery (CAS). Passive computer-assisted navigation and active robotic-assisted surgery systems could achieve a more accurate tunnel placement than conventional techniques (12). A better biomechanical and tridimensional understanding of tunnel placement is therefore essential.

Since 2007, EOS^{tm} imaging has become a reference in musculoskeletal imaging. This biplanar X-Ray machine, based on a Nobel prize-winning invention, can capture the whole body in an upright, physiological load-bearing position with minimized radiation doses and a true 1:1 scale for size and volume. *(Figure 1. Biplanar acquisition of stereoradiographic images using EOS^{tm})* EOS^{tm} transforms the original photons into electrons, minimising image distortion and significantly decreasing radiation exposure; it is associated with an 8 to 10 times decrease in radiation exposure when compared to conventional x-rays and an 800 to 1000 times decrease when compared to a CT-scan (13, 14). Use of this new technology allows precise tridimensional reconstruction of the skeletal system, thus a novel approach to orthopedic pathologies (15). EOS^{tm} is therefore routinely used in spine and lower limb surgery, especially in the pediatric population (14). Many research groups at the *Laboratoire de Recherche en Imagerie et Orthopédie* (LIO de l'ETS, CRCHUM) are focused on improving the reconstruction techniques (16).

Our objective is to evaluate precisely and reproducibly tridimensional positioning of bone tunnels in ACLR. Comparing knee 3D models issued from EOS^{tm} low-irradiation biplanar X-Rays with those issued from computed tomography high definition images will allow a bone morphological description of a previously unseen precision. We want to propose biplanar stereoradiographic imaging as a new reference in tridimensional evaluation of ACLR. Aiming for future clinical and research uses in ACLR, our team would also like to establish a standardized protocol from the acquisition of biplanar images to exporting the 3D model. We hypothesize that stereoradiographic biplanar imaging (EOS^{tm}) will allow us to obtain tridimensional models of the

knee quickly, precisely, in a reproducible fashion, while also exposing the patient to lower radiation compared to CT-Scan. We also believe the oblique orthogonal radiologic projections will allow a better identification of the various components of the knee, including the tunnels. More precisely, based on previous validation study, we expect our 3D surface analysis to be within 2 mm of CT-Scan (16). We expect that the radius of tunnels using EOS^{tm} models will also stay within 2 mm of those from CT-Scan reconstruction and that tunnel position would be within 5 mm (21,22). With 3D models picturing ACLR, we plan on designing a novel frame of reference in guiding the tunnels positioning. This paper presents our tridimensional modeling techniques and the evaluation results.

Methodology

Study subjects

Ten subjects were selected from a cohort, *Prospective collection of clinical and radiological data in knee patients,* taking place at the Centre Hospitalier de l'Université de Montréal (CHUM), in Montreal, QC, Canada, while conforming to the requirements of their ethics committee. Sample size for this study was calculated with an alpha of 5%, a beta of 10%, considering that 2 mm would be a statistically significant difference between imaging modalities when performing a surface analysis. We were expecting standard deviation of 0.3 mm and we used these values for the sample size and power analysis, giving 8 knees per group. Being, to our knowledge, the first group using EOS^{tm} for the tridimensional analysis of tunnel positioning, we aimed for an estimated standard deviation of 2 mm for the apertures' positioning and 5 mm as a significant non-equivalence difference. For this study, radiological data of six men and four

women (seven left knee operations, three right knee) with an age of 33.8 +/- 5.7 years were recovered. The patients were all operated by the same surgeon, with a homogeneous technique: Hamstring graft, single-bundle, constant graft sizing method, anteromedial portal drilling, *"In & Out"* technique and endobutton femoral fixation. The preoperative research protocol included EOS^{tm} (EOS Imaging, Paris, France) bi-planar images acquisition of the lower limbs with AP-Lateral and oblique (45^{o}-45^{o}) views. Six months after the surgery, they underwent an injected contrast enhanced CT-Scan (arthroscan) of both their operated and healthy knee. *(Figure 2. Flow chart)* At that time, they also recorded a second set of bi-planar orthogonal X-Ray images using the same parameters as preoperatively. Unfortunately, one patient's postoperative EOS^{tm} images were unrecoverable.

CT-Scan segmentation

In the first part of this study, the "bronze-standard" 3D models issued from the CT-Scan were established in order to compare each respective EOS^{tm} model. Using the Slice-O-Matic (Tomovision, Magog, Québec) software, a first evaluator, an orthopedic surgery resident, blinded, performed an axial segmentation of nineteen knees. *(Figure 3. CT-Scan segmentation and reconstruction)* Indeed, one out of ten patients did not undergo an arthroscan of his healthy knee. The femur, tibia and their tunnels were precisely identified and distinguished on the CT-Scan images. With this injected CT-Scan, the graft or the native ACL were visualized and segmented for further analysis. This slice by slice segmentation is a long and tedious process. Once all the bony structures were segmented, 3D reconstruction was performed in MatLab (Version 9.5 / Mathworks, MA, USA).

3D Models from EOS imaging

The pairs of orthogonal X-ray images were processed using IdefX software (LIO, Montreal, Quebec, Canada) to reconstruct the 3D models of the femur and tibia personalized to each subject. This was performed starting with a generic 3D model of each segment. Each generic 3D model was then deformed and reconstructed via an as-rigid-as-possible approach. This was based on the moving least squares optimization method until its projected contours on two radiographic planes matched the boundaries of the bones on orthogonal X-rays (16, 17) *(Figure 4. EOS 3D models reconstruction)*. Afterward, identification of the femoral and tibial tunnels on the post-operative acquisitions was performed. To accurately represent theses tunnels, an adjustable truncated cone was designed, added in the IdefX software and fitted independently by our trained evaluators. Another set of EOS^{tm} 3D models was performed by a second evaluator to verify the inter-reproducibility of the entire process *(Figure 5. EOS inter-reproducibility evaluation).* Both evaluators were blinded with respect to any informations on the subjects. Adding both orthogonal projections (AP-Lateral and oblique) of the subjects' pre-operative and post-operative images, each evaluator reconstructed a total of seventy-six knees using EOS^{tm} imaging techniques.

Iconic refitting of 3D Models from both imaging system

The 3D CT-Scan meshes were used as the basis for the validation. As such, an intensity based rigid registration of the 3D CT-Scan to both biplanar X-ray images (EOS^{tm}) was completed. By using mutual information, bony structures issued from CT-Scan were superposed on both EOS^{tm} images. This process was carried on the 144 3D models issued from EOS^{tm} biplanar X-Rays

with their corresponding CT-Scan model. Structures issued from CT-Scan and EOS^{tm} were then in the same reference, which allowed to measure distances between both segmentations *(Figure 6. EOS^{tm} vs CT models comparison).*

3D reconstructions surface evaluation

Bony surfaces issued from EOS^{tm} and CT-Scan models were initially compared. A surface analysis by distance mapping allowed us to establish the differences or errors between the homologous points of the EOS^{tm} and CT-scan reconstructions. No major deformation of the bony structures was observed. Confidence intervals around mean absolute differences were calculated with Student T-test and no outliers were excluded from the analysis. For the inter-reproducibility evaluation, the same surface analysis was applied between the two evaluators' respective models. Absolute errors were measured for the femur and the tibia, but also expressed according to the radiographic projections used for the EOS^{tm} reconstruction (AP-LAT versus Oblique).

Tunnels evaluation parameters

A distinct analysis was performed on the bone tunnels. Different basic parameters were targeted to assess the validity of the EOS^{tm} tunnels representation compared to those obtained from CT-Scan. Euclidean distances between the corresponding tunnels' apertures centers were measured for the femur and tibia (Position Δ). The radius of apertures was also compared between the two imaging modalities (Radius Δ). Furthermore, the distance between the femoral and tibial intra-articular apertures on EOS^{tm} models, which represented a simulated length of the graft, was compared with the actual graft length measured on CT-Scan models. *(Figure 7. EOS vs*

CT models superposition with tunnels parameters) With respect to the bony surfaces analysis, an inter-reproducibility evaluation of these tunnels parameters was performed, respecting the radiographic projections used for the EOS^{tm} reconstruction (AP-LAT vs Oblique).

Statistical analysis

Statistical analysis was accomplished using PRISM software (Version 8 / GraphPad, California, USA). Testing for equivalence between imaging modality was accomplished via a one-sided 95% confidence intervals approach; as mentioned previously, the zone of scientific indifference was determined to be 2 mm for the surface analysis, 5 mm for tunnel position and 2 mm for tunnel radii. Student T-tests were also used to compare results between the different radiographic projections (AP-LAT versus Obliques) to find the one rendering a better precision.

Evaluation of reconstruction time

The time required for a complete 3D reconstruction in IdefX (LIO, Montreal, Quebec, Canada), beginning from the opening the biplanar stereoradiographic images until viewing the knee 3D model with tunnels, was measured. The total reconstruction time of both evaluators was studied for 10 subjects and noted according to the radiographic projections used; AP-lateral versus oblique-oblique. Reconstruction time of EOS^{tm} models was compared to the segmentation time of models issued from CT-Scan using Student T-Test as well.

Results

Table 1. Surface analysis

10 subjects had their knees reconstructed using EOS^{tm} and CT-Scan. A surface analysis calculated that the two imaging modalities, when reconstructing the distal femur, differed by a mean (95% confidence level) of 1.5 mm (1.3-1.6) in AP-LAT, and 1.0 mm (1.0-1.1) in oblique projections. Overall, the minimum and maximum differences for the distal femur reconstructions were 0.01 mm and 11.9 mm, respectively. When performed for the proximal tibia, they differed in average by 1.2 mm (1.0-1.4) in AP-LAT, and 1.1 mm (1.1-1.3) in oblique. For the proximal tibia, we obtained 0.01 mm and 11.2 mm as minimum and maximum differences. All these results respected the 2 mm zone of equivalence. For the projection comparison, the femur models issued from oblique projections showed statistically significant precision ($p<0.001$) and inter-observer reproducibility ($p=0.02$) improvements when compared to the models issued from AP-LAT projections.

Table 2. Tunnel analysis

- referring to *Figure 7. EOS vs CT models superposition with tunnels parameters*

For the femoral tunnel placement analysis between EOS^{tm} and CT-Scan, AP-Lat incidence measured a mean radius difference of 0.8 mm (0.4-1.2), a mean aperture positioning difference of 4.3 mm (3.0-5.7), with an average tunnel orientation difference of 9.3° (7.2-11.4). The simulated graft length differed by 5.5 mm (3.9-7.1) with AP-Lat views. With EOS^{tm} oblique projections, the same parameters were 0.6 mm (0.0-1.2), 4.6 mm (3.5-5.6), and 8.3° (6.6-10.0), respectively, while the simulated graft length differed by 5.3 mm (3.5-7.2). For the tibial tunnel placement analysis, the AP-Lat incidence measured a mean radius difference of 2.3 mm (1.8-2.9),

a mean aperture positioning difference of 7.2 mm (5.4-9.0), giving an average tunnel orientation difference of 12.0° (8.1-15.9). Again, in the oblique views, the equivalent parameters were 1.9 mm (1.4-2.4), 6.5 mm (4.9-8.2), and, 8.9° (6.7-11.1), respectively. Only the radius measurements respected its 2 mm zone of equivalence in both projections. The tunnel position analysis was exceeding the 5 mm threshold using both projections. However, PF1 (femoral tunnel) placement reproducibility with EOS^{tm} models between both observers was significantly better with the oblique projections (p=0.005).

Table 3. Reconstruction time evaluation

Evaluator #1 completed a single AP-LAT EOS^{tm} reconstruction in an average of 6.9 minutes (5.7-8.0) and took 7.0 minutes (6.1-8.0) to reconstruct a model from oblique images. Evaluator #2 completed the same task in 6.4 (5.6-7.1) and 6.8 minutes (5.5-8.1), respectively. On the other hand, a CT-scan segmentation lasted an average of 216.3 minutes (205.9-226.7), this result being significantly longer than the EOS^{tm} reconstruction time (p<0.0001).

Discussion

This study successfully evaluated the validity and reliability of EOS^{tm} low-irradiation biplanar X-Rays in reconstructing 3D models of knees and positioning tunnels drilled for ACLR. We hypothesized that this novel technique would be effective in doing so with a precision approaching that of “bronze-standard” CT-Scan, in a fast and cost-effective manner, while using a low dose radiation technique.

The preoperative and postoperative 3D knee reconstructions’ bony contours with EOS^{TM} were comparable to those obtained with CT-scan. The mean absolute differences calculated with

the surface analysis were well under the pre-established 2 mm threshold, at the level of the femur and the tibia. The results obtained were statistically significant. The overall precision achieved in the reconstructions can be explained by the fact that most of the anatomic landmarks necessary for modeling were well defined and easy to outline bony structures. The markers were therefore placed on the software with a higher degree of confidence. Although both incidences were precise, the femoral 45° views rendered a significantly smaller mean difference, compared to the AP-LAT. This variation can most probably be explained by the absence of superposition of the femoral condyles that is seen on a lateral view, which complicated the identification of landmarks on the AP-Lat images. On the other hand, the AP and 45° views were both precise in recreating bony contours. In general, for the same reasons, the inter-technician reproducibility was at least two time greater at 45° for the femur and tibia, giving a statistically significant difference. Our results are consistent with the initial validation study by Cresson et *al*., where the average reconstruction error of the bones using this technique was found to be 1 mm (16).

To our knowledge, this study is the first to compare the efficiency of EOS^{TM} biplanar XRays to that of CT-scan in ACLR 3D knee reconstructions. Previous studies have attempted similar goals, but using different anatomical locations. Pasha *et al.* compared the use of EOS^{TM} to the CT scan in evaluating the measurement of morphological vertebral parameters in a pediatric population investigated for scoliosis (18). Using a similar methods and comparable materials to ours, they found no significant difference in measurements between the two imaging modalities. They concluded that EOS^{TM} was reliable for vertebral 3D reconstruction. Similarly, Berger *et al.* obtained a smaller than 2 mm difference between total spinal measurements obtained with

EOS™ and CT-scan (19). With respect to the knee, Westberry *et al.* studied the reliability of SterEOS™ (20). However, their study was performed on the entire lower limb, used different measurements, and compared two subsequent examinations with the same technique instead of CT-scan.

While the results for bony structures were satisfactory, the tunnels encountered more variability, depending on the measurement and location. Although most of our tunnel analysis results did not attain statistical significance, some of our measurements respected the pre-established threshold values. For the femoral tunnels, both apertures' radii had a difference of less than 2 mm, but were positioned more than 5 mm away from those obtained with CT-scan. Here, the AP projection has proven to be as precise as the oblique. Furthermore, our preliminary EOS™ models showed that the tunnels, which were cylindrical at the time of surgery, progressed to a truncated cone shape, six months after the operation, due to an integration, ossification and remodeling processes. This phenomenon was considered by programing our software to fit the conical shape of the tunnels. This adjustment is reflected by the small differences of radii obtained. However, this irregular shape could also contribute to discrepancies between the two imaging modalities. At the tibial level, our data was yet again closer to CT-scan in the oblique views, but with no statistical significance. At 45°, the radius difference was equal or less than 2 mm, while the position difference exceeded 5 mm by only a small margin. Position of tibial tunnel aperture (PT2) was significantly more reproducible using oblique projections. This was expected as the superposition of the tibial anatomy on the AP-Lat views made identification of the tunnel

very difficult, compared to the oblique view, in which it was clearly defined from the surrounding structures.

The inter-technician reproducibility analysis was satisfying for the tibial tunnel with an obtained consistency at 45° for all the measurements. The same cannot be said for the femoral tunnel, in which reproducibility showed no relation with incidence, but was adequate for tunnel radii and the lateral aperture of femoral tunnel. Of note, intra-articular (P1) aperture positioning reproducibility was significantly less consistent in AP-Lat, due to the lateral condyles superposition described earlier.

Our study measured tunnel orientation and simulated graft length (defined as the 3D distance between the centers of the distal femoral tunnel aperture and the proximal tibial tunnel aperture), two parameters which had not been widely used in previous research. Both these measurements showed a smaller difference and a better inter-technician reproducibility at 45°, compared to AP-Lat. The greater precision of these two measurements at 45° reflects the general superiority of this projection, since their calculation is based on previous parameters. Lack of comparison makes further interpretation of these parameters difficult, but they can stand as references for future research.

Previous literature lacks any comparable studies. To the best of our knowledge, this study is the first to evaluate EOS^{TM} for integrating ACLR tunnels in 3D reconstructions of knee. Ducouret *et al*. have previously compared MRI to CT-scan using tunnels measurements similar to ours. (21)

They obtained no significant difference between the two methods and concluded in the adequacy of MRI in assessing tunnel position in ACLR, at the expense of cost and accessibility. However, no other study focused on biplanar X-Ray reconstructions for tunnel positioning. Therefore, comparison of our data to literature is hard to achieve.

Concerning the time needed to accomplish a reconstruction, it is evident that models issued from EOS^{tm} images in the IdeFX software were a lot faster to realize. CT-Scan slice segmentation took around 3.5 hours to obtain, even once the evaluators were well trained with the software. On the other hand, both evaluators could complete an EOS^{tm} 3D reconstruction in less than 10 minutes after a proper introduction to the software and technique, demonstrating a quite rapid learning curve. There was no statistically significant difference in time between the projections used, even with the superposition of the femoral condyles on the lateral view. EOS^{tm} reconstruction time analysis of both evaluators concluded similar results being, 6.9 min (5.7-8.0) and 7.0 min (6.1-8.0) for the first evaluator and 6.4 min (5.7-7.1) and 6.8 (5.5-8.1) min for second evaluator.

Although our main objective was achieved, this study has certain limitations. The first limitation is the small sample size used for the study. Including a larger number of subjects would allow us to improve the precision in the results and possibly increase our study's power. For this preliminary project, the number of patients with a postoperative arthroscan was the limiting factor in attaining a large sample size. However, for further studies, accessibility to the EOS^{tm} cabin will allow rapid data collection. Secondly, results obtained can be difficult to compare

directly to previous research since 3D ACLR tunnel positioning analysis with EOS^{tm} are nonexistent. In the future, we hope to develop a mathematical conversion between our methods and previous approaches, using for instance, the widely-used Bernard-Hertel grid. Thirdly, since access to EOS^{tm} machine and software is currently limited in other centers, there will undoubtedly be a learning curve in 3D modeling with these biplanar X-Rays. In order to scale up this method to a clinical setting, while keeping the same precision and reproducibility, we plan on proposing a standardized realization protocol clarifying the steps from the acquisition of stereoradiographic images to the completion of the knee 3D model. Furthermore, even if this method brings significant progress in terms of reconstruction time, there are still many manual segmentation steps. Multiples groups at our research center are focusing on deep machine learning and automatized processes; it's clear that these reconstructions should be fully automatized to be fast and functional in a clinical setup. Moreover, our database consisted of patients who underwent ACL reconstruction by a single surgeon using a single technique. While this method represents a limitation to our study with regards to its external validity, it allowed us to limit confusing factors and evaluate its reliability. We hope that it will open the door for further research to evaluate its generalizability. Finally, Euclidian distances were used to calculate the difference in tunnel apertures positioning. While this method worked well to estimate the magnitude of the differences and to measure the overall precision of EOS^{tm} 3D models, it provided no information on their direction. Indeed, it would have been interesting to be able to break down the distances in vectors to possibly identify anatomic planes in which errors where more prone to occur. This is even more relevant in the lateral view or sagittal plane, to compare our analysis with the Bernard-Hertel Grid.

Conclusion & future directions

Tridimensional modeling with biplanar stereoradiographic X-Rays, a low-irradiation imaging system, showed a precision comparable to computed tomography in ACLR description, with significant reduction in the reconstruction time. Our results also suggest that EOS^{tm} oblique projections show an overall superior accuracy and reproducibility compared to AP-Lat views and should be used in the standard protocols for knee 3D reconstruction. Even if the results of this preliminary study are promising for the knee surface analysis, we strive to improve our methods for the tunnels' analysis. With EOS^{tm} as a reliable 3D platform, our group is currently working on a new intercondylar referential that would isolate parameters with significant per-operative and clinical impacts.

Acknowledgements & Affiliations:

Jacques De Guise & Thierry Cresson ;

- Research funds, royalties and patent licensed from EOS^{tm} company
- Sponsorship by CRSNG RDC, Canada research chairs, Mitacs, MEDTEQ

References

1. Gordon MD SM. Anterior cruciate ligament injuries. 3 ed. Rosemont American Academy of Orthopaedic Surgeons; 2004. 466 p.

2. Rayan F, Nanjayan SK, Quah C, Ramoutar D, Konan S, Haddad FS. Review of evolution of tunnel position in anterior cruciate ligament reconstruction. World J Orthop. 2015;6(2):252-62.

3. Marchant BG, Noyes FR, Barber-Westin SD, Fleckenstein C. Prevalence of nonanatomical graft placement in a series of failed anterior cruciate ligament reconstructions. Am J Sports Med. 2010;38(10):1987-96.

4. Stevenson WW, 3rd, Johnson DL. "Vertical grafts": a common reason for functional failure after ACL reconstruction. Orthopedics. 2007;30(3):206-9.

5. Lee MC, Seong SC, Lee S, Chang CB, Park YK, Jo H, et al. Vertical femoral tunnel placement results in rotational knee laxity after anterior cruciate ligament reconstruction. Arthroscopy. 2007;23(7):771-8.

6. Ajuied A, Wong F, Smith C, Norris M, Earnshaw P, Back D, et al. Anterior cruciate ligament injury and radiologic progression of knee osteoarthritis: a systematic review and metaanalysis. Am J Sports Med. 2014;42(9):2242-52.

7. Parkar AP, Adriaensen M, Vindfeld S, Solheim E. The Anatomic Centers of the Femoral and Tibial Insertions of the Anterior Cruciate Ligament: A Systematic Review of Imaging and Cadaveric Studies Reporting Normal Center Locations. American Journal of Sports Medicine. 2017;45(9):2180-8.

8. Ducsharm M, Banaszek D, Hesse D, Kunz M, Reifel C, Bardana D. Assessing the accuracy of femoral tunnel placement in anatomic ACL reconstruction (913.13). The FASEB Journal. 2014;28(1_supplement):913.13.

9. Miller MD. Editorial Commentary: Does Anybody Really Know What Time It Is? Does Anybody Really Care? Arthroscopy. 2017;33(2):398-9.

10. Mehta V, Petsche T, Rawal AM. Inter- and Intrarater Reliability of the Femoral Tunnel Clock-Face Grading System During Anterior Cruciate Ligament Reconstruction. Arthroscopy: The Journal of Arthroscopic & Related Surgery. 2017;33(2):394-7.

11. Ramme AJ, Wolf BR, Warme BA, Shivanna KH, Willey MC, Britton CL, et al. Surgically oriented measurements for three-dimensional characterization of tunnel placement in anterior cruciate ligament reconstruction. Comput Aided Surg. 2012;17(5):221-31.

12. Luites JW, Wymenga AB, Blankevoort L, Kooloos JM, Verdonschot N. Development of a femoral template for computer-assisted tunnel placement in anatomical double-bundle ACL reconstruction. Comput Aided Surg. 2011;16(1):11-21.

13. Deschenes S, Charron G, Beaudoin G, Labelle H, Dubois J, Miron MC, et al. Diagnostic imaging of spinal deformities: reducing patients radiation dose with a new slot-scanning X-ray imager. Spine. 2010;35(9):989-94.

14. Ilharreborde B, Dubousset J, Le Huec JC. Use of EOS imaging for the assessment of scoliosis deformities: application to postoperative 3D quantitative analysis of the trunk. European spine journal : official publication of the European Spine Society, the European Spinal Deformity Society, and the European Section of the Cervical Spine Research Society. 2014;23 Suppl 4:S397-405.

15. Illes T, Somoskeoy S. The EOS imaging system and its uses in daily orthopaedic practice. Int Orthop. 2012;36(7):1325-31.

16. Cresson T, Branchaud D, Chav R, Godbout B, Guise JAd, editors. 3D shape reconstruction of bone from two x-ray images using 2D/3D non-rigid registration based on moving leastsquares deformation. SPIE Medical Imaging; 2010: SPIE.

17. Zeighami A, Dumas R, Kanhonou M, Hagemeister N, Lavoie F, de Guise JA, et al. Tibiofemoral joint contact in healthy and osteoarthritic knees during quasi-static squat: A bi-planar X-ray analysis. Journal of biomechanics. 2017;53:178-84.

18. Pasha S, Schlosser T, Zhu X, Mellor X, Castelein R, Flynn J. Application of Low-dose Stereoradiography in In Vivo Vertebral Morphologic Measurements: Comparison With Computed Tomography. Journal of pediatric orthopedics. 2017.

19. Berger S, Hasler CC, Grant CA, Zheng G, Schumann S, Buchler P. A software program to measure the three-dimensional length of the spine from radiographic images: Validation and reliability assessment for adolescent idiopathic scoliosis. Computer methods and programs in biomedicine. 2017;138:57-64.

20. Westberry DE, Carpenter AM. 3D Modeling of Lower Extremities With Biplanar Radiographs: Reliability of Measures on Subsequent Examinations. Journal of pediatric orthopedics. 2017.

21. Ducouret E, Loriaut P, Boyer P, Perozziello A, Pesquer L, Mounayer C, et al. Tunnel positioning assessment after anterior cruciate ligament reconstruction at 12 months: Comparison between 3D CT and 3D MRI. A pilot study. Orthopaedics & Traumatology: Surgery & Research. 2017;103(6):937-42.

22. Hui C, Pi Y, Swami V, Mabee M, Jaremko JL. A Validation Study of a Novel 3-Dimensional MRI Modeling Technique to Identify the Anatomic Insertions of the Anterior Cruciate Ligament. Orthopaedic journal of sports medicine. 2016;4(12):2325967116673797.

Tables

Table 1. Surface analysis

	EOS vs CT comparison (n=19)		EOS Inter-technician reproducibility (n=36)	
Distal Femur	Mean absolute Δ (mm) (CI (a= 5%))		Mean absolute Δ (mm) (CI (a= 5%))	
AP-Lat	1,5 §	(1,3 - 1,6)	2,5	(1,6 - 3,4)
45°	1,0 §*	(1,0- 1,1)	1,2 §*	(0,8 - 1.5)
Proximal Tibia				
AP-Lat	1,2 §	(1,0 - 1,4)	3,0	(1,9 - 4,2)
45°	1,1 §	(1,1 - 1,3)	1,4 §*	(1,0 - 1,8)

§: respecting zone of equivalence (a = 95%)
*: $p<0.05$ for Student-T test between projections used (Obliques vs AP-LAT)

Table 2. Tunnel analysis

	EOS vs CT Analysis (n=9)				EOS Inter technician reproducibility (n=9)			
	AP-Lat		**45°**		**AP-Lat**		**45°**	
Femoral tunnel	Mean (CI (a= 5%))		Mean (CI (a= 5%))		Mean (CI (a= 5%))		Mean (CI (a= 5%))	
Total radius Δ (mm)	0,8 §	(0,4 -1,2)	0,6 §	(0,0 -1,2)	0,5 §	(0,3 - 0,8)	0,6 §	(0,4 – 0,9)
PF1 radius Δ (mm)	0,8 §	(0,3 -1,2)	0,6 §	(0,0 -1,2)	0,5 §	(0,3 - 0,7)	0,8 §	(0,5 - 1,0)
PF2 radius Δ (mm)	0,8 §	(0,4 -1,2)	0,6 §	(0,0 -1,2)	0,6 §	(0,2 – 0,9)	0,5 §	(0,2 - 0,8)
Total position Δ (mm)	4,3	(3,0 -5,7)	4,6	(3,5 -5,6)	5,1	(3,0 - 7,1)	3,5	(1,1 – 5,9)
PF1 position Δ (mm)	4,4	(3,0 -5,8)	4,5	(3,4 -5,6)	6,5	(3,9 - 9,1)	1,8 §*	(0,0 - 4,4)
PF2 position Δ (mm)	4,3	(3,0 -5,6)	4,6	(3,6 -5,6)	3,6 §	(2,9 - 4,3)	5,1	(2,1 - 8,1)
Δ Tunnel orientation (°)	9,3	(7,2 -11,4)	8,3	(6,6 -10,0)	7,8	(3,6 -12,0)	4,3	(1,8 -6,8)
Tibial tunnel								
Total radius Δ (mm)	2,3	(1,8 -2,9)	1,9	(1,4 - 2,4)	0,7 §	(0,4 - 0,9)	0,4 §	(0,2 - 0,7)
PT1 radius Δ (mm)	2,5	(1,9 -3,0)	2,0	(1,5 -2,6)	0,6 §	(0,4 - 0,7)	0,4 §	(0,3 - 0,6)
PT2 radius Δ (mm)	2,2	(1,7 -2,8)	1,8	(1,2 -2,3)	0,7 §	(0,4 - 1,1)	0,4 §	(0,1 - 0,7)
Total position Δ (mm)	7,2	(5,4 -9,0)	6,5	(4,9 - 8,2)	4,6	(2,7 - 6,4)	3,5	(1,6 - 5,4)
PT1 position Δ (mm)	7,3	(5,3 -9,2)	6,6	(4,9 -8,3)	5,3	(3,6 - 7,0)	4,2	(3,0 - 5,4)
PT2 position Δ (mm)	7,2	(5,4 -8,9)	6,5	(4,9 -8,0)	3,8	(1,8 - 5,9)	2,8 §	(0,8 – 4,9)
Δ Tunnel orientation (°)	12,0	(8,1 -15,9)	8,9	(6,7 -11,1)	8,0	(4,2 -11,8)	2,7*	(1,4 - 4,0)
Simulated graft length								
Δ PF1 - PT1 length (mm)	5,5	(3,9 -7,1)	5,3	(3,5 - 7,2)	3,5	(2,0 - 5,0)	3,0	(1,6 - 4,3)

§: respecting zone of equivalence (a =95%)
*: $p<0.05$ for Student-T test between projections used (Obliques vs AP-LAT)

Table 3. Time Analysis

EOS reconstruction (n=10)		Mean (min)	(CI (a= 5%))
Evaluator 1	AP-Lat	6,9	(5,7 - 8,0)
	Oblique	7,0	(6,1 - 8,0)
Evaluator 2	AP-Lat	6,4	(5,6 - 7,1)
	Oblique	6,8	(5,5 - 8,1)
CT-Scan segmentation (n=9)		216,3 *	(205,9 - 226,7)

*: $p<0.05$ for Student-T test between modality used (EOS vs CT)

Figures

Figure 1. Biplanar acquisition of stereoradiographic images using EOS[tm]

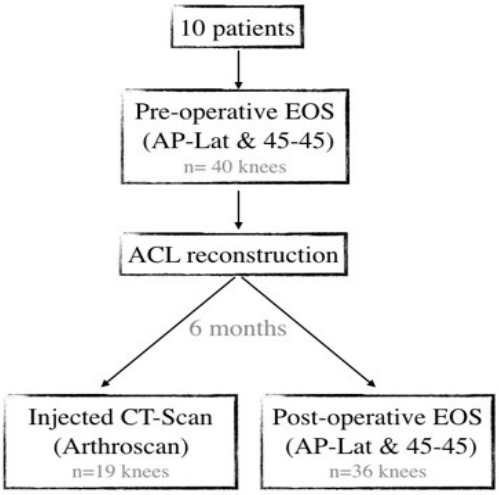

Figure 2. Flow chart

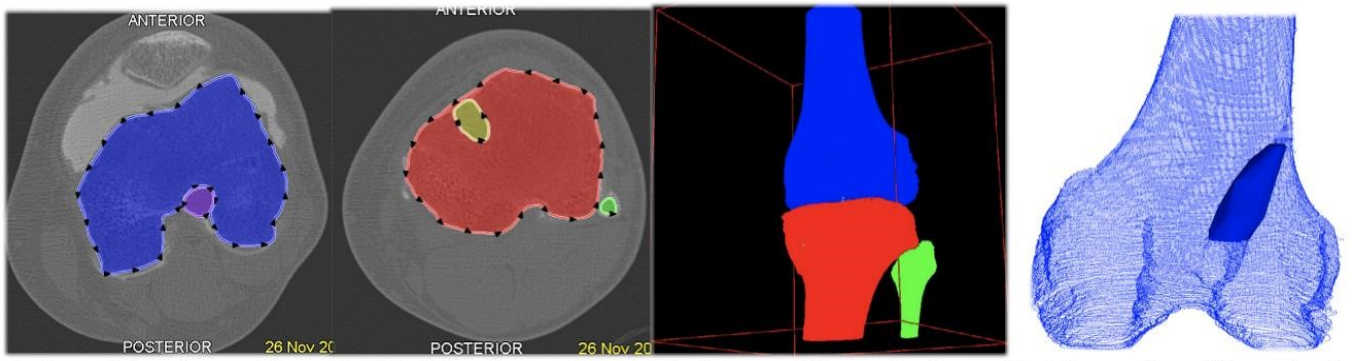

A. Femur & tunnel segmentation B. Tibia & tunnel segmentation C. Arthroscan 3D reconstruction D. Arthroscan femur 3D reconstruction

Figure 3.CT-Scan segmentation and reconstruction

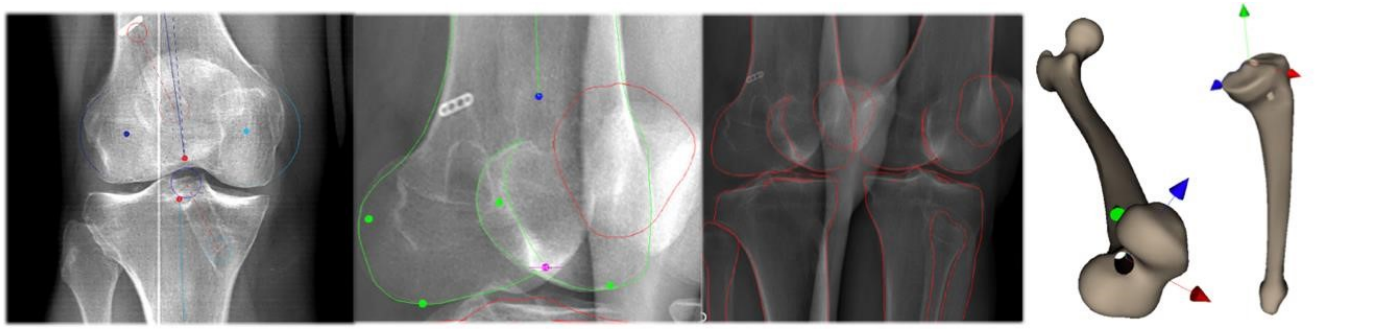

A. Anatomical landmarks identification B. Femur generic 3D model ajustment C. Femoral and tibial bony contours D. Femoral and tibial 3D models with tunnels

Figure 4. EOS 3D models reconstruction

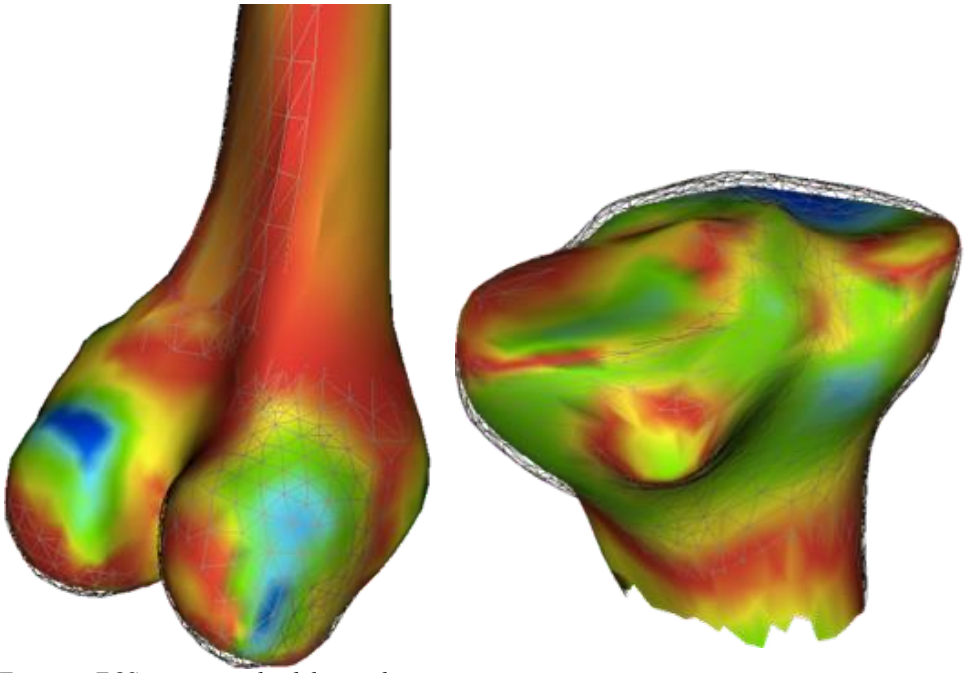

Figure 5 EOS inter reproducibility evaluation

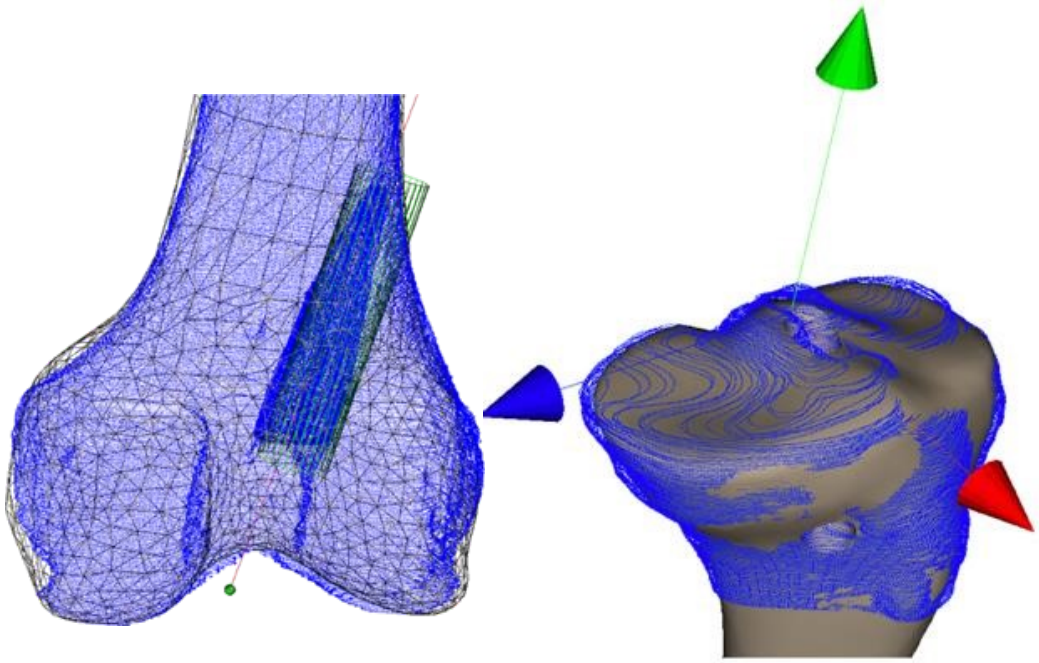

Figure 6. EOS vs CT Models comparison

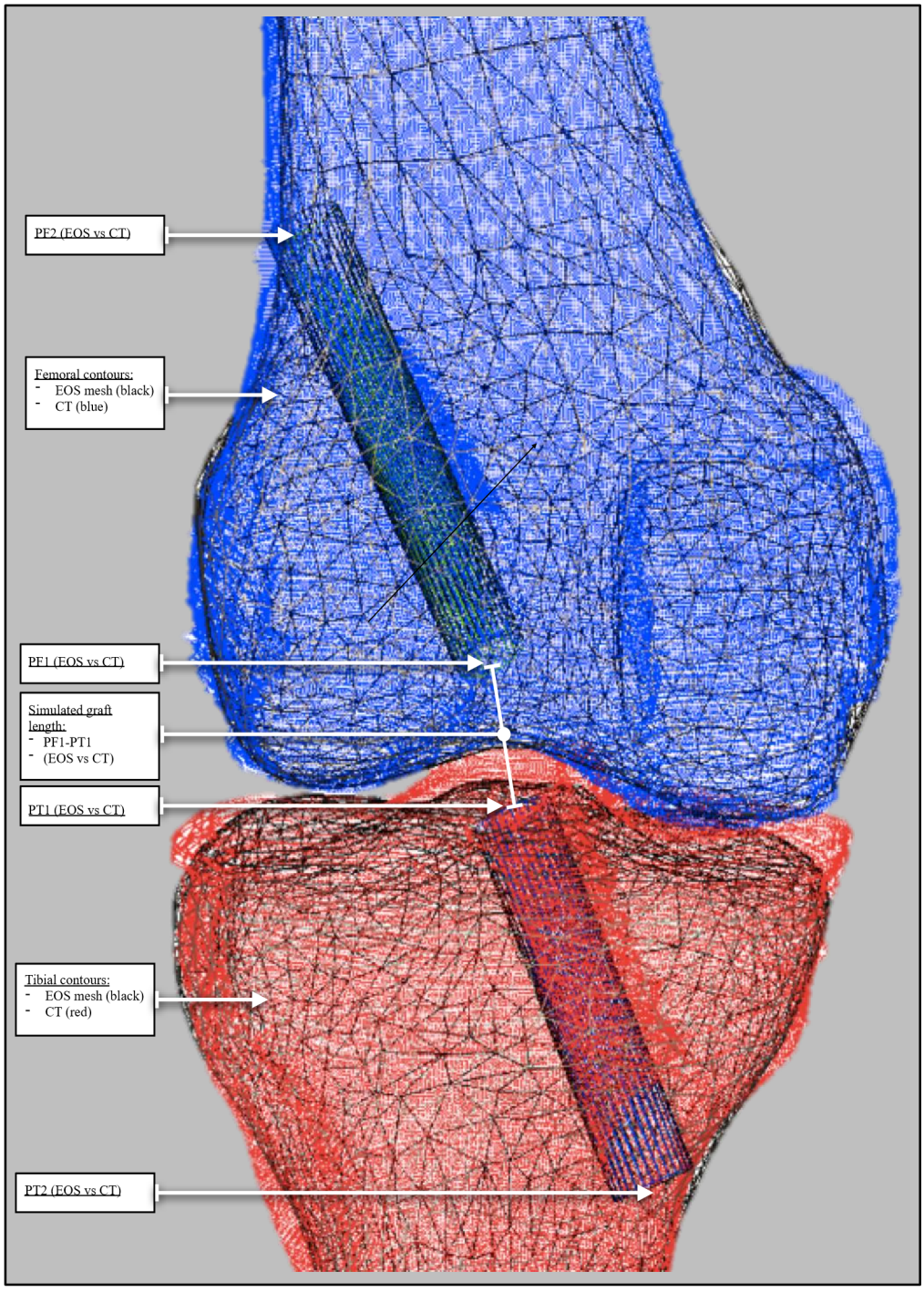

Figure 7. EOS & CT models superposition with tunnels parameters

Chapitre 2: Femoral tunnel placement analysis in ACL reconstruction using a novel tridimensional referential with biplanar stereoradiographic (EOS^{tm}) imaging

Accepté, en voie de publication ;

The Orthopaedic Journal of Sports Medicine

Article

Femoral tunnel placement analysis in ACL reconstruction using a novel tridimensional referential with biplanar stereo-radiographic (EOS^{tm}) imaging

MONTREUIL, Julien[1,2] ; LAVOIE, Frédéric[3] ; SALEH, Joseph ; CRESSON, Thierry[1] ; DE GUISE, Jacques A.[1]

Affiliations

1. Laboratoire de recherche en Imagerie et Orthopédie de l'ETS (LIO)
2. McGill Division of Orthopaedic Surgery, Montreal General Hospital (MGH)
3. Service de chirurgie orthopédique, Centre Hospitalier de l'Université de Montréal (CHUM)
4. Faculté de Médecine, Université de Sherbrooke

Abstract word count: 310

Text Word count: 5775

Contributions statement

JM designed and conceptualized the study, performed segmentations, reconstructions, analysis, interpretation of results and drafted the manuscript. *FL* designed and conceptualized the study, performed analysis, interpretation of results and revised the manuscript. Also obtained research ethics committee approval for data collection. *JS* performed segmentations, reconstructions and assisted in drafting the manuscript. *TC* & *JdG* supervised all computerization tasks, including providing personalized software for modeling and analysis. All authors have read and approved the final submitted manuscript.

Address for Correspondence:

Julien Montreuil MD

Laboratoire de recherche en Imagerie et Orthopédie de l'ETS (LIO) du Centre de Recherche du Centre Hospitalier de l'Université de Montréal (CRCHUM)

900 St Denis St, Montreal, QC , H2X 0A9

Abstract

Objectives: Non-anatomic graft placement is common and an important cause of ACL reconstruction (ACLR) failure. We aim to describe the femoral tunnel placement in ACLR, while using a new comprehensive three-dimensional cylindrical coordinate system combining both the traditional clock-face technique and the quadrant method. Our objective is to validate this technique and evaluate its reproducibility.

Methods: Thirty-seven subjects who underwent an ACLR had their knee and their tunnels 3D reconstructed using EOS^{tm} imaging. We designed an automated cylindrical referential software individualized to each subject's distal femur morphology. Cylinder parameters were collected automatically from each observer's series of reconstructions. For validation, each independent observer manually measured the corresponding parameters on a lateral view of 3D contours and on the stereoradiographic images of the corresponding subject.

Results: The average cylinder produced from the first observer reconstructions series had a 30.0^{o} (28.4-31.5) orientation, 40.4 mm (39.3-41.4) length and a diameter of 19.3 mm (18.6-20.0). For the second observer, the same metrics were 29.7^{o} (28.1-31.3), 40.7 mm (39.7-41.8) and 19.7 mm (18.8-20,6), respectively. Our method showed moderate inter-test intraclass correlation (ICC) between all three measuring techniques both for length (r=0.68) and diameter (r=0.63), but with poor correlation for orientation (r=0.44). In terms of inter-observer reproducibility of the automatized method, similar results were obtained; with excellent correlation for length (r=0.95; p<0.001) and moderate for diameter (r=0.66; p<0.001). With this referential, we described the placement of the thirty-seven subjects individual femoral

tunnel aperture, giving an average difference of less than 10 mm from the historical anatomic description of *Bernard et al.*

Conclusion:

This novel tridimensional cylindrical coordinate system, using biplanar stereoradiographic low irradiation imaging system, showed a precision comparable to standard manual measurements in ACLR femoral tunnel placement description. Our results also suggest that automatized cylinders issued from EOS^{tm} 3D models show moderate accuracy and reproducibility. This technique will open up to multiple pre-operative, per-operative and postoperative possibilities in ACLR.

Key Words:

- Knee, ACL, tridimensional modeling, Stereoradiographic imaging, biomechanics of ligament, Imaging and Radiology (General)

What is known about this subject?

- ACL reconstruction is a common procedure due to the incidence of the injury. The femoral sided anatomic footprint of the anterior cruciate ligament has been widely studied across last decades. The common mistakes in its surgical placement as well as their impact on the biomechanics of the graft have been studied. Efforts have been made to develop techniques achieving accurate placement of the tunnels. These can

be based on anatomic landmarks, visual reference system, tridimensional imaging or even computer-assisted navigation.

What this study adds to existing knowledge:

- While multiple reference systems were proposed to locate the femoral insertion, few of them, to our knowledge, have used a tridimensional coordinate system. The EOS^{tm} imaging system with its stereoradiographic acquisition, allows a rapid, easy and precise tridimensional reconstruction of bony structures. While being used in spine deformity surgery, its application on the appendicular skeleton is limited. This study is innovative in its approach to the tridimensional modeling of the knee, tailored for the anterior cruciate ligament reconstruction.

Introduction

The anterior cruciate ligament (ACL) is an important stabilizer of the knee and is frequently injured. On a worldwide basis, epidemiologic studies demonstrate that around 400 000 anterior cruciate ligament reconstructions (ACLR) are performed each year[29]. Non-anatomic graft placement is common and an important cause of ACLR failure[25]. Mispositioning ranging from 25-65% has been reported [1]. Common errors can lead to a vertical graft, instability and impingement at the intercondylar notch. Furthermore, anterior placement of femoral tunnel can lead to restriction and tightness of the graft in knee flexion. An additional anteromedial portal has been preferred over the transtibial technique for its trend toward

anatomical placement, better resisting the anterior tibial translation and rotational forces [9,17,26]. Of the many available techniques used in ACLR for femoral tunnel positioning, the clock-face technique remains commonly employed even after concerns were reported due to its interobserver reliability [10,21]. Indeed, the use of a two-dimensional reference in a three-dimensional volume limits its applicability. The Bernard and Hertel quadrant method has been widely used and standardized since its initial description [2,12,27]. The grid coordinates, in a sagittal plane, are impossible to apply directly during a knee arthroscopy without additional fluoroscopy [15,18]. Description of new anatomic landmarks guiding arthroscopic tunnel placement, like the apex of the deep cartilage (ADC), and efforts to prove its reproducibility are encouraging [11]. However, the two-dimensional quadrant coordinates are used even with the newer Computed-Assisted Surgery (CAS) techniques; either for navigation or for active robotic surgery [3,22,28]. Globally, few three-dimensional descriptions of femoral tunnel positioning were proposed since the quadrant method, in 1997.

After being introduced commercially in 2007, the EOS^{tm} X-ray machine is now being studied for a variety of orthopedic pathologies, especially in spine surgery. This technology captures biplanar X-ray images in an upright, physiologic, position with a true 1:1 scale for both size and volume. Based on the work on particle detection of nobel prize-winning physicist Georges Charpak, this imaging system emits lower doses of radiation then conventional X-rays [14]. (FIGURE 1) From these simultaneous orthogonal views, the generation of a skeletal three-dimensional model is simplified. Our group previously compared reconstructions using EOS^{tm}

and CT-Scan; models from biplanar stereoradiographic images were rapid to obtain and precise, while keeping a good inter-reproducibility. In fact, for the femur, we obtained a mean (95% confidence level) error of 1.0 mm (1.0-1.1) for the surface analysis between the EOS^{tm} models compared to the CT reconstructions when using oblique projections. With the same oblique projections, the inter-technician reproducibility study of EOS^{tm} reconstructions resulted in an absolute difference of 1.2 mm (0.8-1.5). (*Montreuil et al. Unpublished*)

In this study, we will focus on describing the femoral tunnel placement in ACLR, while using a new comprehensive three-dimensional cylindrical reference. In using this cylindrical coordinate system, we hypothesize that it will combine both the traditional clock-face technique and the quadrant method. This coordinate system will respect arthroscopic terminology using High-Low and Deep-Shallow axises.[26] Our objective is to validate this technique and evaluate its reproducibility. Based on other 3D studies, we expect that this cylindrical template will correspond to Bernard's grid within 5 mm in length in the shallow/deep axis and 2 mm in diameter for the medio-lateral and high-low axises [9,22]. Furthermore, this method will help in evaluating post-operative tunnel positioning. We plan on comparing actual femoral tunnel aperture position to a described target that is within the range of the known anatomic 5th and 95th percentiles [27]. In the deep-shallow axis, this will correspond to 24% and 37%, respectively, whereas for the high-low axis, the values correspond to 28% and 43%, respectively [27]. Overall, we believe this method will allow for pre-operative

planning, intra-operative guidance and post-operative feedback of femoral tunnel placement in ACLR. This paper presents our tridimensional modeling techniques and its evaluation results.

Methodology

Study subjects

Thirty-seven subjects were selected from a cohort participating in the, *Prospective collection of clinical and radiological data in knee patients,* taking place at the *Centre Hospitalier de l'Université de Montréal* (CHUM), in Montreal, QC, Canada. This was previously approved by the local ethics committee. Sample size for this study was calculated with an alpha of 5% and a beta of 10%. Radiological data of twenty-five men and twelve women (twenty-one right knees and sixteen left knees operation) with an age of 31,8 +/- 3,0 years were collected. The patients were all operated from 2008 to 2011 by the same surgeon, with a homogeneous technique: Hamstring graft, single-bundle, constant graft sizing method, anteromedial femoral portal drilling, *"In & Out"* technique and endobutton femoral fixation. The research protocol included pre-operative EOS^{tm} (EOS Imaging, Paris, France) bi-planar image acquisition of the lower limbs consisting of AP-Lateral and oblique (45^{o}-45^{o}) views. Six months after the surgery they recorded a second set of bi-planar orthogonal X-Ray images using the same parameters as preoperatively.

3D Models from EOS imaging including tunnels

The pairs of orthogonal X-ray images were processed using IdefX software (LIO, Montreal, Quebec, Canada) to reconstruct the 3D models of the femur and tibia personalized to each subject. As proposed by our previous study *(Montreuil et al. unpublished),* we used the oblique

views to create these models as it facilitated identification of anatomical landmarks while minimizing superposition. The reconstruction was performed starting from a generic 3D model of each segment. Each generic 3D model was deformed and reconstructed via an as-rigid-as-possible approach. This is based on the "moving least squares optimization method" that requires the projected contours from two radiographic planes to match the boundaries of the bones on orthogonal X-rays [6,34]. Then, identification of the femoral and tibial tunnels on the postoperative acquisitions was performed. To represent theses tunnels, an adjustable truncated cone was designed since the lateral portion of the tunnel was narrower due to an integration and ossification process at the time of the post-operative EOS^{tm} acquisition. This conical shape was added in the IdefX software and was fitted manually by our trained evaluators. Another set of EOS^{tm} 3D models was performed by a second evaluator to verify the inter-rater reproducibility of the entire process. Both evaluators were blinded with respect to any information of the subjects. A total of seventy-four post-operative 3D models with tunnels were obtained. (FIGURE 2)

Cylindrical referential conception

For the purpose of this study, the arthroscopic terminology using High-Low and Deep-Shallow axises was respected in the methodology (FIGURE 3) [26]. A cylindrical description of the femoral tunnel positioning in the intercondylar notch allows the combination of two known techniques, the clock-face and the Bernard & Hertel quadrant method, in a unique tridimensional fashion. We defined this cylindrical coordinate system with a standard 3-axis system (X,Y,Z). Starting from the origin, a radius (X), an angle (Y) then followed by a depth (Z)

coordinate allows for the description of any point on the cylinder. (FIGURE 4.) With this reference being fitted and fixed in the middle of the intercondylar notch, the radius and the angle would be given in a similar fashion as the clock-face technique. The deep/shallow coordinate, along the long axis of the cylinder, would reproduce the quadrant method. This method allowed us to acknowledge the extensive literature behind these two techniques.

Cylindrical reference fixation

After deciding on the components of the coordinate system, we proceeded with the fixation of the referential within boundaries. 3D models issued from EOS^{tm} imaging in IdeFX software (LIO, Montreal, Quebec, Canada) have predefined regions which includes the intercondylar notch. Thus, notch surface mapping of every individual model allowed creation of an automatic and personalized fitted cylinder for every subject. (FIGURE 5) The diameter and orientation were obtained by minimizing the distance between homologous points on a generic cylinder against the intercondylar notch. In the sagittal plane, in concordance with the initial Quadrant method description, this technique oriented the cylinder as parallel as possible to the roof of the intercondylar notch corresponding to the Blumensaat line. It also defined the higher and lower borders of the cylindrical coordinate system. The anterior and posterior edges of the lateral femoral condyle served as borders to extend the Z axis in the same way as Bernard & Hertel described the deep and shallow parameters. The origin of the Z axis was placed at the posterior outlet of the notch, at the deepest coordinate. Since the ACL is located deep in the notch, extrapolation from a shallow origin would lead to imprecisions [8]. 3D reconstructions

issued from EOS^{tm} also provide known metrics like the bicondylar axis and the posterior condyle line. When viewing the cylinders from a frontal plane, the X-axis of the cylindrical referential was defined as parallel to the posterior condyle line. The Y-axis is therefore at ninety degrees and centered on the highest point of the notch. (FIGURE 6a-6b) As previously stated, the diameter was individualized and represent the high-low and mediolateral limits of the cylinder. Theses origins and boundaries of the cylinder were computed, and thirty-seven cylinders were automatically created for both evaluator's postoperative models. All computations of the proposed methods were performed with Mathlab software (Version 9.5 / Mathworks, MA, USA) in addition to the standard functions using IdeFX (LIO, Montreal, Quebec, Canada).

Cylindrical reference validation

In order to validate this automatized technique, the orientation, length and diameter of these 74 cylinders were extracted and compared to two manual measurements techniques. As well, we executed an inter-test reliability study between the automatized method, the manual 3D measures and the x-ray measures. With respect to the 3D manual measures, the projected contours of the 3D models from a perfectly lateral view were obtained. Then, it allowed for a clear identification of the intercondylar notch roof corresponding to the Blumensaat line as seen on a true lateral stereo-radiographic image. Manual x-ray measures were performed as initially described in the quadrant method [2]. The length and diameter were first compared between the three measuring modalities. In the sagittal plane, the cylinder length was measured from the anterior to posterior edges of the lateral femoral condyle along

the Blumensaat line. The diameter of the cylinder was measured at the lowest aspect of the lateral femoral condyle, at 90 degrees from the long axis of the cylinder. Finally, the cylinder's orientation was calculated as the angle between the distal femur's anatomic axis and the cylinder's Z axis on a lateral view. This same angle was manually measured on every 3D contour and on the corresponding lateral stereo-radiographic image. (FIGURE 7) (FIGURE 8). Estimates for ICC and their 95% confidence intervals were calculated using SPSS statistical package Version 25 (SPSS Inc, Chicago, IL) based on a mean-rating (k = 3), absolute-agreement, 2-way mixed effects model. The same software was used to perform paired T-tests with Pearson correlation for the inter-observer reliability study of the 3 parameters. PRISM software (GraphPad, California, USA) was used for illustration of correlation matrices. As a reference, ICC values of less than 0.5 are indicative of poor reliability, values between 0.5 and 0.75 indicate moderate reliability, values between 0.75 and 0.9 indicate good reliability, and values greater than 0.90 indicate excellent reliability [4,19,31].

Anatomic tunnel placement location

Based on the coordinate system implemented, it is possible to describe and project any desired point. Most importantly, this study attempts to highlight the anatomic position of femoral tunnel aperture. Being on the cylinder's surface, this target has the individualized radius as the X coordinate. Furthermore, the initial Bernard study described the anatomical femoral tunnel position as being at 28.5% in the Y axis (high/low). With basic trigonometrics, a 28.5% position along the medial wall of the lateral femoral condyle translates into two possible angles in our referential depending on the side operated. These angles are 0.45 radians for the

left knee and 2.69 radians for the right knee. Not surprisingly, these two angles that were generated correspond to the commonly described anatomic 2 o'clock (left) and 10 o'clock (right) positions. With the final coordinate being the depth along the Z axis, we used Bernard & Hertel's initial description to place our target position. This point was placed at 24,8% from the posterior edge of the lateral femoral condyle.

According to our tridimensional referential, the ideal point coordinate for a left ACL is then;

- *P (1.00 x notch radius, 0.45 rad, 0.248 x length)*
- (FIGURE 9)

Note that this technique can be adapted to any eventual expression and confirmation of an ideal placement for a single or double bundle femoral tunnel placement.

Post-operative description of the actual tunnel aperture position

The post-operative tunnel identification was performed on the thirty-seven subjects by both evaluators. We described the actual positioning of the femoral tunnel aperture in our cylindrical coordinate system by intersecting the axis of the femoral tunnel with the surface of the cylinder. We were able to express every tunnel's crossing point with the same coordinate system (Radius, Angle, Length). (FIGURE 10) The actual and ideal points both being on the cylinder, the radius "X-coordinate" remains constant. However, differences were seen in terms of height (angle) and in the deep/shallow position along the intercondylar notch. These results were plotted as a "modified grid".

Results

Initially cylinder parameters were collected automatically from each observer's series of 3D reconstruction (*Auto*). Then, each independent observer manually measured the same parameters on 3D contours (*Manual-3D*) and on the stereoradiographic images (*Manual-XR*). For the metrics obtained by the automatized method, the first observer's cylinder had a mean orientation of 30,0º (95% CI (28,4-31,5)), a length of 40,4 mm (39,3-41,4) and diameter of 19,3 mm (16,6-20,0). The same metrics for the second observer's series were 29,7 º (28,1-31,3), 40,7 mm (39,7-41,8) and 19,7 mm (18,8-20,6), respectively (TABLE 1 & GRAPH 1). Using a paired T-Test, the first observer's automatized cylinder had an average orientation of 5,6º (3,8-7,4) less than the manual-3D technique. This same measurement was 9,2 º (7,6-10,8) for the second observer. When comparing the automatized method to manual-XR measurements, observer one had an orientation absolute difference of 4,9 º (3,0-6,7) and observer two had a difference of 7,7 º (5,6-9,8). For the length, the first observer's automatized cylinder was on average 5,5 mm (4,5-6,5) shorter than manual-3D measures, while the same parameter was 1,6 mm (0,82,5) for the second observer. In terms of comparison with the manual-XR, observer one obtained an automatized length 4,3 mm (3,2-5,4) shorter than by x-rays, while observer two measured 0,3 mm (-1,6-2,2) longer. For the diameter, the first observer's automatized cylinder, on average, was 2,4 mm (1,6-3,1) smaller than with manual-3D measures, while it was found to be 0,7 mm (-1,8-0,4) larger for the second observer. In terms of comparison with the manually measured diameter on x-rays, observer one obtained an automatized diameter 2,4 mm (1,2-3,5) smaller than with x-rays, while observer two was 0,5 mm (1,1-2,1) smaller. (TABLE 2 –3 & GRAPH 2-3)

For all three measuring modalities, inter-test correlation (r) was calculated independently, along with a global intra-class correlation coefficient (ICC) for every parameter of the cylinder. They all demonstrated positive correlations (GRAPH 4). For the orientation, the automatized versus manual-3D method gave a moderate correlation (r=0,50; p<0,001), while both the automatized versus manual-XR and the manual-3D compared to the manual-XR gave a poor correlation; (r=0,18; p=0,28) and (r=0,13; p=0,45), respectively. However, for the length, the automatized versus both manual-3D and manual-XR measures gave moderate correlations; (r=0,60; p<0,001) and (r=0,66; p<0,001), respectively. Also, manual-XR compared to manual-3D measures showed a good correlation (r=0,76; p<0,001). For the diameter, the automatized compared to manual-3D measures gave a poor correlation (r=0,40; p=0,015), while the automatized to manual-XR gave a moderate correlation (r=0,50; p=0,002). The manual-3D and manual-XR also had a moderate correlation (r=0,56; p<0,001). Overall, the global inter-test correlation gave a poor correlation for the orientation (r=0,44; 95% CI (0,080,68)). However, the length and the diameter both showed moderate overall correlation of 0,68 (0,15-0,87), and 0,63 (0,33-0,80), respectively (TABLE 4).

For the inter-observer reliability, the automatized, manual-3D and manual-XR measured cylinders all had a poor inter-observer correlation for the orientation; (r=0,29; p=0,08), (r=0,14; p=0,41); (r=0,48; p<0,001), respectively. For the length, the automatized method gave an excellent correlation (r=0,95; p<0,001), while the manual-3D and manual-XR both had a moderate correlation between observers with; (r=0,66; p<0,001) and (r=0,45;

p<0,001), respectively. For the diameter, the automatized, manual-3D, manual-XR, all gave a moderate correlation between observers; (r=0,64; p<0,001), (r=0,53; p<0,001) and (r=0,72; p<0,001), respectively (TABLE 5).

Finally, we displayed the coordinates of each subject's femoral tunnel aperture in the cylindrical coordinate system for both observer's series of reconstruction (GRAPH 5). As stated earlier, using basic trigonometrics, the Y-axis high/low coordinate is given by a sinus ratio of its corresponding angle. The target point was then placed according to the initial description by Bernard; 24.8% in shallow/deep Z-axis and 28.5% in high/low Y-axis. The population 5th to 95th percentile anatomic footprint, as studied by *Parkar et al.* were also templated as limits. The mean coordinates at the center of the femoral tunnel aperture for the first observer's series were 37.6 +/- 4.6 degrees (or 0.66 +/- 0.08 radians) and 41.0 +/- 3.0 % in length. The same parameters for second observer's series were 38.3 +/- 5.7 degrees (0.66 +/- 0.1 radians) and 42.0 +/- 3.0 % in length. The average Euclidian distance between the actual and anatomic tunnel position was 8.1 +/- 1.1 mm for the first observer's series and 9.5 +/- 1.5 mm for the second observer's series.

Discussion

This study successfully evaluated the validity and reliability of a novel cylindrical coordinate system in the analysis of ACLR femoral tunnel placement. This cylindrical referential was developed with the use of 3D models issued from EOS^{tm} biplanar x-rays, which provides a low radiation, highly efficient alternative to computed tomography. We were able to validate these

automatized cylinders with parameters that were measured manually on corresponding 3D models, as well as on the initial x-rays images. This cylindrical coordinate system allowed us to illustrate femoral tunnel placement in a previously unseen tridimensional fashion. To define coordinates of the anatomic placement in this 3D reference, we were able to execute mathematical conversions and merge two previously studied approaches; the Clock-face and the Bernard-Hertel quadrant method.

Tridimensional modeling demonstrates clear advantages in ACLR tunnel placement. It is able to represent the actual morphology of the intercondylar notch as seen by the surgeon during an arthroscopic surgery. Recently, 3D reconstruction using computed tomography scans gained popularity because of its improved bony description. However, for ACLR, most of proposed techniques using 3D-CT actually produce a 2D analysis with the quadrant method on a medial view of the lateral condyle. Few groups actually described the ACLR femoral aperture with three-dimensional coordinates. To our knowledge, *Luites et al.,* with a well-designed computer navigation software, are the only group that also used a cylindrical referential in describing ACLR [23]. However, it is based on real-time navigation with opto-electric cameras and dynamic reference bases (DRBs). Thus, availability and applicability of such per-operative digitization system as well as the inability to produce pre-operative planning are major limitations of this technique. Since multiple groups at our research center are focusing on deep machine learning and automatized processes, we were able to design a cylindrical referential that could automatically be produced from an EOS^{tm} 3D knee reconstruction. While the present

paper outlines the initial technique to fit a cylindrical reference in the intercondylar notch, we are aware that further refinements could take into account that the notch dimensions are often variable and that the shape of the Blumensaat line is not always straight [16,20]. To our knowledge, we are the first group to use biplanar stereo-radiographic imaging to describe femoral tunnel positioning in ACLR.

The parameters targeted for the validation of the cylinder were the orientation, the length and the diameter. These metrics were compared between three modalities; the automatized method, a manual measure on the 3D contours and manual measures on lateral x-rays as initially described by the quadrant method. While the orientation of the intercondylar notch roof is not widely reported, the reported deep/shallow length and high/low height in the literature are consistent with our results [5,7,9,20,24,33]. From all three parameters, the angle between the cylinder's long axis and the anatomic distal femur axis is undoubtedly the one that accounted the most variability. The natural bowing of the femur in the sagittal plane combined with subjective manual measurements could explain the variability between the measuring modalities. For further studies, other landmarks for the orientation could be used. On the other hand, the length and diameter of the automatized cylinders were consistently within the previously identified targets, being 5 mm for length and 2 mm for diameter, when compared to the standard manual measures on lateral x-rays. Following the same tendency, our method showed adequate inter-test ICC between all three measuring techniques both for length and diameter, while giving a poor correlation for orientation. In terms of inter-observer reproducibility, similar results were obtained; with a moderate to excellent correlation for

length and diameter. Most importantly, our results show a better reproducibility with the automatized process than the standard manual measurements. We believe that overall, the cylinder's length, which is also influenced by its orientation within the distal femur represents the most important parameter. Overall, our results support the adequacy of the proposed method for the length determination. As well, we would like to refine the analysis for the diameter even if acceptable results were obtained. Comparing a three-dimensional technique with a monoplanar distance in the high/low axis could explain the discrepancies obtained. Also, since the manual techniques (EOS^{tm} contours and XR) were exposed to human operator errors in obtaining a perfect lateral image, malrotation could contribute to the differences observed. In fact, both observers needed to manually rotate the transparent 3D model before proceeding with their measurements. Similarly, some biplanar stereoradiographic x-rays acquisitions did not display a perfect lateral image of the operated knee. While we are satisfied with the validation of this cylindrical coordinate system, we believe that adjusting these factors could improve the overall precision of our method.

Displaying the location of all apertures on a single graph allows to analyze tridimensional femoral tunnel placement in a novel fashion. While acknowledging the discrepancies in the literature concerning the location of the ideal femoral tunnel placement, we opted to compare our reconstructions with an anatomic placement as historically described by Bernard. We also included the population anatomic 5-95th percentile interval as shared by *Parkar et al*. in their systematic review. Compared to these targets, both observers' series displayed an average post-operative femoral tunnel placed in a shallower and higher position in the intercondylar

notch. In fact, from a frontal perspective, the tunnels' aperture had an angular component of around 10 degrees more than the ideal 2 & 10 o'clock position. The Euclidian distance between the center of actual femoral tunnel aperture and the anatomic target underline the overall precision of the tunnel placement. Both observers' series showed a distance less than 10 mm. Proportionally, the average reamer used for femoral tunnel drilling in ACLR has a diameter of 7 or 8 mm. The impact of this difference in femoral tunnel placement on the biomechanics of the knee has not yet been determined.

Finally, this technique will open the door to multiple pre-operative, per-operative and postoperative possibilities in ACLR, as well as in other knee surgeries. In our opinion, the efficiency of the low-irradiating biplanar stereoradiographic imaging combined with the recent progress in automatization and deep learning will allow for a tailored pre-operative approach in ACLR. During the surgery, this three-dimensional referential could also be use with augmented reality for navigation or to customize a surgical guide in order to avoid grossly misplaced tunnels. In fact, previous studies show that visual aids improve precision and reliability of tunnel placement in ACLR [13,30]. Finally, post-operative 3D feedback on tunnel placement could also be beneficial as underlined by previous studies [32]. On the other hand, the present method still entails certain limitations. As previously stated, our group will need to improve some parameters in the conception of the cylindrical reference, notably the orientation. Our technique will also need to consider that the notch dimensions are often variable and that the shape of the Blumensaat line is not always straight. Furthermore, the accessibility of such a system is limited, restricting our knowledge on the reproducibility

amongst different centers. This reproducibility will need to be established before scaling our technique. Collecting data from other institutions using EOS^{tm} will augment the sample size, while providing subjects operated by other surgeons with different surgical techniques. This should improve the precision and generalizability of our method.

Conclusion & future directions

This novel tridimensional cylindrical coordinate system, using biplanar stereoradiographic X-Rays, a low-irradiation imaging system, showed a precision comparable to standard manual measurements in ACLR femoral tunnel placement description. Our results also suggest that automatized cylinders issued from EOS^{tm} show an adequate accuracy and reproducibility. Even if the results of this preliminary study are promising, we strive to improve our methods by refining further parameters to evaluate and re-validate the present method, especially focusing on the spatial orientation. We also plan on scaling up the study in other centers using the EOS^{tm} imaging technology with different orthopaedic surgeons.

Acknowledgements & Affiliations:

Jacques De Guise & Thierry Cresson ;

- Research funds, royalties and patent licensed from EOS company
- Sponsorship by CRSNG RDC, Canada research chairs, Mitacs, MEDTEQ

References

1. Behrend H, Stutz G, Kessler MA, Rukavina A, Giesinger K, Kuster MS. Tunnel placement in anterior cruciate ligament (ACL) reconstruction: quality control in a teaching hospital. *Knee Surg Sports Traumatol Arthrosc.* 2006;14(11):1159-1165.

2. Bernard M, Hertel P, Hornung H, Cierpinski T. Femoral insertion of the ACL. Radiographic quadrant method. *The American journal of knee surgery.* 1997;10(1):1421; discussion 21-12.

3. Burkart A, Debski RE, McMahon PJ, et al. Precision of ACL tunnel placement using traditional and robotic techniques. *Comput Aided Surg.* 2001;6(5):270-278.

4. Cicchetti DV. Guidelines, criteria, and rules of thumb for evaluating normed and standardized assessment instruments in psychology. *Psychological Assessment.* 1994;6(4):284-290.

5. Colombet P, Robinson J, Christel P, et al. Morphology of anterior cruciate ligament attachments for anatomic reconstruction: a cadaveric dissection and radiographic study. *Arthroscopy.* 2006;22(9):984-992.

6. Cresson T, Branchaud D, Chav R, Godbout B, Guise JAd. 3D shape reconstruction of bone from two x-ray images using 2D/3D non-rigid registration based on moving least-squares deformation. Paper presented at: SPIE Medical Imaging2010.

7. Davis TJ, Shelbourne KD, Klootwyk TE. Correlation of the intercondylar notch width of the femur to the width of the anterior and posterior cruciate ligaments. *Knee Surgery, Sports Traumatology, Arthroscopy.* 1999;7(4):209-214.

8. Edwards A, Bull AM, Amis AA. The attachments of the anteromedial and posterolateral fibre bundles of the anterior cruciate ligament. Part 2: femoral attachment. *Knee Surg Sports Traumatol Arthrosc.* 2008;16(1):29-36.

9. Forsythe B, Kopf S, Wong AK, et al. The location of femoral and tibial tunnels in anatomic double-bundle anterior cruciate ligament reconstruction analyzed by threedimensional computed tomography models. *J Bone Joint Surg Am.* 2010;92(6):14181426.

10. Han Y, Hart A, Martineau PA. Is the clock face an accurate, precise, and reliable measuring tool for anterior cruciate ligament reconstruction? *Arthroscopy.* 2014;30(7):849-855.

11. Hart A, Han Y, Martineau PA. The Apex of the Deep Cartilage: A Landmark and New Technique to Help Identify Femoral Tunnel Placement in Anterior Cruciate Ligament Reconstruction. *Arthroscopy.* 2015;31(9):1777-1783.

12. Hwang MD, Piefer JW, Lubowitz JH. Anterior cruciate ligament tibial footprint anatomy: systematic review of the 21st century literature. *Arthroscopy.* 2012;28(5):728-734.

13. Ilahi OA, Mansfield DJ, Urrea LH, 2nd, Qadeer AA. Reliability and reproducibility of several methods of arthroscopic assessment of femoral tunnel position during anterior cruciate ligament reconstruction. *Arthroscopy.* 2014;30(10):1303-1310.

14. Illes T, Somoskeoy S. The EOS imaging system and its uses in daily orthopaedic practice. *Int Orthop.* 2012;36(7):1325-1331.

15. Inderhaug E, Larsen A, Waaler PA, Strand T, Harlem T, Solheim E. The effect of intraoperative fluoroscopy on the accuracy of femoral tunnel placement in singlebundle anatomic ACL reconstruction. *Knee Surg Sports Traumatol Arthrosc.* 2017;25(4):1211-1218.

16. Iriuchishima T, Ryu K, Aizawa S, Fu FH. Blumensaat's line is not always straight: morphological variations of the lateral wall of the femoral intercondylar notch. *Knee Surg Sports Traumatol Arthrosc.* 2016;24(9):2752-2757.

17. Jepsen CF, Lundberg-Jensen AK, Faunoe P. Does the position of the femoral tunnel affect the laxity or clinical outcome of the anterior cruciate ligament-reconstructed knee? A clinical, prospective, randomized, double-blind study. *Arthroscopy.* 2007;23(12):1326-1333.

18. Kawakami Y, Hiranaka T, Matsumoto T, et al. The accuracy of bone tunnel position using fluoroscopic-based navigation system in anterior cruciate ligament reconstruction. *Knee Surg Sports Traumatol Arthrosc.* 2012;20(8):1503-1510.

19. Koo TK, Li MY. A Guideline of Selecting and Reporting Intraclass Correlation Coefficients for Reliability Research. *Journal of chiropractic medicine.* 2016;15(2):155163.

20. Koukoubis TD, Glisson RR, Bolognesi M, Vail TP. Dimensions of the intercondylar notch of the knee. *The American journal of knee surgery.* 1997;10(2):83-87; discussion 87-88.

21. Kraeutler MJ, Patel KV, Hosseini A, Li G, Gill TJ, Bravman JT. Variability in the Clock Face View Description of Femoral Tunnel Placement in ACL Reconstruction Using MRIBased Bony Models. *The journal of knee surgery.* 2018.

22. Luites JW, Wymenga AB, Blankevoort L, Eygendaal D, Verdonschot N. Accuracy of a computer-assisted planning and placement system for anatomical femoral tunnel

positioning in anterior cruciate ligament reconstruction. *The international journal of medical robotics + computer assisted surgery : MRCAS.* 2014;10(4):438-446.

23. Luites JW, Wymenga AB, Blankevoort L, Kooloos JM, Verdonschot N. Development of a femoral template for computer-assisted tunnel placement in anatomical doublebundle ACL reconstruction. *Comput Aided Surg.* 2011;16(1):11-21.

24. Luites JWH, Wymenga AB, Blankevoort L, Kooloos JGM. Description of the attachment geometry of the anteromedial and posterolateral bundles of the ACL from arthroscopic perspective for anatomical tunnel placement. *Knee Surgery Sports Traumatology Arthroscopy.* 2007;15(12):1422-1431.

25. Marchant BG, Noyes FR, Barber-Westin SD, Fleckenstein C. Prevalence of nonanatomical graft placement in a series of failed anterior cruciate ligament reconstructions. *Am J Sports Med.* 2010;38(10):1987-1996.

26. Musahl V, Plakseychuk A, VanScyoc A, et al. Varying femoral tunnels between the anatomical footprint and isometric positions: effect on kinematics of the anterior cruciate ligament-reconstructed knee. *Am J Sports Med.* 2005;33(5):712-718.

27. Parkar AP, Adriaensen M, Vindfeld S, Solheim E. The Anatomic Centers of the Femoral and Tibial Insertions of the Anterior Cruciate Ligament: A Systematic Review of Imaging and Cadaveric Studies Reporting Normal Center Locations. *American Journal of Sports Medicine.* 2017;45(9):2180-2188.

28. Petermann J, Kober R, Heinze R, Frölich JJ, Heeckt PF, Gotzen L. Computer-assisted planning and robot-assisted surgery in anterior cruciate ligament reconstruction. *Operative Techniques in Orthopaedics.* 2000;10(1):50-55.

29. Rayan F, Nanjayan SK, Quah C, Ramoutar D, Konan S, Haddad FS. Review of evolution of tunnel position in anterior cruciate ligament reconstruction. *World J Orthop.* 2015;6(2):252-262.

30. Schep NW, Stavenuiter MH, Diekerhof CH, et al. Intersurgeon variance in computerassisted planning of anterior cruciate ligament reconstruction. *Arthroscopy.* 2005;21(8):942-947.

31. Shrout PE, Fleiss JL. Intraclass correlations: uses in assessing rater reliability. *Psychological bulletin.* 1979;86(2):420-428.

32. Sirleo L, Innocenti M, Innocenti M, Civinini R, Carulli C, Matassi F. Post-operative 3D CT feedback improves accuracy and precision in the learning curve of anatomic ACL femoral tunnel placement. *Knee Surg Sports Traumatol Arthrosc.* 2017.

33. Zantop T, Wellmann M, Fu FH, Petersen W. Tunnel positioning of anteromedial and posterolateral bundles in anatomic anterior cruciate ligament reconstruction: anatomic and radiographic findings. *Am J Sports Med.* 2008;36(1):65-72.

34. Zeighami A, Dumas R, Kanhonou M, et al. Tibio-femoral joint contact in healthy and osteoarthritic knees during quasi-static squat: A bi-planar X-ray analysis. *Journal of biomechanics.* 2017;53:178-184.

Tables & Graphs

1. Table 1. Cylinder overall parameters evaluation

		Observer 1			Observer 2		
Parameter	Modality	Mean	Inf	Sup	Mean	Inf	Sup
Angle							
(degrees)	Automatized	30,0	28,4	31,5	29,7	28,1	31,3
	Manual-EOS	35,6	33,6	37,5	38,8	37,6	40,0
	Manual-XR	34,8	33,6	36,0	37,4	36,1	38,6
Length							
(mm)	Automatized	40,4	39,3	41,4	40,7	39,7	41,8
	Manual-EOS	45,8	44,7	46,9	42,3	41,1	43,6
	Manual-XR	44,7	43,3	46,1	40,4	38,5	42,3
Diameter							
(mm)	Automatized	19,3	18,6	20,0	19,7	18,8	20,6
	Manual-EOS	21,7	20,9	22,4	19,1	18,5	19,7
	Manual-XR	21,7	20,4	22,9	20,3	18,9	21,7

2. Table 2. Observer 1 inter-test paired T-test

Observer 1			
	Modality	Mean	95% CI
Angle (deg)			
	A vs E	- 5,59	- 7,42 ; - 3,76
	A vs XR	- 4,86	- 6,71 ; - 3,00
Length (mm)			
	A vs E	- 5,46	- 6,47 ; - 4,46
	A vs XR	- 4,33	- 5,43 ; - 3,23
Diameter (mm)			
n=37	A vs E	- 2,37	- 3,15 ; - 1,58
a=5%	A vs XR	- 2,35	- 3,46 ; - 1,23

3. Table 3. Observer 2 inter-test paired T-test

Observer 2			
	Modality	**Mean**	**95% CI**
Angle (deg)			
	A vs E	- 9,18	- 10,75 ; - 7,60
	A vs XR	- 7,71	- 9,82 ; - 5,61
Length (mm)			
	A vs E	- 1,61	- 2,46 ; - 0,75
	A vs XR	0,33	- 1,58 ; 2,24
Diameter (mm)			
n=37	A vs E	0,66	- 0,44 ; - 1,75
a=5%	A vs XR	- 0,54	- 2,14 ; - 1,07

4. Table 4. Inter-test global intra-class correlation (ICC)

Global inter-test ICC		
Parameter	**ICC**	**95% CI**
Angle	0,44	0,08 ; 0,68
Length	0,68	0,15 ; 0,87
Diameter	0,63	0,33 ; 0,80

5. Table 5. Inter-observer correlation

Inter-observer correlation			
Parameter	**Modality**	**ICC**	**sig.**
Angle			
	Automatized	0,29	0,08
	Manual-EOS	0,14	0,41
	Manual-XR	0,48	< 0,01
Length			
	Automatized	0,95	< 0,01
	Manual-EOS	0,66	< 0,01
	Manual-XR	0,45	0,01
Diameter			
	Automatized	0,64	< 0,01
a=5%	Manual-EOS	0,53	< 0,01
n=37	Manual-XR	0,72	< 0,01

6. Graph 1. Inter-test cylinder validation box-plot for all three parameters

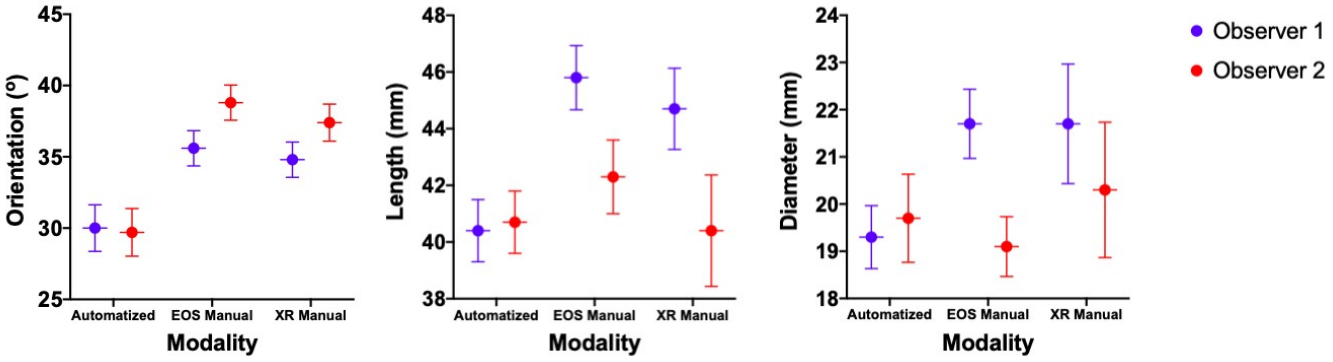

7. Graph 2. Obs. 1 cylinder inter-test box-plot for all three parameters

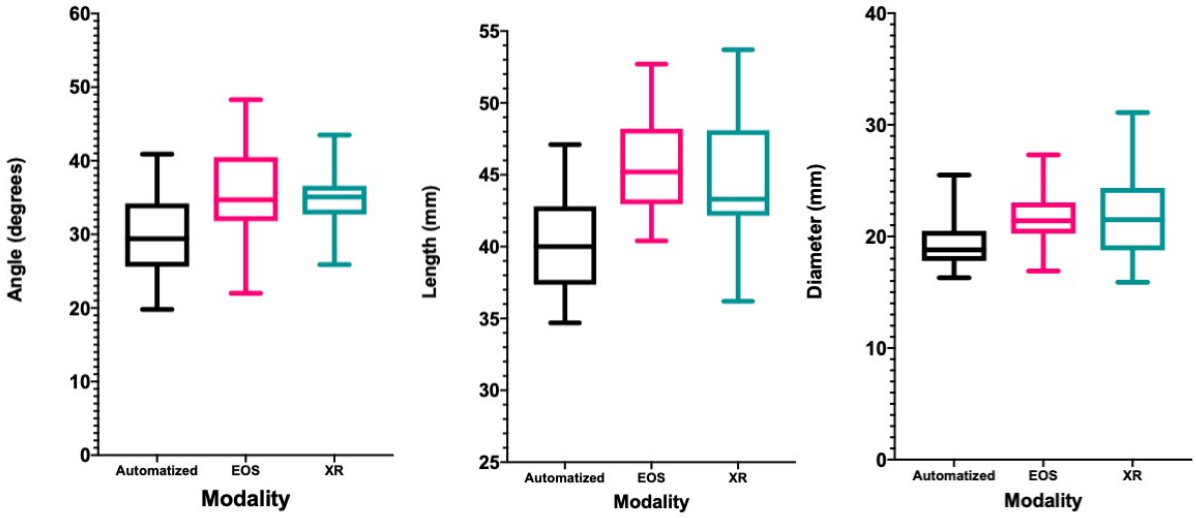

8. Graph 3. Obs. 2 cylinder inter-test box-plot for all three parameters

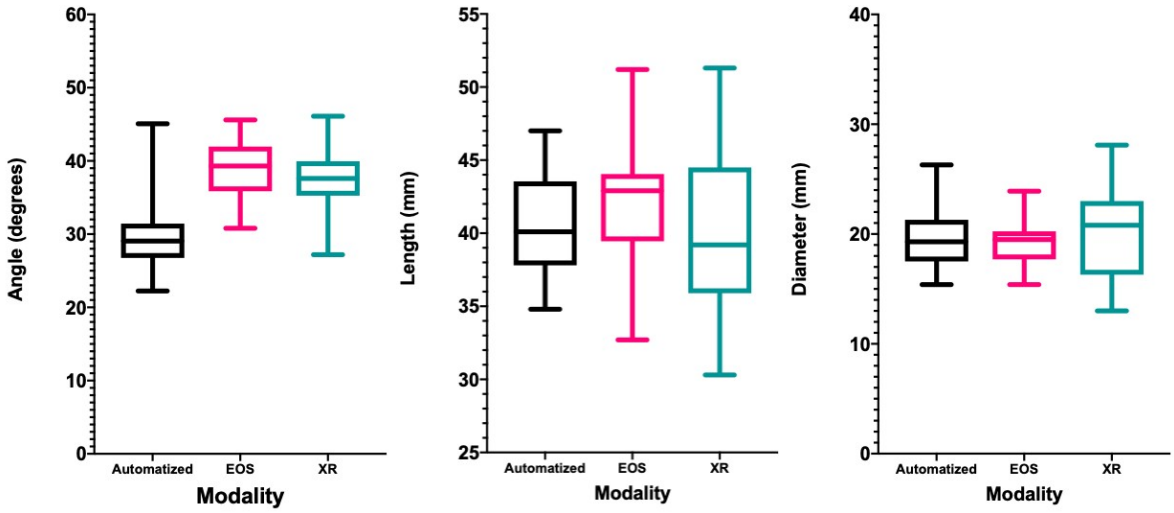

9. Graph 4. Inter-test Pearson correlation matrices for all three parameters

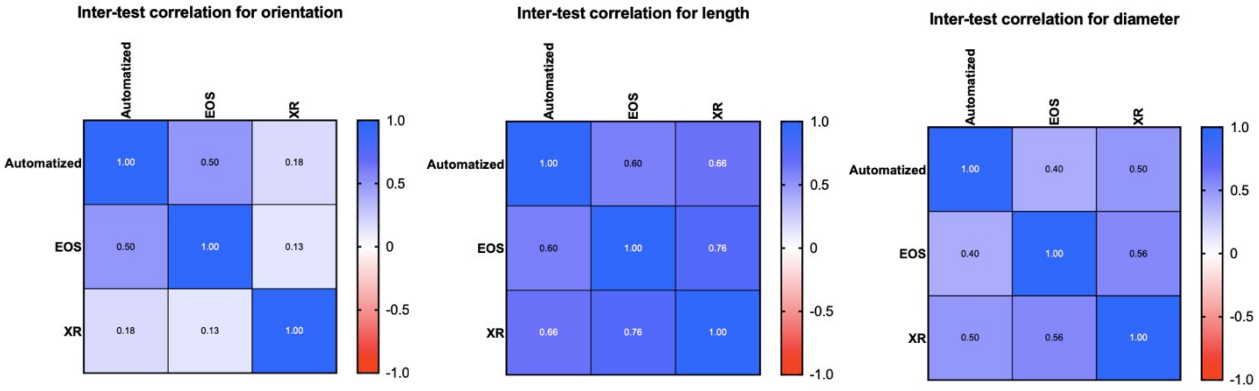

10. Graph 5. Actual tunnels apertures placement

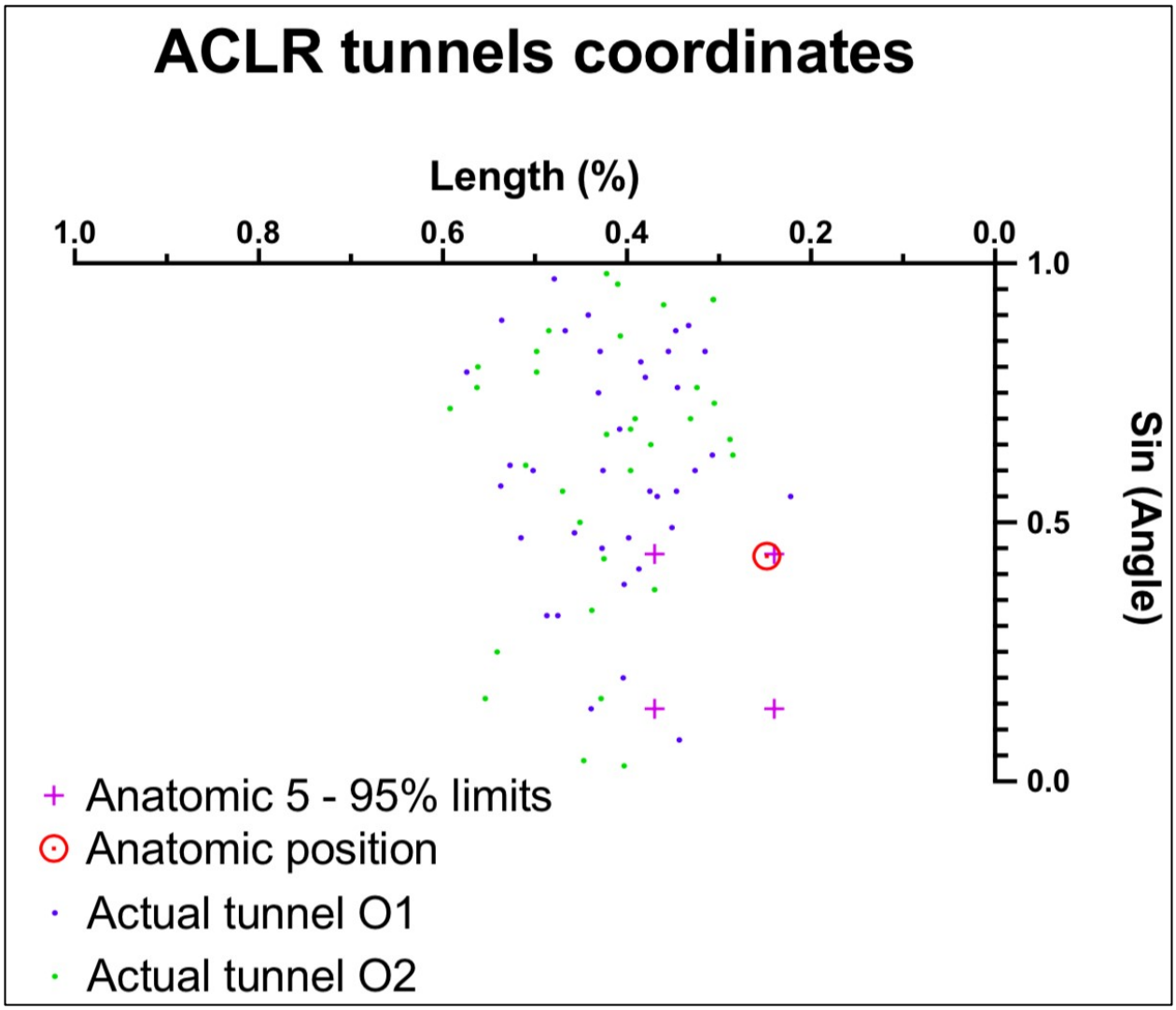

Figures

Figure 1. EOS^{tm} imaging

Figure 1. EOS^{tm} imaging

Figure 2. EOS^{tm} 3D reconstruction methods

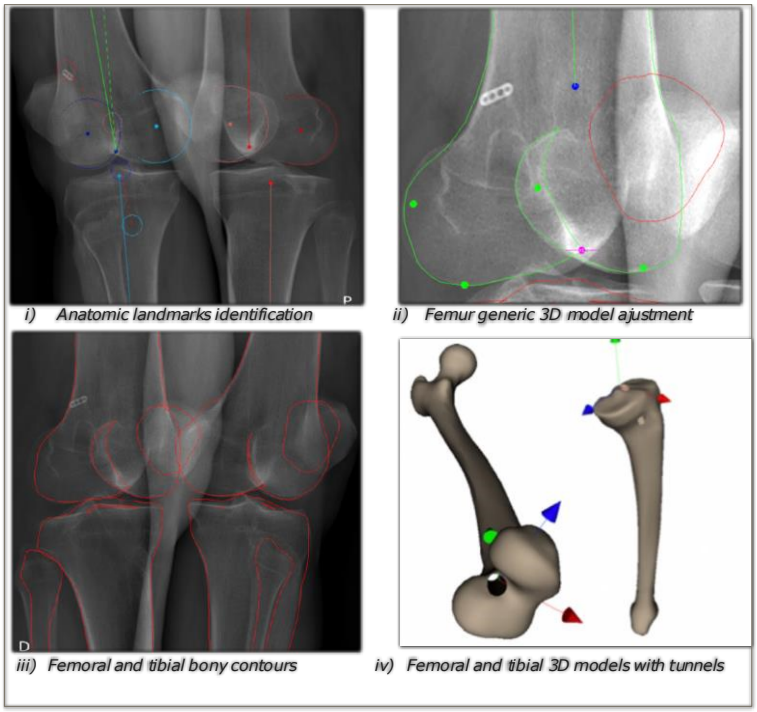

Figure 2. EOS^{tm} 3D reconstruction method

Figure 3. Knee arthroscopic terminology

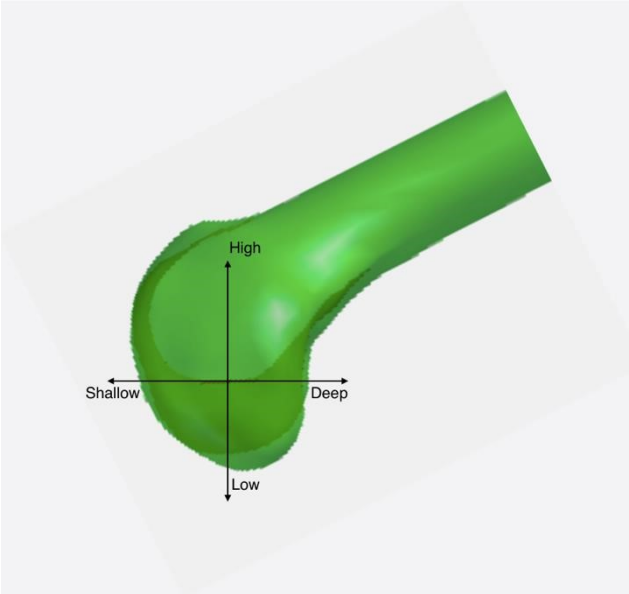

Figure 3. Knee arthroscopic terminology

Figure 4. Cylindrical coordinate system

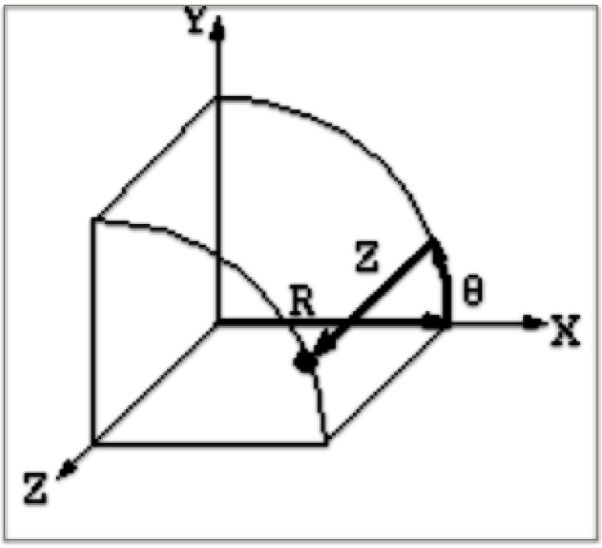

Figure 4. Cylindrical coordinate system

Figure 5. Intercondylar notch surface mapping with EOS^{tm}

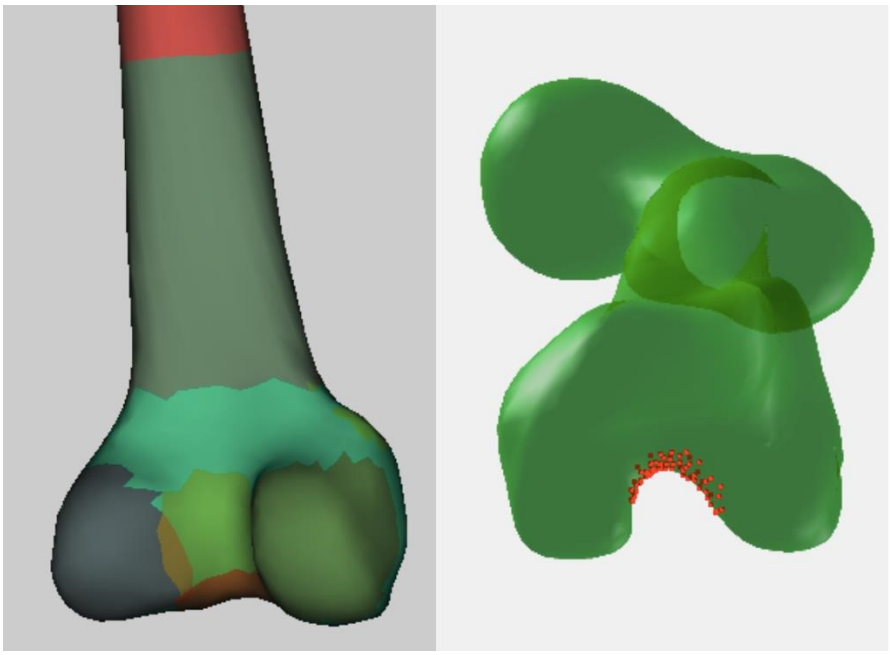

Figure 5. Intercondylar notch surface mapping with EOS^{tm}

Figure 6a-6b. Frontal and Sagittal view cylinder

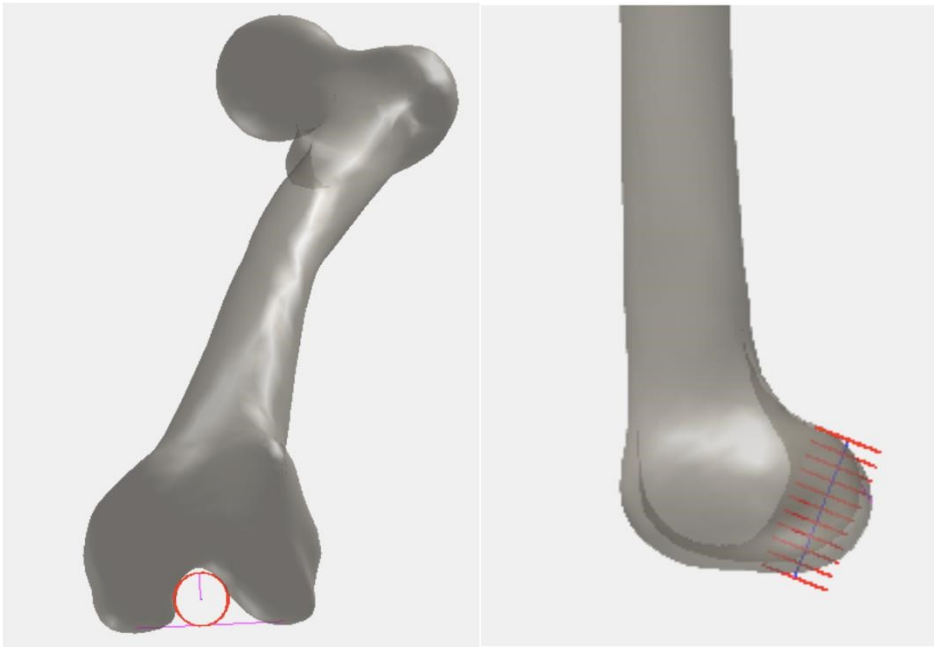

Figure 6a. Cylinder frontal view

Figure 6b. Cylinder sagittal view

Figure 7. Manual measurements on 3D contours

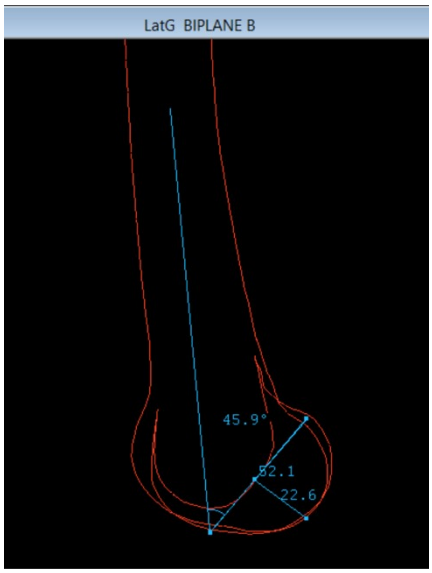

Figure 7. Manual measurements on 3D contours

Figure 8. Manual measurements on lateral stereoradiographic images

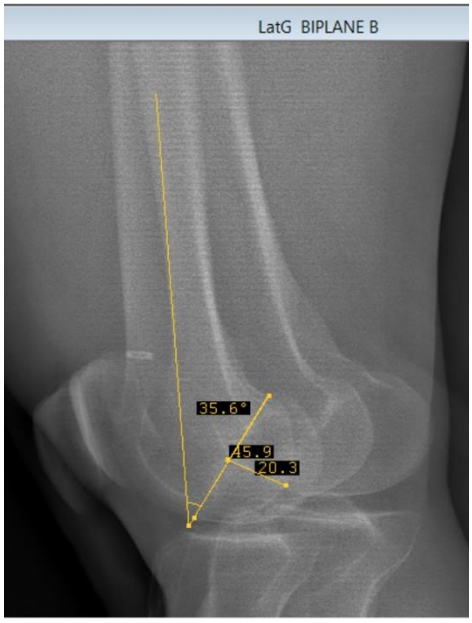

Figure 8. Manual measurements on lateral stereoradiographic image

Figure 9. Tridimensional location of anatomic femoral ACL insertion

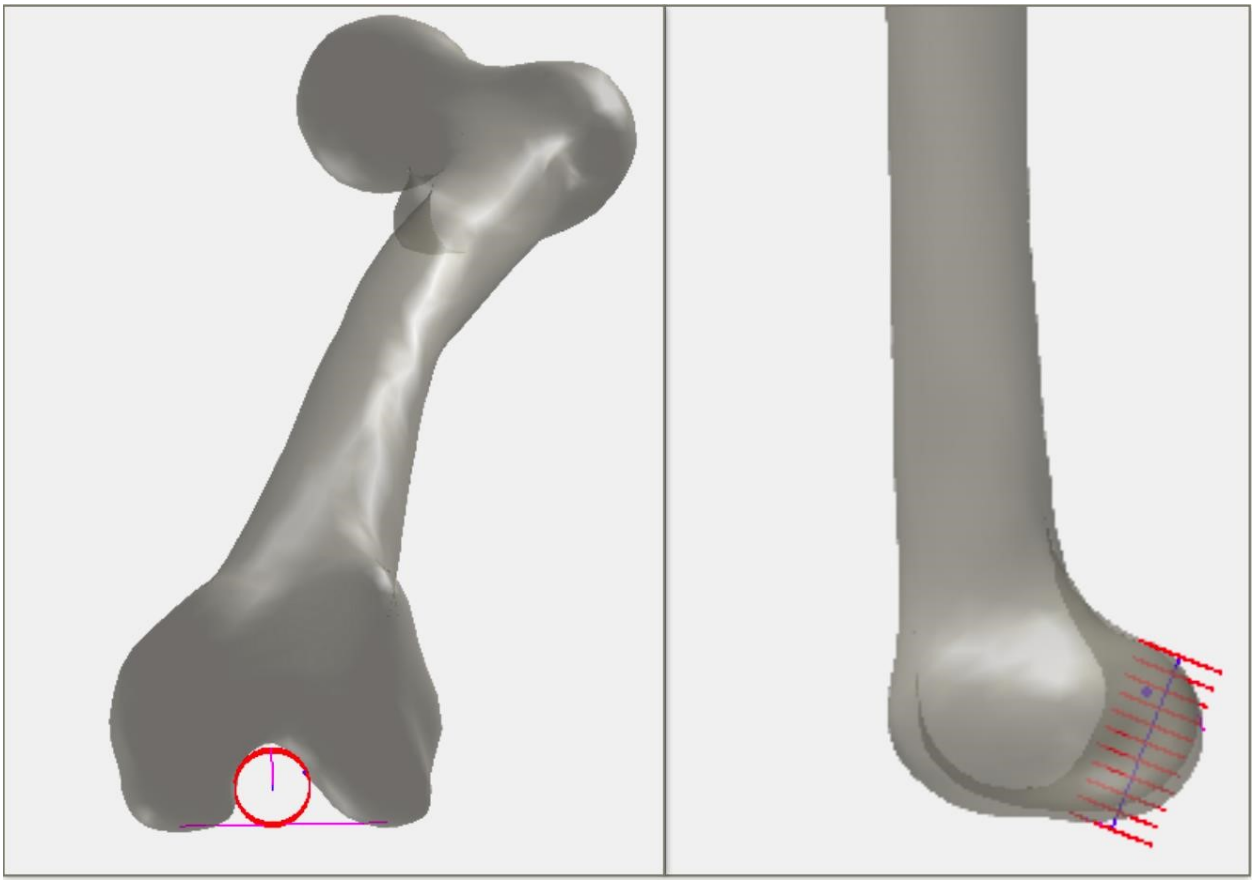

Figure 9. Tridimensional location of anatomic femoral ACL insertion

Figure 10. Actual femoral tunnel aperture compared to anatomic femoral

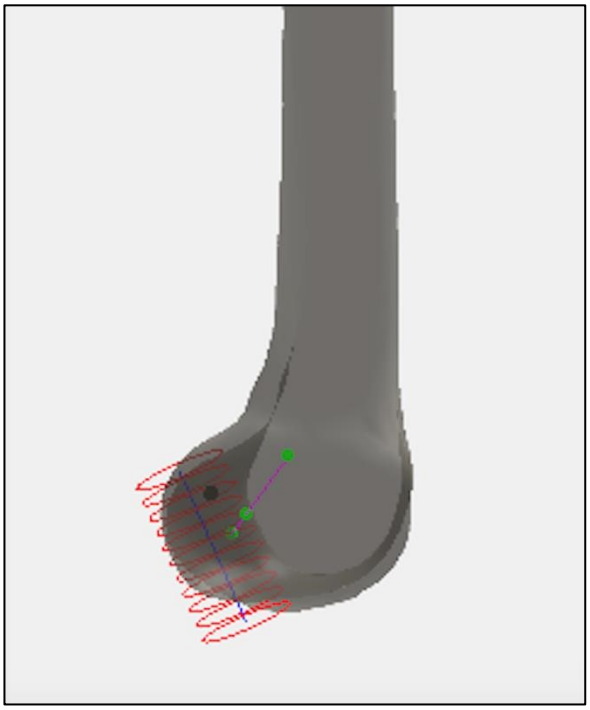

Figure 10. Actual femoral tunnel aperture compared to anatomic femoral ACL insertion

Discussion

Ce mémoire a exploré l'application de l'imagerie biplanaire stéréoradiographique dans l'analyse tridimensionelle de la reconstruction du ligament croisé antérieur du genou. Le premier chapitre, *Biplanar stereo-radiographic imaging as a new reference in tridimensional evaluation of tunnels positioning in ACL reconstruction,* visait principalement à valider les reconstructions tridimensionnelles du genou provenant de l'imagerie EOS^{mc}. Le deuxième chapitre, *Femoral tunnel placement analysis in ACL reconstruction using a novel tridimensional referential with biplanar stereo-radiographic (EOS^{tm}) imaging,* de son côté, a présenté une nouvelle méthode pour décrire les coordonnées tridimensionnelles du tunnel fémoral.

Premièrement, la précision, reproductibilité et rapidité des reconstructions 3D issues d'EOS^{mc} ont été évaluées en les comparant à celles issues de tomodensitométrie. L'analyse surfacique des reconstructions du fémur et du tibia a démontré une équivalence au CT-Scan par une différence moyenne de moins de 2 mm entre les deux types de reconstruction. Plus encore, utiliser les modèles EOS^{mc} issues d'incidences obliques a amélioré significativement la précision et reproductibilité par une identification facilitée des repères anatomiques et une superposition minimisée. L'analyse de la rapidité des reconstructions est sans équivoque : les modèles 3D issus d'EOS^{mc} sont environ 30 fois plus rapide à obtenir qu'une segmentation d'un CT-Scan et ce, après la maîtrise des deux techniques par les évaluateurs. La validation de ces reconstructions a ensuite permis de développer un nouveau référentiel dans l'échancrure intercondylienne décrivant le positionnement tridimensionnel du tunnel fémoral tel qu'exploré dans le deuxième chapitre du mémoire.

En effet, dans un deuxième temps, à partir des reconstructions 3D EOS^{mc}, nous avons proposé un référentiel cylindrique, combinant la technique de l'Horloge ainsi que la grille de Bernard & Hertel, comme un moyen efficace de décrire objectivement l'emplacement de l'ouverture intra-articulaire du tunnel fémoral. Selon ce référentiel tridimensionnel, le point idéal de l'attache fémorale du LCA serait donc sur le mur médial du condyle fémoral latéral, à une angulation de 0.45 radians de l'horizon

et à 24,8% de la longueur de l'échancrure intercondylienne à partir de sa limite postérieure. Les paramètres utilisés pour la validation de ce référentiel automatisé étaient donc la longueur, le diamètre et l'angulation de ce cylindre. Les résultats automatisés ont été comparés avec deux autres méthodes de mesure : manuellement sur rayons-X et sur les contours 3D. Le référentiel programmé a démontré une corrélation modérée pour la longueur (r=0.68) et le diamètre (r=0.63) du cylindre, mais une faible corrélation pour l'orientation (r=0.44). Cette méthode automatisée a également démontré des résultats semblables quant à la reproductibilité inter-évaluateur : une excellente corrélation pour longueur (r=0.95), modérée pour le diamètre (r=0.66), mais faible pour l'orientation (r=0.29). Notons que cette reproductibilité était supérieure à la méthode manuelle sur les contours 3D. Avec ce référentiel, nous avons pu identifier l'emplacement réel de l'ouverture intra-articulaire du tunnel fémoral chez 37 patients opérés pour une reconstruction du LCA. Bref, grâce à ce projet pilote, notre groupe se penchera sur l'amélioration des paramètres du référentiel cylindrique, notamment l'orientation, afin d'améliorer la précision tout en s'adaptant aux variations individuelles dans la morphologie de l'échancrure intercondylienne. Nous croyons que cette méthode ouvre la porte à une multitude d'applications préopératoires, d'outils peropératoires ainsi que de méthodes d'évaluation post-opératoires.

Conclusion

Le présent mémoire a permis de démontrer que l'imagerie biplanaire stéréoradiographique du système EOS^{tm} est un outil fiable pour la modélisation tridimensionnelle du genou. Afin d'assurer sa généralisabilité, notre groupe a également proposé un protocole de réalisation optimisant la précision des reconstructions (en annexe). Ce travail porte spécialement sur une description tridimensionnelle de la reconstruction du ligament croisé antérieur. La solution innovatrice proposée par notre groupe consiste en un référentiel cylindrique positionné dans l'échancrure intercondylienne décrivant la position du tunnel fémoral. La validité et la reproductibilité de ce référentiel ont été établies. Il a été possible de décrire les coordonnées tridimensionnelles du centre anatomique du ligament croisé antérieur dans ce nouveau référentiel qui guide un placement optimal du tunnel fémoral. Somme toute, plusieurs aspects biomécaniques de la reconstruction du ACL devront être considérer pour accompagner les avancés du présent projet. D'abord, se pencher sur l'insertion tibiale du LCA sera crucial. L'impact biomécanique et clinique des différents positionnements tridimensionnels du tunnel fémoral dans l'échancrure intercondylienne restent également à préciser. Ainsi, lorsqu'identifié, l'emplacement idéal, possiblement différent de la position anatomique utilisée dans ce travail, pourra être utilisé avec le présent référentiel. De plus, les avancés récents en intelligence artificielle et en automatisation permettront d'accélérer considérablement les techniques complexes de reconstructions 3D, sans compromettre leur précision. Par les groupes effectuant des travaux dans ce domaine, en particulier dans notre institution, il ne sera pas surprenant d'assister aux progrès de l'imagerie tridimensionnelle qui permettront de mieux comprendre les pathologies de l'articulation complexe qu'est le genou.

Bibliographie

Ahn JH, Jeong HJ, Ko CS, Ko TS, Kim JH. Three-dimensional reconstruction computed tomography evaluation of tunnel location during single-bundle anterior cruciate ligament reconstruction: a comparison of transtibial and 2-incision tibial tunnel-independent techniques. Clinics in Orthopedic Surgery. 2013;5(1):26-35.

Ajuied A, Wong F, Smith C, et al. Anterior cruciate ligament injury and radiologic progression of knee osteoarthritis: a systematic review and meta-analysis. Am J Sports Med. 2014;42(9):2242-2252.

Arnoczky SP. Anatomy of the anterior cruciate ligament. Clinical orthopaedics and related research. 1983(172):19-25.

Bedi A, Maak T, Musahl V, et al. Effect of tibial tunnel position on stability of the knee after anterior cruciate ligament reconstruction: is the tibial tunnel position most important? Am J Sports Med. 2011;39(2):366-373.

Behrend H, Stutz G, Kessler MA, Rukavina A, Giesinger K, Kuster MS. Tunnel placement in anterior cruciate ligament (ACL) reconstruction: quality control in a teaching hospital. Knee Surg Sports Traumatol Arthrosc. 2006;14(11):1159-1165.

Berger S, Hasler CC, Grant CA, Zheng G, Schumann S, Buchler P. A software program to measure the three-dimensional length of the spine from radiographic images: Validation and reliability assessment for adolescent idiopathic scoliosis. Computer methods and programs in biomedicine. 2017;138:57-64.

Bernard M, Hertel P, Hornung H, Cierpinski T. Femoral insertion of the ACL. Radiographic quadrant method. The American journal of knee surgery. 1997;10(1):14-21; discussion 2112.

Bird JH, Carmont MR, Dhillon M, et al. Validation of a new technique to determine midbundle femoral tunnel position in anterior cruciate ligament reconstruction using 3dimensional computed tomography analysis. Arthroscopy. 2011;27(9):1259-1267.

Boden BP, Dean GS, Feagin JA, Jr., Garrett WE, Jr. Mechanisms of anterior cruciate ligament injury. Orthopedics. 2000;23(6):573-578.

Brown MJ, Carter T. ACL Allograft: Advantages and When to Use. Sports medicine and arthroscopy review. 2018;26(2):75-78.

Burkart A, Debski RE, McMahon PJ, et al. Precision of ACL tunnel placement using traditional and robotic techniques. Comput Aided Surg. 2001;6(5):270-278.

Burnett QM, 2nd, Fowler PJ. Reconstruction of the anterior cruciate ligament: historical overview. The Orthopedic clinics of North America. 1985;16(1):143-157.

Cicchetti DV. Guidelines, criteria, and rules of thumb for evaluating normed and standardized assessment instruments in psychology. Psychological Assessment. 1994;6(4):284-290.

Colombet P, Robinson J, Christel P, et al. Morphology of anterior cruciate ligament attachments for anatomic reconstruction: a cadaveric dissection and radiographic study. Arthroscopy. 2006;22(9):984-992.

Colvin AC, Shen W, Musahl V, Fu FH. Avoiding pitfalls in anatomic ACL reconstruction. Knee Surg Sports Traumatol Arthrosc. 2009;17(8):956-963.

Crespo B, Aga C, Wilson KJ, et al. Measurements of bone tunnel size in anterior cruciate ligament reconstruction: 2D versus 3D computed tomography model. J Exp Orthop. 2014;1(1):2.

Cresson T, Branchaud D, Chav R, Godbout B, Guise JAd. 3D shape reconstruction of bone from two x-ray images using 2D/3D non-rigid registration based on moving least-squares deformation. Paper presented at: SPIE Medical Imaging2010.

Dabirrahmani D, Christopher Hogg M, Walker P, Biggs D, Mark Gillies R. Comparison of isometric and anatomical graft placement in synthetic ACL reconstructions: A pilot study. Computers in Biology and Medicine. 2013;43(12):2287-2296.

Dambros JM, Florencio R, Junior OV, Kuhn A, Saggin J, de Freitas Spinelli L. Radiological Analysis of Bone Tunnel Position in Anterior Cruciate Ligament Reconstruction Surgery: Comparison between the Open Technique and Arthroscopy Via an Anteromedial Portal. Rev Bras Ortop. 2011;46(3):270-275.

Davis TJ, Shelbourne KD, Klootwyk TE. Correlation of the intercondylar notch width of the femur to the width of the anterior and posterior cruciate ligaments. Knee Surgery, Sports Traumatology, Arthroscopy. 1999;7(4):209-214.

de Abreu-e-Silva GM, de Oliveira M, Maranhao GS, et al. Three-dimensional computed tomography evaluation of anterior cruciate ligament footprint for anatomic single-bundle reconstruction. Knee Surgery Sports Traumatology Arthroscopy. 2015;23(3):770-776.

Deschenes S, Charron G, Beaudoin G, et al. Diagnostic imaging of spinal deformities: reducing patients radiation dose with a new slot-scanning X-ray imager. Spine. 2010;35(9):989-994.

Domnick C, Raschke MJ, Herbort M. Biomechanics of the anterior cruciate ligament: Physiology, rupture and reconstruction techniques. World J Orthop. 2016;7(2):82-93.

Ducouret E, Loriaut P, Boyer P, et al. Tunnel positioning assessment after anterior cruciate ligament reconstruction at 12 months: Comparison between 3D CT and 3D MRI. A pilot study. Orthopaedics & Traumatology: Surgery & Research. 2017;103(6):937-942.

Ducsharm M, Banaszek D, Hesse D, Kunz M, Reifel C, Bardana D. Assessing the accuracy of femoral tunnel placement in anatomic ACL reconstruction (913.13). The FASEB Journal.

2014;28(1_supplement):913.913.

Edwards A, Bull AM, Amis AA. The attachments of the anteromedial and posterolateral fibre bundles of the anterior cruciate ligament. Part 2: femoral attachment. Knee Surg Sports Traumatol Arthrosc. 2008;16(1):29-36.

Fernandes TL, Fregni F, Weaver K, Pedrinelli A, Camanho GL, Hernandez AJ. The influence of femoral tunnel position in single-bundle ACL reconstruction on functional outcomes and return to sports. Knee Surgery, Sports Traumatology, Arthroscopy. 2014;22(1):97-103.

Fernandes TL, Martins N, Watai FD, Neto CA, Pedrinelli A, Hernandez AJ. 3D COMPUTER TOMOGRAPHY FOR MEASUREMENT OF FEMORAL POSITION IN ACL RECONSTRUCTION. Acta Ortopedica Brasileira. 2015;23(1):11-15.

Ferretti AMD. A Historical Note on Anterior Cruciate Ligament Reconstruction. Journal of Bone & Joint Surgery - American Volume. 2003;85(5):970-971.

Ferretti M, Doca D, Ingham SM, Cohen M, Fu FH. Bony and soft tissue landmarks of the ACL tibial insertion site: an anatomical study. Knee Surg Sports Traumatol Arthrosc. 2012;20(1):62-68.

Forsythe B, Kopf S, Wong AK, et al. The location of femoral and tibial tunnels in anatomic double-bundle anterior cruciate ligament reconstruction analyzed by three-dimensional computed tomography models. J Bone Joint Surg Am. 2010;92(6):1418-1426.

Foster TE, Wolfe BL, Ryan S, Silvestri L, Kaye EK. Does the graft source really matter in the outcome of patients undergoing anterior cruciate ligament reconstruction? An evaluation of autograft versus allograft reconstruction results: a systematic review. Am J Sports Med. 2010;38(1):189-199.

Fu FH. The clock-face reference: simple but nonanatomic. Arthroscopy. 2008;24(12):1433; author reply 1434.

Fu FH, Bennett CH, Lattermann C, Ma CB. Current trends in anterior cruciate ligament reconstruction. Part 1: Biology and biomechanics of reconstruction. Am J Sports Med. 1999;27(6):821-830.

Fu FH, Schulte KR. Anterior cruciate ligament surgery 1996. State of the art? Clinical orthopaedics and related research. 1996(325):19-24.

Garofalo R, Moretti B, Kombot C, Moretti L, Mouhsine E. Femoral tunnel placement in anterior cruciate ligament reconstruction: rationale of the two incision technique. Journal of orthopaedic surgery and research. 2007;2:10.

Gordon MD SM. Anterior cruciate ligament injuries. 3 ed. Rosemont American Academy of Orthopaedic Surgeons; 2004.

Grassi A, Nitri M, Moulton SG, et al. Does the type of graft affect the outcome of revision anterior cruciate ligament reconstruction? a meta-analysis of 32 studies. The bone & joint journal. 2017;99-b(6):714-723.

Han Y, Hart A, Martineau PA. Is the clock face an accurate, precise, and reliable measuring tool for anterior cruciate ligament reconstruction? Arthroscopy. 2014;30(7):849-855.

Harner CD, Marks PH, Fu FH, Irrgang JJ, Silby MB, Mengato R. Anterior cruciate ligament reconstruction: endoscopic versus two-incision technique. Arthroscopy. 1994;10(5):502512.

Hart A, Han Y, Martineau PA. The Apex of the Deep Cartilage: A Landmark and New Technique to Help Identify Femoral Tunnel Placement in Anterior Cruciate Ligament Reconstruction. Arthroscopy. 2015;31(9):1777-1783.

Hart A, Sivakumaran T, Burman M, Powell T, Martineau PA. A Prospective Evaluation of Femoral Tunnel Placement for Anatomic Anterior Cruciate Ligament Reconstruction Using 3-Dimensional Magnetic Resonance Imaging. Am J Sports Med. 2018;46(1):192-199.

Hensler D, Working ZM, Illingworth KD, Tashman S, Fu FH. Correlation between femoral tunnel length and tunnel position in ACL reconstruction. Journal of Bone & Joint Surgery - American Volume. 2013;95(22):2029-2034.

Horie M, Muneta T, Yamazaki J, et al. A modified quadrant method for describing the femoral tunnel aperture positions in ACL reconstruction using two-view plain radiographs. Knee Surg Sports Traumatol Arthrosc. 2015;23(4):981-985.

Hosseini A, Lodhia P, Van de Velde SK, et al. Tunnel position and graft orientation in failed anterior cruciate ligament reconstruction: a clinical and imaging analysis. Int Orthop. 2012;36(4):845-852.

Hui C, Pi Y, Swami V, Mabee M, Jaremko JL. A Validation Study of a Novel 3-Dimensional MRI Modeling Technique to Identify the Anatomic Insertions of the Anterior Cruciate Ligament. Orthopaedic journal of sports medicine. 2016;4(12):2325967116673797.

Hwang MD, Piefer JW, Lubowitz JH. Anterior cruciate ligament tibial footprint anatomy: systematic review of the 21st century literature. Arthroscopy. 2012;28(5):728-734.

Ilahi OA, Mansfield DJ, Urrea LH, 2nd, Qadeer AA. Reliability and reproducibility of several methods of arthroscopic assessment of femoral tunnel position during anterior cruciate ligament reconstruction. Arthroscopy. 2014;30(10):1303-1310.

Ilharreborde B, Dubousset J, Le Huec JC. Use of EOS imaging for the assessment of scoliosis deformities: application to postoperative 3D quantitative analysis of the trunk. European spine journal : official publication of the European Spine Society, the European Spinal Deformity Society, and the European Section of the Cervical Spine Research Society. 2014;23 Suppl 4:S397-405.

Illes T, Somoskeoy S. The EOS imaging system and its uses in daily orthopaedic practice. Int Orthop. 2012;36(7):1325-1331.

Illingworth KD, Hensler D, Working ZM, Macalena JA, Tashman S, Fu FH. A Simple Evaluation of Anterior Cruciate Ligament Femoral Tunnel Position The Inclination Angle and Femoral Tunnel Angle. American Journal of Sports Medicine. 2011;39(12):2611-2618.

Inderhaug E, Larsen A, Waaler PA, Strand T, Harlem T, Solheim E. The effect of intraoperative fluoroscopy on the accuracy of femoral tunnel placement in single-bundle anatomic ACL reconstruction. Knee Surg Sports Traumatol Arthrosc. 2017;25(4):12111218.

Iriuchishima T, Ryu K, Aizawa S, Fu FH. Blumensaat's line is not always straight: morphological variations of the lateral wall of the femoral intercondylar notch. Knee Surgery, Sports Traumatology, Arthroscopy. 2016;24(9):2752-2757.

Iriuchishima T, Shirakura K, Fu FH. Graft impingement in anterior cruciate ligament reconstruction. Knee Surg Sports Traumatol Arthrosc. 2013;21(3):664-670.

Jepsen CF, Lundberg-Jensen AK, Faunoe P. Does the position of the femoral tunnel affect the laxity or clinical outcome of the anterior cruciate ligament-reconstructed knee? A clinical, prospective, randomized, double-blind study. Arthroscopy. 2007;23(12):13261333.

Kai S, Kondo E, Kitamura N, et al. A quantitative technique to create a femoral tunnel at the averaged center of the anteromedial bundle attachment in anatomic double-bundle anterior cruciate ligament reconstruction. BMC musculoskeletal disorders. 2013;14:189.

Kato Y, Maeyama A, Lertwanich P, et al. Biomechanical comparison of different graft positions for single-bundle anterior cruciate ligament reconstruction. Knee Surg Sports Traumatol Arthrosc. 2013;21(4):816-823.

Kawakami Y, Hiranaka T, Matsumoto T, et al. The accuracy of bone tunnel position using fluoroscopic-based navigation system in anterior cruciate ligament reconstruction. Knee Surg Sports Traumatol Arthrosc. 2012;20(8):1503-1510.

Kieser CW, Jackson RW. Eugen Bircher (1882-1956) the first knee surgeon to use diagnostic arthroscopy. Arthroscopy. 2003;19(7):771-776.

Kim DH, Lim WB, Cho SW, Lim CW, Jo S. Reliability of 3-Dimensional Computed Tomography for Application of the Bernard Quadrant Method in Femoral Tunnel Position Evaluation After Anatomic Anterior Cruciate Ligament Reconstruction. Arthroscopy. 2016;32(8):16601666.

Kim Y, Lee BH, Mekuria K, et al. Registration accuracy enhancement of a surgical navigation system for anterior cruciate ligament reconstruction: A phantom and cadaveric study. Knee. 2017;24(2):329-339.

Klos TV, Habets RJ, Banks AZ, Banks SA, Devilee RJ, Cook FF. Computer assistance in arthroscopic anterior cruciate ligament reconstruction. Clinical orthopaedics and related research. 1998(354):65-69.

Koo TK, Li MY. A Guideline of Selecting and Reporting Intraclass Correlation Coefficients for Reliability Research. Journal of chiropractic medicine. 2016;15(2):155-163.

Kopf S, Forsythe B, Wong AK, et al. Nonanatomic tunnel position in traditional transtibial single-bundle anterior cruciate ligament reconstruction evaluated by three-dimensional computed tomography. J Bone Joint Surg Am. 2010;92(6):1427-1431.

Kostogiannis I, Ageberg E, Neuman P, Dahlberg LE, Friden T, Roos H. Clinically assessed knee joint laxity as a predictor for reconstruction after an anterior cruciate ligament injury: a prospective study of 100 patients treated with activity modification and rehabilitation. Am J Sports Med. 2008;36(8):1528-1533.

Koukoubis TD, Glisson RR, Bolognesi M, Vail TP. Dimensions of the intercondylar notch of the knee. The American journal of knee surgery. 1997;10(2):83-87; discussion 87-88.

Kraeutler MJ, Patel KV, Hosseini A, Li G, Gill TJ, Bravman JT. Variability in the Clock Face View Description of Femoral Tunnel Placement in ACL Reconstruction Using MRI-Based Bony Models. The journal of knee surgery. 2018.

Laporte S, Skalli W, de Guise JA, Lavaste F, Mitton D. A biplanar reconstruction method based on 2D and 3D contours: application to the distal femur. Computer methods in biomechanics and biomedical engineering. 2003;6(1):1-6.

Larson RL, Tailon M. Anterior Cruciate Ligament Insufficiency: Principles of Treatment. The Journal of the American Academy of Orthopaedic Surgeons. 1994;2(1):26-35.

Lee BH, Kum DH, Rhyu IJ, Kim Y, Cho H, Wang JH. Clinical advantages of image-free navigation system using surface-based registration in anatomical anterior cruciate ligament reconstruction. Knee Surgery Sports Traumatology Arthroscopy. 2016;24(11):3556-3564.

Lee DH, Kim HJ, Ahn HS, Bin SI. Comparison of femur tunnel aperture location in patients undergoing transtibial and anatomical single-bundle anterior cruciate ligament reconstruction. Knee Surg Sports Traumatol Arthrosc. 2016;24(12):3713-3721.

Lee JK, Lee S, Seong SC, Lee MC. Anatomy of the anterior cruciate ligament insertion sites: comparison of plain radiography and three-dimensional computed tomographic imaging to anatomic dissection. Knee Surgery Sports Traumatology Arthroscopy. 2015;23(8):22972305.

Lee MC, Seong SC, Lee S, et al. Vertical femoral tunnel placement results in rotational knee laxity after anterior cruciate ligament reconstruction. Arthroscopy. 2007;23(7):771-778.

Lee SR, Jang HW, Lee DW, Nam SW, Ha JK, Kim JG. Evaluation of femoral tunnel positioning using 3-dimensional computed tomography and radiographs after single bundle anterior

cruciate ligament reconstruction with modified transtibial technique. Clinics in Orthopedic Surgery. 2013;5(3):188-194.

Leong NL, Petrigliano FA, McAllister DR. Current tissue engineering strategies in anterior cruciate ligament reconstruction. Journal of biomedical materials research Part A. 2014;102(5):1614-1624.

Lertwanich P, Martins CAQ, Asai S, Ingham SJM, Smolinski P, Fu FH. Anterior Cruciate Ligament Tunnel Position Measurement Reliability on 3-Dimensional Reconstructed Computed Tomography. Arthroscopy: The Journal of Arthroscopic & Related Surgery. 2011;27(3):391-398.

Luites JW, Wymenga AB, Blankevoort L, Eygendaal D, Verdonschot N. Accuracy of a computer-assisted planning and placement system for anatomical femoral tunnel positioning in anterior cruciate ligament reconstruction. The international journal of medical robotics + computer assisted surgery : MRCAS. 2014;10(4):438-446.

Luites JW, Wymenga AB, Blankevoort L, Kooloos JM, Verdonschot N. Development of a femoral template for computer-assisted tunnel placement in anatomical double-bundle ACL reconstruction. Comput Aided Surg. 2011;16(1):11-21.

Luites JWH, Wymenga AB, Blankevoort L, Kooloos JGM. Description of the attachment geometry of the anteromedial and posterolateral bundles of the ACL from arthroscopic perspective for anatomical tunnel placement. Knee Surgery Sports Traumatology Arthroscopy. 2007;15(12):1422-1431.

Marcacci M, Zaffagnini S, Iacono F, Neri MP, Loreti I, Petitto A. Arthroscopic intra- and extra-articular anterior cruciate ligament reconstruction with gracilis and semitendinosus tendons. Knee Surg Sports Traumatol Arthrosc. 1998;6(2):68-75.

Marchant BG, Noyes FR, Barber-Westin SD, Fleckenstein C. Prevalence of nonanatomical graft placement in a series of failed anterior cruciate ligament reconstructions. Am J Sports Med. 2010;38(10):1987-1996.

Markatos K, Kaseta MK, Lallos SN, Korres DS, Efstathopoulos N. The anatomy of the ACL and its importance in ACL reconstruction. European journal of orthopaedic surgery & traumatology : orthopedie traumatologie. 2013;23(7):747-752.

Markolf KL, Mensch JS, Amstutz HC. Stiffness and laxity of the knee--the contributions of the supporting structures. A quantitative in vitro study. J Bone Joint Surg Am. 1976;58(5):583-594.

Marshall JL, Wang JB, Furman W, Girgis FG, Warren R. The anterior drawer sign: what is it? The Journal of sports medicine. 1975;3(4):152-158.

McConkey MO, Amendola A, Ramme AJ, et al. Arthroscopic Agreement Among Surgeons on Anterior Cruciate Ligament Tunnel Placement. American Journal of Sports Medicine. 2012;40(12):2737-2746.

Mehta V, Petsche T, Rawal AM. Inter- and Intrarater Reliability of the Femoral Tunnel ClockFace Grading System During Anterior Cruciate Ligament Reconstruction. Arthroscopy: The Journal of Arthroscopic & Related Surgery. 2017;33(2):394-397.

Meuffels DE, Potters JW, Koning AHJ, Brown CH, Verhaar JAN, Reijman M. Visualization of postoperative anterior cruciate ligament reconstruction bone tunnels Reliability of standard radiographs, CT scans, and 3D virtual reality images. Acta Orthopaedica. 2011;82(6):699-703.

Miller MD. Editorial Commentary: Does Anybody Really Know What Time It Is? Does Anybody Really Care? Arthroscopy. 2017;33(2):398-399.

Mohtadi N, Chan D, Barber R, Oddone Paolucci E. A Randomized Clinical Trial Comparing Patellar Tendon, Hamstring Tendon, and Double-Bundle ACL Reconstructions: PatientReported and Clinical Outcomes at a Minimal 2-Year Follow-up. Clinical journal of sport medicine : official journal of the Canadian Academy of Sport Medicine. 2015;25(4):321331.

Mountcastle SB, Posner M, Kragh JF, Jr., Taylor DC. Gender differences in anterior cruciate ligament injury vary with activity: epidemiology of anterior cruciate ligament injuries in a young, athletic population. Am J Sports Med. 2007;35(10):1635-1642.

Murray MM, Flutie BM, Kalish LA, et al. The Bridge-Enhanced Anterior Cruciate Ligament Repair (BEAR) Procedure: An Early Feasibility Cohort Study. Orthopaedic journal of sports medicine. 2016;4(11):2325967116672176.

Musahl V, Burkart A, Debski RE, Van Scyoc A, Fu FH, Woo SL. Anterior cruciate ligament tunnel placement: Comparison of insertion site anatomy with the guidelines of a computer-assisted surgical system. Arthroscopy. 2003;19(2):154-160.

Musahl V, Plakseychuk A, VanScyoc A, et al. Varying femoral tunnels between the anatomical footprint and isometric positions: effect on kinematics of the anterior cruciate ligament-reconstructed knee. Am J Sports Med. 2005;33(5):712-718.

Nau T, Teuschl A. Regeneration of the anterior cruciate ligament: Current strategies in tissue engineering. World J Orthop. 2015;6(1):127-136.

Noyes FR, Matthews DS, Mooar PA, Grood ES. The symptomatic anterior cruciate-deficient knee. Part II: the results of rehabilitation, activity modification, and counseling on functional disability. J Bone Joint Surg Am. 1983;65(2):163-174.

Ortiz A. The EOS Imaging System: Promising Technology in Skeletal Imaging. Radiologic technology. 2017;88(4):448-450.

Paessler HH, Deneke J, Dahners LE. Augmented repair and early mobilization of acute anterior cruciate ligament injuries. Am J Sports Med. 1992;20(6):667-674.

Park SH, Moon SW, Lee BH, et al. Arthroscopically blind anatomical anterior cruciate ligament reconstruction using only navigation guidance: a cadaveric study. Knee. 2016;23(5):813-819.

Parkar AP, Adriaensen M, Vindfeld S, Solheim E. The Anatomic Centers of the Femoral and Tibial Insertions of the Anterior Cruciate Ligament: A Systematic Review of Imaging and Cadaveric Studies Reporting Normal Center Locations. American Journal of Sports Medicine. 2017;45(9):2180-2188.

Parkar AP, Adriaensen MEAPM, Fischer-Bredenbeck C, et al. Measurements of tunnel placements after anterior cruciate ligament reconstruction — A comparison between CT, radiographs and MRI. The Knee. 2015;22(6):574-579.

Parkinson B, Gogna R, Robb C, Thompson P, Spalding T. Anatomic ACL reconstruction: the normal central tibial footprint position and a standardised technique for measuring tibial tunnel location on 3D CT. Knee Surg Sports Traumatol Arthrosc. 2017;25(5):1568-1575.

Parkinson B, Robb C, Thomas M, Thompson P, Spalding T. Factors That Predict Failure in Anatomic Single-Bundle Anterior Cruciate Ligament Reconstruction. Am J Sports Med. 2017;45(7):1529-1536.

Pasha S, Schlosser T, Zhu X, Mellor X, Castelein R, Flynn J. Application of Low-dose Stereoradiography in In Vivo Vertebral Morphologic Measurements: Comparison With Computed Tomography. Journal of pediatric orthopedics. 2017.

Pearle AD, McAllister D, Howell SM. Rationale for Strategic Graft Placement in Anterior Cruciate Ligament Reconstruction: I.D.E.A.L. Femoral Tunnel Position. American journal of orthopedics (Belle Mead, NJ). 2015;44(6):253-258.

Petermann J, Kober R, Heinze R, Frölich JJ, Heeckt PF, Gotzen L. Computer-assisted planning and robot-assisted surgery in anterior cruciate ligament reconstruction. Operative Techniques in Orthopaedics. 2000;10(1):50-55.

Phan B, Sohn K-M, Wang J-H, Koo S. Automatic computation of bernard quadrant in the distal femur. 2016.

Prodromos CC, Han Y, Rogowski J, Joyce B, Shi K. A meta-analysis of the incidence of anterior cruciate ligament tears as a function of gender, sport, and a knee injury-reduction regimen. Arthroscopy. 2007;23(12):1320-1325.e1326.

Ramme AJ, Wolf BR, Warme BA, et al. Surgically oriented measurements for threedimensional characterization of tunnel placement in anterior cruciate ligament reconstruction. Comput Aided Surg. 2012;17(5):221-231.

Ratliff AH. Ernest William Hey Groves and his contributions to orthopaedic surgery. Bristol medico-chirurgical journal (1963). 1983;98(367):98-103.

Rayan F, Nanjayan SK, Quah C, Ramoutar D, Konan S, Haddad FS. Review of evolution of tunnel position in anterior cruciate ligament reconstruction. World J Orthop. 2015;6(2):252-262.

Reynaud O, Batailler C, Lording T, Lustig S, Servien E, Neyret P. Three dimensionalCT analysis of femoral tunnel position after ACL reconstruction. A prospective study of one hundred and thirty five cases. Int Orthop. 2017;41(11):2313-2319.

Robbrecht C, Claes S, Cromheecke M, et al. Reliability of a semi-automated 3D-CT measuring method for tunnel diameters after anterior cruciate ligament reconstruction: A comparison between soft-tissue single-bundle allograft vs. autograft. Knee. 2014;21(5):926-931.

Robert HE, Bouguennec N, Vogeli D, Berton E, Bowen M. Coverage of the Anterior Cruciate Ligament Femoral Footprint Using 3 Different Approaches in Single-Bundle Reconstruction A Cadaveric Study Analyzed by 3-Dimensional Computed Tomography. American Journal of Sports Medicine. 2013;41(10):2375-2383.

Sabczynski J, Dries SP, Hille E, Zylka W. Image-guided reconstruction of the anterior cruciate ligament. The international journal of medical robotics + computer assisted surgery : MRCAS. 2004;1(1):125-132.

Sadoghi P, Kropfl A, Jansson V, Muller PE, Pietschmann MF, Fischmeister MF. Impact of tibial and femoral tunnel position on clinical results after anterior cruciate ligament reconstruction. Arthroscopy. 2011;27(3):355-364.

Samuelsen BT, Webster KE, Johnson NR, Hewett TE, Krych AJ. Hamstring Autograft versus Patellar Tendon Autograft for ACL Reconstruction: Is There a Difference in Graft Failure Rate? A Meta-analysis of 47,613 Patients. Clinical orthopaedics and related research. 2017;475(10):2459-2468.

Sati M, Stäubli HU, Bourquin Y, Kunz M, Käsermann S, Nolte L-P. Clinical integration of computer-assisted technology for arthroscopic anterior cruciate ligament reconstruction. Operative Techniques in Orthopaedics. 2000;10(1):40-49.

Sati M, Stäubli HU, Bourquin Y, Kunz M, Nolte LP. Real-Time Computerized in Situ Guidance System for ACL Graft Placement. Computer Aided Surgery. 2002;7(1):25-40.

Schep NW, Stavenuiter MH, Diekerhof CH, et al. Intersurgeon variance in computerassisted planning of anterior cruciate ligament reconstruction. Arthroscopy. 2005;21(8):942-947.

Schillhammer CK, Reid JB, 3rd, Rister J, et al. Arthroscopy Up to Date: Anterior Cruciate Ligament Anatomy. Arthroscopy. 2016;32(1):209-212.

Schindler OS. Surgery for anterior cruciate ligament deficiency: a historical perspective. Knee Surg Sports Traumatol Arthrosc. 2012;20(1):5-47.

Shimodaira H, Tensho K, Akaoka Y, Takanashi S, Kato H, Saito N. Tibial Tunnel Positioning Technique Using Bony/Anatomical Landmarks in Anatomical Anterior Cruciate Ligament Reconstruction. Arthroscopy Techniques. 2017;6(1):e49-e55.

Shino K, Iuchi R, Tachibana Y, Matsuo T, Ohori T, Mae T. Intraoperative Landmarks for Tunnel Placement in Anatomical Anterior Cruciate Ligament Reconstruction. Operative Techniques in Orthopaedics. 2017;27(1):38-42.

Shrout PE, Fleiss JL. Intraclass correlations: uses in assessing rater reliability. Psychological bulletin. 1979;86(2):420-428.

Sirleo L, Innocenti M, Innocenti M, Civinini R, Carulli C, Matassi F. Post-operative 3D CT feedback improves accuracy and precision in the learning curve of anatomic ACL femoral tunnel placement. Knee Surg Sports Traumatol Arthrosc. 2017.

Stevenson WW, 3rd, Johnson DL. "Vertical grafts": a common reason for functional failure after ACL reconstruction. Orthopedics. 2007;30(3):206-209.

Sudhahar TA, Glasgow MM, Donell ST. Comparison of expected vs. actual tunnel position in anterior cruciate ligament reconstruction. Knee. 2004;11(1):15-18.

Swami VG, Cheng-Baron J, Hui C, Thompson R, Jaremko JL. Reliability of Estimates of ACL Attachment Locations in 3-Dimensional Knee Reconstruction Based on Routine Clinical MRI in Pediatric Patients. The American Journal of Sports Medicine. 2013;41(6):1319-1329.

Takahashi M, Doi M, Abe M, Suzuki D, Nagano A. Anatomical study of the femoral and tibial insertions of the anteromedial and posterolateral bundles of human anterior cruciate ligament. Am J Sports Med. 2006;34(5):787-792.

Taketomi S, Inui H, Nakamura K, et al. Clinical outcome of anatomic double-bundle ACL reconstruction and 3D CT model-based validation of femoral socket aperture position. Knee Surgery Sports Traumatology Arthroscopy. 2014;22(9):2194-2201.

Tensho K, Kodaira H, Yasuda G, et al. Anatomic double-bundle anterior cruciate ligament reconstruction, using CT-based navigation and fiducial markers. Knee Surgery Sports Traumatology Arthroscopy. 2011;19(3):378-383.

Tensho K, Shimodaira H, Aoki T, et al. Bony Landmarks of the Anterior Cruciate Ligament Tibial Footprint: A Detailed Analysis Comparing 3-Dimensional Computed Tomography Images to Visual and Histological Evaluations. Am J Sports Med. 2014;42(6):1433-1440.

Torg JS, Conrad W, Kalen V. Clinical diagnosis of anterior cruciate ligament instability in the athlete. Am J Sports Med. 1976;4(2):84-93.

van der List JP, Zuiderbaan HA, Nawabi DH, Pearle AD. Impingement following anterior cruciate ligament reconstruction: comparing the direct versus indirect femoral tunnel position. Knee Surg Sports Traumatol Arthrosc. 2017;25(5):1617-1624.

van Eck CF, Kropf EJ, Romanowski JR, et al. Factors that influence the intra-articular rupture pattern of the ACL graft following single-bundle reconstruction. Knee Surg Sports Traumatol Arthrosc. 2011;19(8):1243-1248.

Vermersch T, Lustig S, Reynaud O, Debette C, Servien E, Neyret P. CT assessment of femoral tunnel placement after partial ACL reconstruction. Orthopaedics & Traumatology: Surgery & Research. 2016;102(2):197-202.

Westberry DE, Carpenter AM. 3D Modeling of Lower Extremities With Biplanar Radiographs: Reliability of Measures on Subsequent Examinations. Journal of pediatric orthopedics. 2017.

Westermann R, Sybrowsky C, Ramme A, Amedola A, Wolf BR. Three-Dimensional Characterization of the Anterior Cruciate Ligament's Femoral Footprint. Journal of Knee Surgery. 2014;27(1):53-58.

Witonski D, Dorman T. [Anterior cruciate ligament reconstruction by autogenous bonepatellar tendon-bone graft: correlation between bone-tunnel position and clinical results].
Chir Narzadow Ruchu Ortop Pol. 2003;68(1):29-33.

Wolf BR, Ramme AJ, Britton CL, Amendola A, Grp MK. Anterior Cruciate Ligament Tunnel Placement. Journal of Knee Surgery. 2014;27(4):309-317.

Wybier M, Bossard P. Musculoskeletal imaging in progress: the EOS imaging system. Joint, bone, spine : revue du rhumatisme. 2013;80(3):238-243.

Yasuda K, van Eck CF, Hoshino Y, Fu FH, Tashman S. Anatomic single- and double-bundle anterior cruciate ligament reconstruction, part 1: Basic science. Am J Sports Med. 2011;39(8):1789-1799.

Zantop T, Wellmann M, Fu FH, Petersen W. Tunnel positioning of anteromedial and posterolateral bundles in anatomic anterior cruciate ligament reconstruction: anatomic and radiographic findings. Am J Sports Med. 2008;36(1):65-72.

Zeighami A, Dumas R, Kanhonou M, et al. Tibio-femoral joint contact in healthy and osteoarthritic knees during quasi-static squat: A bi-planar X-ray analysis. Journal of biomechanics. 2017;53:178-184.

Liste des publications

Articles

Chapter 1 - Biplanar stereo-radiographic imaging as a new reference in tridimensional evaluation of tunnels positioning in ACL reconstruction

Journal of Orthopaedic Research (under review)

Chapter 2 – Femoral tunnel placement analysis in ACL reconstruction using a novel tridimensional referential with biplanar stereo-radiographic (EOS^{tm}) imaging

The American Journal of Sports Medicine (under review)

Présentations par affiche et podium

Chapitre 1- Biplanar stereo-radiographic imaging as a new reference in tridimensional evaluation of tunnels positioning in ACL reconstruction

- 8^{e} Journée scientifique du CRCHUM. 26 octobre 2017. Montréal, Québec. Prix : Meilleure présentation par affiche
- Orthopaedic reseach society (ORS) 2019 Annual meeting. 2-5 février 2019. Austin, Texas.
- Arthroscopy Association of North America (AANA) 2019 Annual meeting. Orlando, Florida.

Chapitre 2- Femoral tunnel placement analysis in ACL reconstruction using a novel tridimensional referential with biplanar stereo-radiographic (EOS^{tm}) imaging

- Canadian Orthopaedic Residents Association (CORA) 2019 Annual Meeting. 19-22 Juin 2019. Montréal, Québec.
  Prix: Meilleure présentation podium

Protocole de réalisation

Reconstruction 3D de membres inférieurs

Dans le cadre du projet

Biplanar stereo-radiographic imaging as a new reference in tridimensional evaluation of tunnels positioning in ACL reconstruction

MONTREUIL, Julien[1,2] ; LAVOIE, Frédéric[2] ; THIBEAULT, Felix[4] ; CRESSON, Thierry[1] ; DE GUISE, Jacques A.[1]

Affiliations
1. Laboratoire de recherche en Imagerie et Orthopédie de l'ETS (LIO)
2. McGill Division of Orthopaedic Surgery, Montreal General Hospital (MGH)
3. Service de chirurgie orthopédique, Centre Hospitalier de l'Université de Montréal (CHUM)
4. Faculté de Médecine, Université de Montréal

Table des matières

Version préliminaire

Des modifications pourraient être apportées de concert avec l'équipe du LIO avant toute utilisation

Avant-Propos

Ce protocole a été réalisé dans le cadre du projet de *Biplanar stereo-radiographic imaging as a new reference in tridimensional evaluation of tunnels positioning in ACL reconstruction,* par Montreuil et al., à la Maîtrise en sciences biomédicales, option musculosquelettique de l'Université de Montréal.

Ce présent guide est destiné aux futurs étudiants/chercheurs du LIO désirant parfaire leur technique de reconstruction 3D des membres inférieurs à partir des images radiographiques *EOS* et à l'aide du logiciel IdefX. Tout au long de la reconstruction, nous y joindrons des précisions anatomiques qui devraient aider à la réalisation des modèles.

Rappel sur l'imagerie EOS

Notons que le système d'imagerie EOS est un système d'imagerie corporelle biplanaire stéréo-radiographique. Cette technologie est issue des travaux du physicien Georges Charpak dans la détection des rayons X. Celui-ci s'en est mérité le Prix Nobel de Physique en 1992. Ce type d'imagerie est donc fondé sur des capteurs radiologiques basse-dose. Avec cette faible irradiation, l'utilisation en pédiatrie en devient très intéressante. Dans la dernière décennie, ses applications en imagerie tridimensionnelle musculosquelettique ont été multiples. Un certain avantage de ce système d'imagerie est également que le patient demeure dans une position fonctionnelle de mise en charge. Les paramètres cliniques extraits de ces images à l'échelle sont ainsi fiables.

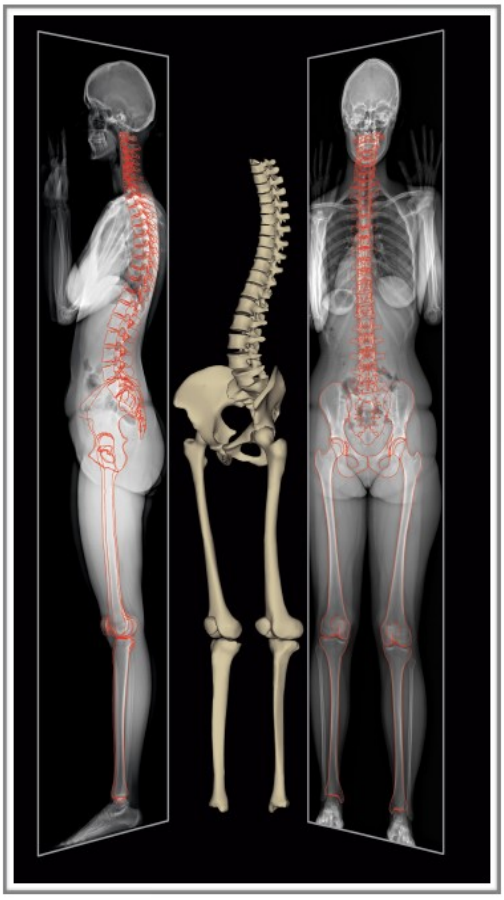

Pour commencer

I. Lancez IdefX

II. Nouvelle analyse
   A. Type de Cabine: EOS 2 ou autres réglages appropriés
   B. Structures à reconstruire:
      1. Sélectionnez le sexe du patient: le modèle générique 3D sera différent selon le sexe, notamment au bassin
      2. Dans le cadre du présent projet, seul les membres inférieurs seront reconstruits
      3. Confirmer

III. Sélection des images
   A. Associez les images d'incidences Postéro-Antérieure et Latérale correspondantes aux choix PA & LAT
      1. Ou 2 incidences obliques orthogonales, le cas échéant

   B. Une fois ouvertes, assurez-vous que les images correspondent bien aux projections désirées.

   C. Dans ce protocole de réalisation des projections obliques sont utilisées. Pour les reconstructions de genoux, la superposition des condyles fémoraux rend difficile les segmentations avec l'incidence latérale

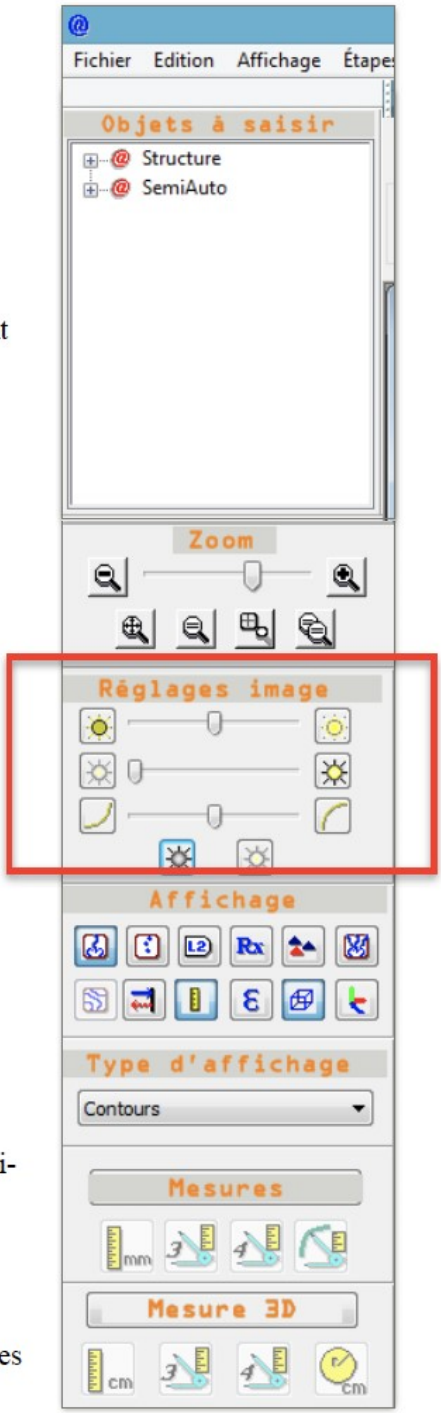

Commandes et raccourcis utiles

- Maj + Clic gauche tenu: Déplacer l'image
- Maj + Roulette: Zoom
- Touche « M » : faire disparaître les modèles
- F11: optimisation de l'affichage des fenêtres sous forme de colonnes
- Contraste des images: l'encadré rouge dans le menu déroulant (tel qu'illustré ci-contre) permet d'ajuster le contraste de vos images afin de bien identifier vos structures anatomiques

Plusieurs autres raccourcis sont disponibles, mais nous préférons vous présenter les modalités de base et éviter toute complexité additionnelle.

Préambule anatomique du membre inférieur

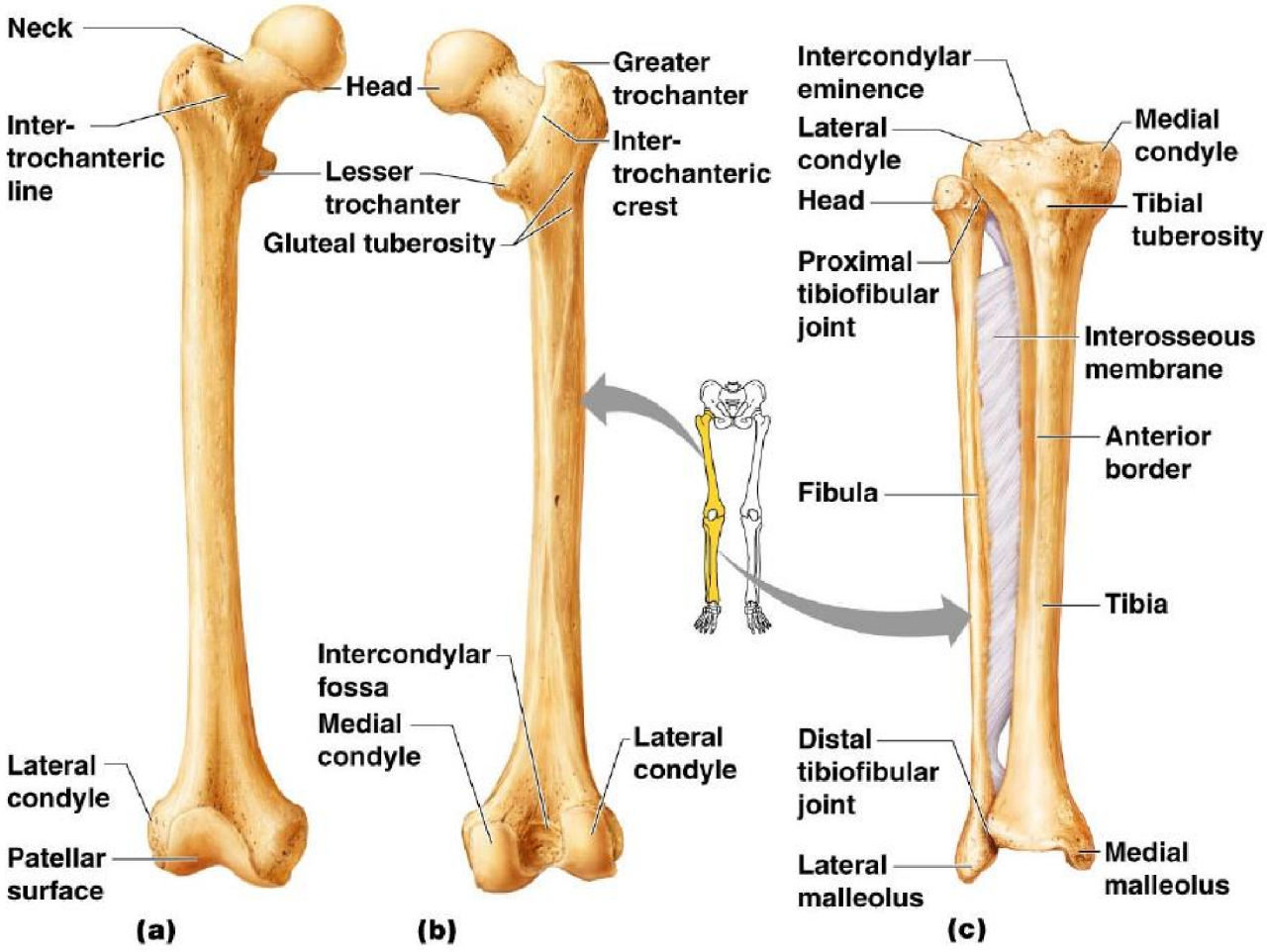

Étape 1: Identification des repères anatomiques

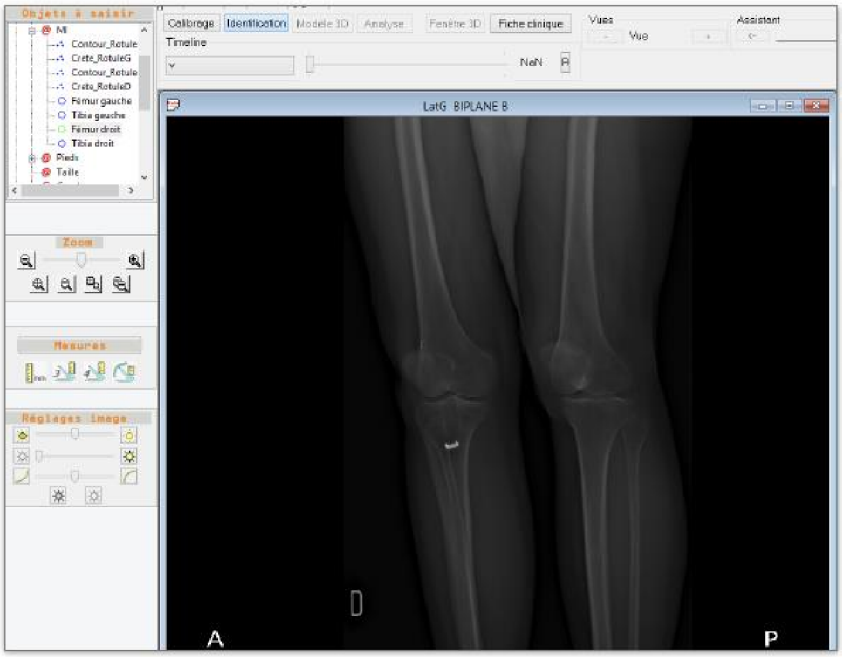

Dans le menu déroulant au coin supérieur gauche, sélectionnez *MI* dans l'onglet *Structures*

I. <u>Identification</u>

A. Après avoir sélectionner l'objet correspondant au côté désiré

B. Identifiez dans la première projection
   1. Centre de la tête fémorale
   2. Centre de l'échancrure intercondylienne
   3. Centre de la diaphyse, au niveau de la jonction entre le tiers moyen et le tiers distal du fémur

- Répétez dans la seconde projection. Notez que les modifications effectuées sont simultanément opérées sur la première image.

C. Ensuite, pour le tibia, identifiez sur la première projection
   1. Centre des épines tibiales
   2. Centre du tibia distal

- Répétez dans la seconde projection.

II. <u>DÉTECTER</u> (icône au coin inférieur gauche, dans le menu actions)

Les références du modèle générique sont ainsi positionnées, c'est à partir de celui-ci que vous ferez les ajustements.

Étape 2: Macro-ajustements

À partir de maintenant, vous naviguerez dans l'onglet assistant de génération du modèle 3D du haut de la fenêtre. L' ajustement du modèle générique du membre inférieur se fait en deux temps: plus grossièrement, puis plus précisément. À ce point-ci, il faut donc effectuer les macro-ajustements du modèle 3D de référence.

I. Ajustements en plusieurs étapes

A. Tête fémorale
   - la taille et la position de la tête fémorale,

B. Fémur distal
   - Centre des condyles, taille des condyles, extrémité distale de l'échancrure intercondylienne

C. Tibia proximal
   - Centre tibia proximal au niveau des épines tibiales

D. Tibia Distal
   - Centre du tibia distal au niveau du plafond tibial

E. Fibula
   - dans le cadre du présent projet, la fibula n'était pas reconstruite

Une fois ces étapes accomplies, vous serez prêts à passer aux micro-ajustements.

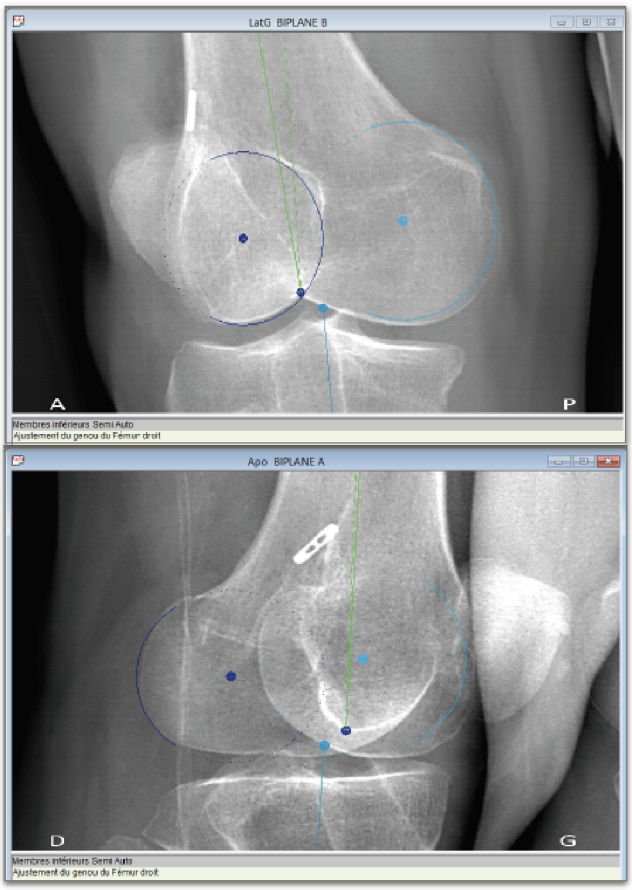

Étape 3: Micro-ajustements

Cette étape s'avère à être la plus longue et rigoureuse. Procédant encore systématiquement vous devez, avec les poignées correspondantes, identifier et ajuster :

1. Fémur proximal
   - Tête fémorale, grand trochanter, petit trochanter

2. Femur Distal
   - Diaphyse discale Condyle médiale et latérale, échancrure intercondylienne

3. Diaphyse fémorale

4. Tibia proximal
   - Plateau tibial médial et latéral, Épines tibiales

5. Tibia distal
   - Malléole médiale, latérale et plafond tibial

À ce moment, la reconstruction 3D du membre inférieur est complétée.

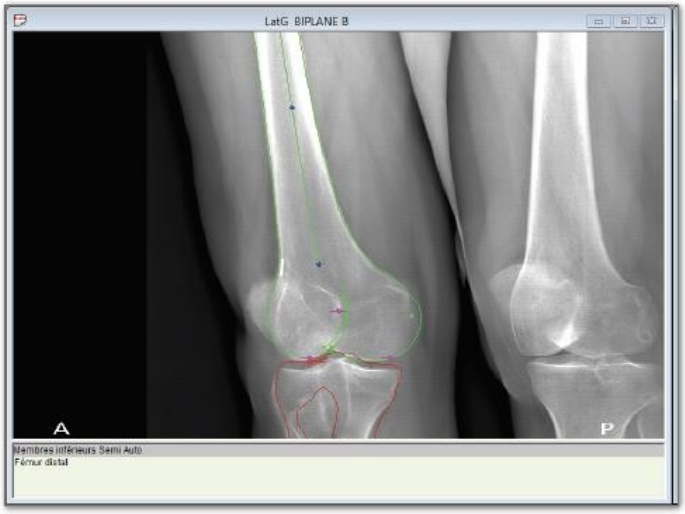

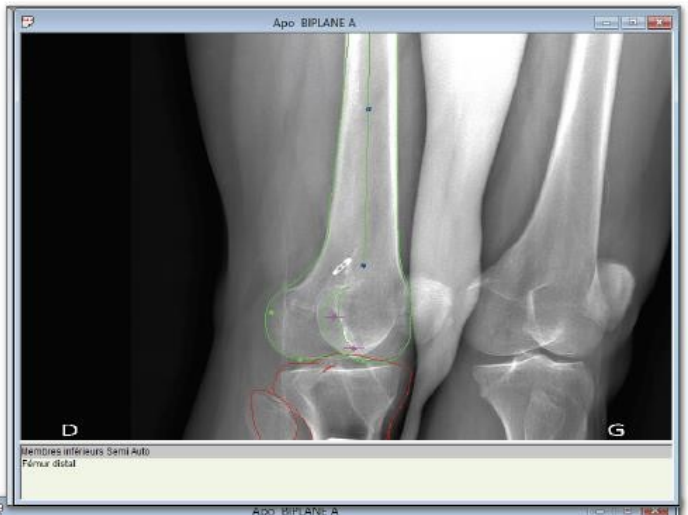

À cette étape, la *Fenêtre 3D* (ci-contre) permet de visualiser et vérifier vos changements en temps réel sur le modèle 3D. En utilisant la touche F11, vous optimiserez l'affichage des 3 fenêtres (AP, LAT, 3D) sous forme de colonnes.

Assurez-vous de bien sauvegarder votre progression.

Aperçu de la reconstruction (Fenêtre 3D)

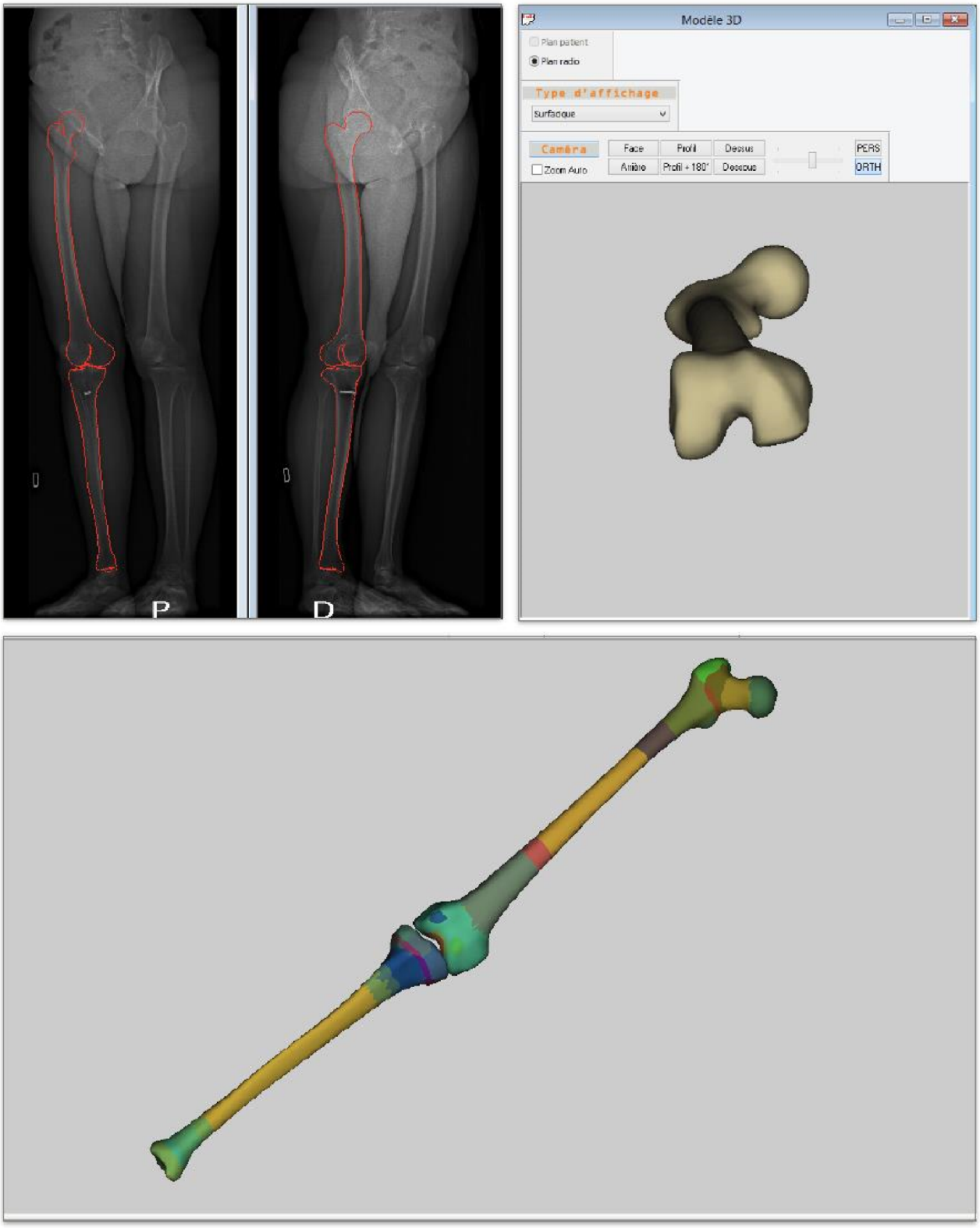

Étape 4: Identification des tunnels

La dernière partie de la reconstruction consiste à identifier les tunnels osseux au fémur et au tibia créés durant la chirurgie de reconstruction du ligament croisé antérieur.

I. Retournez dans le menu déroulant objets à saisir, par l'onglet identification

II. Sélectionnez TunnelsLCA
   A. Tunnel_F pour celui au niveau du fémur
   B. Tunnel_T pour celui au niveau du tibia

III. Par les mêmes principes que précédemment, positionnez les tunnels en ajustant leur longueur, orientation et surtout le diamètre des points intra et extra-articulaire.

- Encore une fois, les ajustements doivent être effectués sur les deux projections.

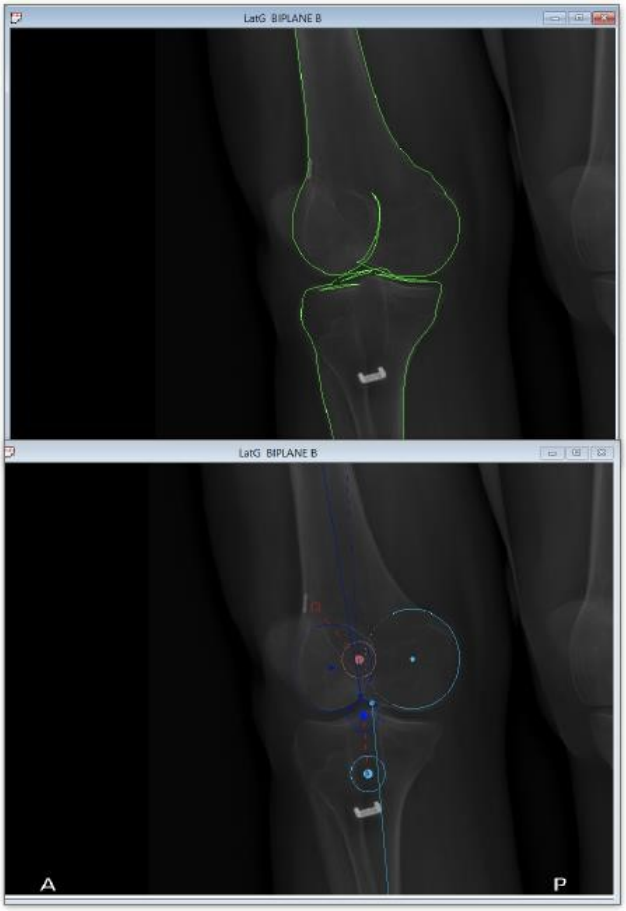

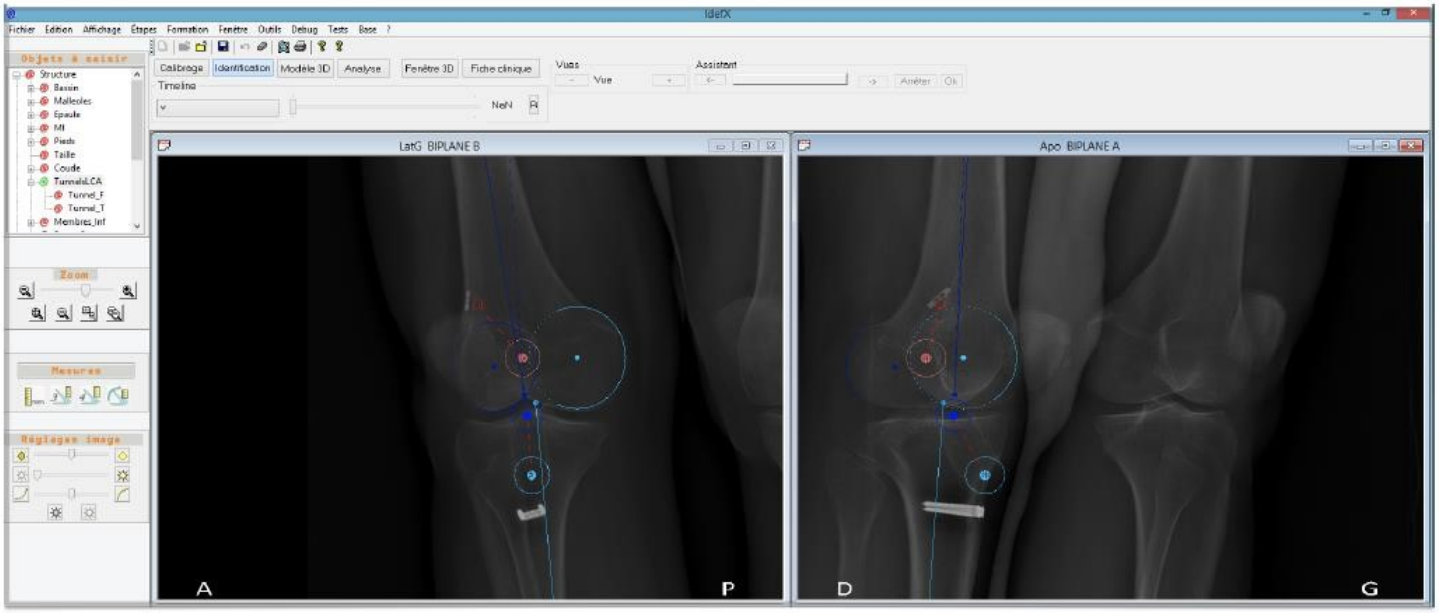

Étape 5: Enregistrer et exportation du modèle 3D

La reconstruction est complétée.

Assurez-vous de bien sauvegarder votre progression et d'exporter votre fichier en format « WRL » ou dans celui désiré en utilisant le menu déroulant fichier.

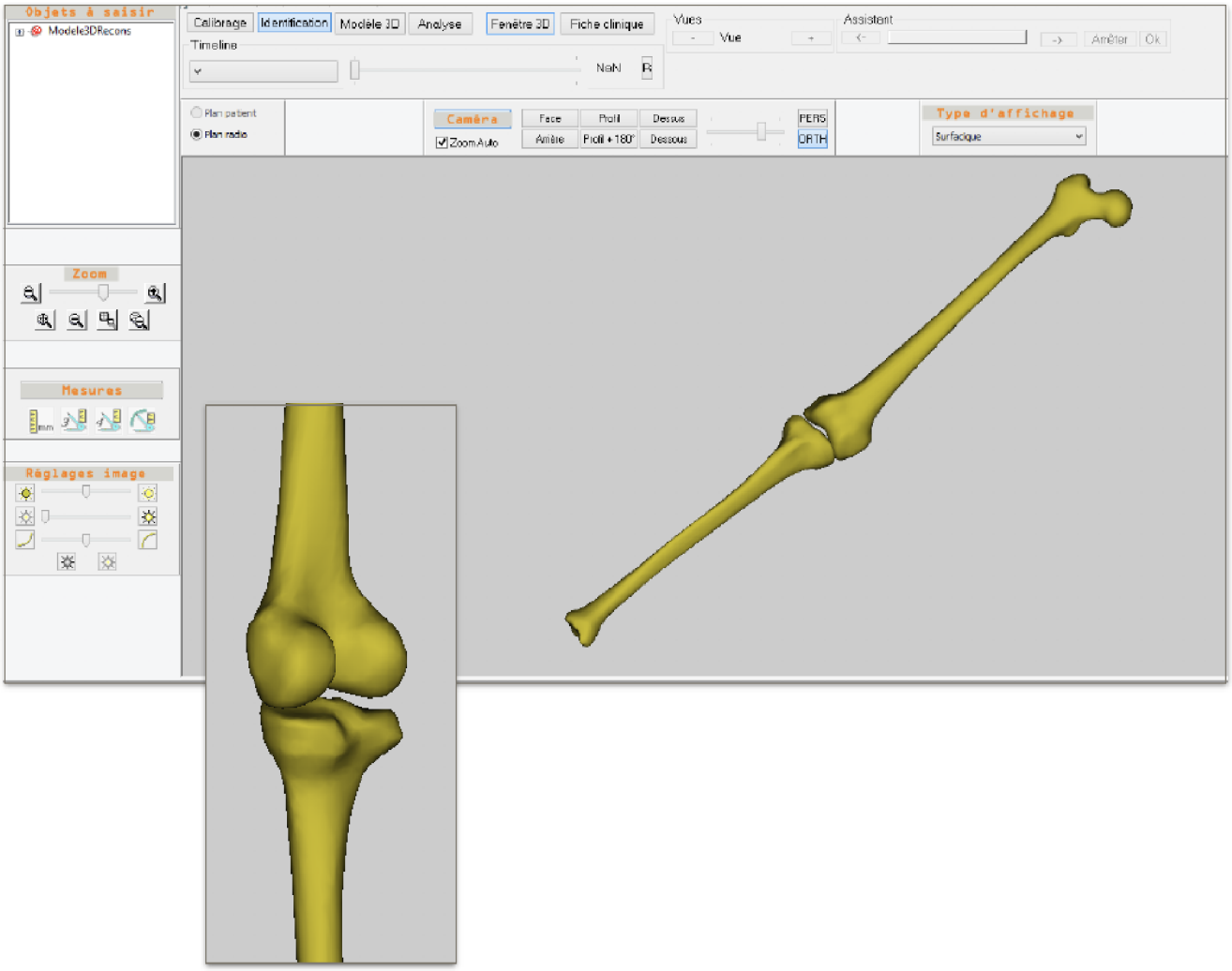

Annexe B – Approbation des auteurs chapitre 1

Titre du 1er article:

Biplanar stereo-radiographic imaging as a new reference in tridimensional evaluation of tunnels positioning in ACL reconstruction

Énoncé :

Par la présente, je reconnais avoir pris connaissance du contenu du manuscrit, être en accord avec les conclusions tirées et avec la publication dans le présent mémoire.

Signatures des coauteurs :

[redacted]

Julien Montreuil

[redacted]

Frédéric Lavoie

[redacted]

Félix Thibeault

[redacted]

Thierry Cresson

[redacted]

Jacques A. De Guise

Annexe C – Approbation des auteurs chapitre 2

Titre du 2e article :

Femoral tunnel placement analysis in ACL reconstruction using a novel tridimensional referential with biplanar stereo-radiographic (EOS™) imaging.

Énoncé :

Par la présente, je reconnais avoir pris connaissance du contenu du manuscrit, être en accord avec les conclusions tirées et avec la publication dans le présent mémoire.

Signatures des coauteurs :

Julien Montreuil

Frédéric Lavoie

Joseph Saleh

Thierry Cresson

Jacques A. De Guise